University of South Wales
2053151

# A STUDY OF LEAD SEPARATION FROM ELECTRIC ARC FURNACE STEEL MAKING DUSTS USING A CEMENTATION PROCESS

BY

ABDUL CADER MOHAMED RASHEED

THESIS SUBMITTED TO THE C.N.A.A. IN PARTIAL FULFILMENT IN CANDIDATURE FOR THE DEGREE OF DOCTOR OF PHILOSOPHY

DEPARTMENT OF CHEMICAL ENGINEERING
THE POLYTECHNIC OF WALES
TREFOREST, PONTYPRIDD
MID GLAMORGAN

In collaboration with G.K.N. Tremorfa Steel Works, Cardiff.

DECEMBER, 1981

## INTRODUCTION

The wastes containing potentially valuable metals and other materials are continuing to be generated in increasing quantities, while the world's resources of ores and minerals are gradually dwindling. Many of the wastes contain large tonnages of valuable metals and the methods of disposal often cause environmental pollution. Recently recycling of wastes has become attractive mainly due to higher costs of both minerals and energy.

During the steel making processes a large amount of wastes is generated, mainly in the form of dusts, slurries, fumes and sludges. The annual production of such wastes in the U.K. amounts to 2.5 to 3.0 million tonnes. For the year 1974/5 the British Steel Corporation produced ferrous wastes estimated at 2217 x $10^3$ tonnes, of which 522,000 tonnes were dumped, the rest was recycled.[1]

In the present study particular attention is paid to the recovery of potentially valuable metals and iron oxides from the electric arc furnace dusts. The production of steel dusts amounts to over 2 million tonnes per year,[2,3] containing approximately 1,100,000 tonnes of iron, 100,000 tonnes of zinc, 20,000 tonnes of manganese and 10,000 tonnes of lead. However, very little of them re-enter the industrial cycle.

The major factors limiting the recycling of electric arc furnace (e.a.f.) dusts are chemical compositions, small

particle size and the presence of a high level of undesirable residual elements. The following brief descriptions of the existing processes in the iron and steel industry are included to identify the problem and the origin of the wastes.

In the blast furnace operation the charge-ore (pellets or sinter), lime stone and coke are fed to the furnace. Simultaneously a stream of pre-heated air is blown in at the bottom of the furnace. During the reaction ('melt'), molten slag and exit gases are formed. The fumes are carried away by the gases. It is estimated that fines arising in this operation are about 1 - 2% of the iron produced.[1] From the total wet dusts produced 25% of it is recycled and the rest is dumped in lagoons. The dry dust is recycled through the ore preparation plant.

The molten pig iron or cast iron produced in the blast furnace is then converted to steel by one of the steel making processes. The principal method is the L.D. (Linz-Donawitz) process, where oxygen is top-jetted into the bath of molten iron fluxed with burnt lime. The wastes arise as dry and wet fines. The dust produced is about 2.0% of the steel production and the dust is estimated to contain 2 - 3% of zinc.[1,6] The collected dust is processed through a sintering plant in order to agglomerate for a product which is acceptable for recycling into the blast furnace.

Another popular method of steel making is by the electric arc furnace. The electric arc furnace process handles

about 10% of the steel production in the U.K.[1,4,5] It is becoming increasingly prominant in recent years and the steel production by this method will continue to increase in the future. The furnace is a cylindrical refractory lined vessel into which the scrap is charged. An electric arc is supplied through the carbon or graphite electrode system, which melts the scrap. The zinc and lead compounds present in the scrap (usually galvanised steel) are reduced and volatized. The fumes carry the volatized lead and zinc as oxides. The level of zinc in the e.a.f. dusts can vary from 7.0 to 40.0%[1,4,5,6] depending mainly on the quality of the scrap charged. The lead content is known to be in the range of 0.50 to 10.0%. During the course of an electric arc furnace operation, up to 20kg. of flue dust can be generated per metric tonne of steel produced.[6] The British Steel Corporation alone produces 49,000 tonnes of e.a.f. dusts per year, which are estimated to contain approximately 8,000 tonnes of zinc and 2,000 tonnes of lead.[1] The total e.a.f. dusts produced contains the equivalent of 10% of the total zinc consumed in the U.K.[1,7] The dusts produced can not be recycled in their existing physical state, they are currently disposed of as waste material in various land filling operations or left on sites in different locations.

Considerable efforts have been and are being made to find a suitable use for this material[8] The unsatisfactory physical and chemical properties make the dust undesirable to be recharged to any type of steel making furances. Many

pyrometallurgical and a few hydrometallurgical treatments have been attempted.

In the present research an attempt is made to separate the non-ferrous metals present in the e.a.f. dust by hydrometallurgy involving alkaline leaching. During the leaching of the dust, the iron compounds are found to remain in solid form. The non-ferrous metal fraction enters the solution and is separated from the iron compounds during filtration. The recovery of lead and zinc from the filtrate is investigated. The residue left after leaching (iron compounds) is to be upgraded to return to the furnace.

Lead is separated from the alkaline leach liquor by the technique of cementation using zinc as the precipitant metal. The word cementation is widely used to describe several unrelated scientific endeavours. Sometimes the terminology is used for adsorption of carbon into iron at high temperatures to form a hard material known as cementite.[9] It is also used to describe the process where the surface of a metal or alloy is impregnated with another substance in order to improve the physical resistance to corrosion, abrasiveness and heat. Another meaning of this word is used in coating of metals with ceramics. In the mining industry it is used for filling operation of a cavity or plugging a hole in a mine shaft with suitable filler material.

The meaning of the word cementation in this work is used in the context of a series of reactions, where lead ion from the leach liquor is precipitated by a more electropositive metal zinc. The name cementation is generally regarded as being derived from the spanish word "cementaction" which means precipitation.

Cementation reactions are known to have been in existence for centuries. In the early days the process was treated more as an art than a sicence. The alchemist also referred to the use of iron with mine waters for producing copper[10] During the early part of the nineteenth century cementation had been used to produce copper on a large scale. However, it was during the beginning of this century that some factors affecting the excess consumption of iron during cementation of copper was recognised.

Reactions of this type have been used in industry for a long time as a means of extracting metals from solutions.[11] The techniques are also used for

(i) the purification of process streams

(ii) the precipitation of copper from leach streams and mine water with scrap iron

(iii) the recovery of metals such as Cu, Ag, Au, Se, and Cd from their solutions

# C H A P T E R  T W O

LITERATURE SURVEY

Several techniques have been tried by many investigators[12 - 21] to find a suitable process for the recycling of electric arc furnace (e.a.f.) dusts. However, most of these techniques are based on pyrometallurgical approach, in which the non-ferrous metals are wasted. The presence of a large tonnage of electric arc furnace dusts containing potentially valuable metals necessitates the study of methods by which ferrous and non-ferrous metals can be recovered.

## 2.1. PROCESSES FOR RECYCLING E.A.F. DUSTS.

### 2.1.1 Pyrometallurgical Processes.

There are a few existing effective methods to treat electric arc furnace and blast furnace dusts. Most of these processes are concerned with the recovery of iron from wastes. A well known process in pyrometallurgy is the Waelz process[1,13] usually used in the treatment of concentrates, residues, drosses, low grade ores, etc. It is also used in the upgrading of zinc wastes.[13] In this process a heated rotary kiln is charged with a mixed feed of waste materials and fine coal, which is allowed to meet a stream of hot air flowing countercurrently. The operating termperature of the kiln is about 1200$^{o}$C. At this temperature the zinc will be vaporized and converted to the oxide fume in the air stream. The oxidized product is collected as light oxide in the electrostatic precipitators.[5,6]

Ban etal.[14] patented an invention of a method of recovering iron and zinc separately from waste materials produced in steel making processes. The method involves the following steps.

(i) the waste materials are mixed with coal and limestone

(ii) the mixture is made into pellets

(iii) the pellets are sintered in a grate

(iv) the sintered pellets are then transferred to a buried electric arc furnace, where the zinc is volatized and collected as an overhead gas.

Iron and slag are removed from the furnace and separated by conventional methods.

Thom[15] invented a method of producing sponge iron from the furnace dust by pelletizing the dry dust and heating it in a reducing gas stream flowing countercurrently in the presence of particulate carbonaceous material and flux. The temperature of the kiln is sufficiently high (1000 - 1200$^{o}$C) to reduce the iron oxide to sponge iron and vaporize the zinc and lead. This process claims a 96 to 99.90% reduction of iron oxide to metallic sponge iron. Tests were carried out using dust from open-hearth furnaces (now phased out).

The Bureau of Mines of U.S.A. studied a sulphuric acid leaching for steel making dusts.[16] In this process the acid leaching is followed by pyrometallurgical treatments to recover separately zinc, lead and iron products. Electric arc furnace dusts containing up to 40% or more of zinc were reported to be leached in sulphuric acid and the impure zinc sulphate solutions is used as a fertilizer additive.

Cochran and George[17] and also Holowaty[18] suggested a reduction-volatization method for separating the metals from e.a.f. dusts. In order to improve the economics of this process, they recommended a large regional plant to serve several steel companies. However, the above proposal was not accepted by any steel manufacturers.

Higby and Fukubayashi[2,3] conducted laboratory research to develop a pyrometallurgical process to recover zinc and lead from electric arc furnace dust. Investigations were carried out on both powdered and pelletized steel dust in an electrically heated quartz tube. The operating temperature ranged from 1050 - 1150$^{o}$C. The electric arc furnace dust was mixed with carbon and heated in an oxygen free atmosphere. Only a single reduction stage was involved and they reported that 99% of the zinc can be removed. A similar technique was employed by them for the recovery of zinc and lead from brass smelter dust.

Powell et al[19,20] investigated the possible recovery of nickel and molybdenum from wastes generated in the stainless

steel manufacturing plants. Lead and zinc present in the wastes are recovered as by products in the form of oxides. Their method consists of pellitizing the wastes and then smelting them using a reductant. Pelletizing was carried out in an 18 inch diameter drum pelletizer, using a water spray and an approx. 5.0% Portland cement to serve as a binder. The pellets were air and oven dried, The smelting was carried out in a coreless induction furnace using carbon, silicon carbide crucibles for dry pellets. They found that reduction materials such as coke breeze, lignite char and granular graphite were effective. The operating temperatures ranged from 1400 to 1600$^{o}$C and they found that higher temperatures were more effective. Lead and zinc were recovered at lower temperatures. An appreciable amount of manganese also evolved with the fume carrying zinc and lead. However, their investigations were primarily concerned with producing a recyclable iron product. The process claims a similar degree of achievement to other pyrometallurgical processes described.

Barnard et al[6] carried out a series of investigations into the recycling of steel making dusts. Samples from open-hearth furnaces, basic oxygen furnaces and electric arc furnaces were independently treated in the following manner:-

(a) The various dust samples were pelletized with 0.8% bentonite in a reducing atmosphere (carbon monoxide) to produce an iron material low in zinc and lead. The final products obtained were reported to have a higher iron content with lead and zinc reduced to a very low level.

(ii) Sulphating the dust by mixing with sulphuric acid followed by leaching to remove copper and zinc, as soluble sulphates. The method claims to yield pellets with high iron content. The leach liquor containing copper and lead did not receive much attention.

(iii) Pelletization of various mixutres of dusts containing carbon, zinc and lead followed by roasting to eliminate the non-ferrous metals.

In the above investigations it is claimed that lead and zinc can be readily evolved in a reducing atmosphere, giving iron products with less than 0.20% lead and zinc. The sulphating and leaching of electric arc furnace dusts were primarily to leach out copper and zinc. However, the end products were enriched in sulphur content, a most undesirable constituent for the furnace operation.

In a recent publication[21] a new process which is about to commence production in West Germany is discussed. The process is based on a modified Waelz kiln for treating steel making dusts. The project is carried out by Metallgesellschaft at its Bergelius zinc smelter near Duisberg. The project involves the use of an existing smelter to accept charges composed of up to 25% zinc ashes and some high grade dust from steel electric arc furnaces. The dust can be charged directly to the smelter without being oxidized by a Waelz kiln

Basically, it is a method by which low grade inputs can be metallurgically altered so that the Waelz kiln will achieve separation.

Research is reported to be underway in Japan[21] for the development of processes to increase material capacity at the smelters so that the electric arc furnace wastes can be recycled on a significant scale.

Larpenteur et al[22] found that if steel making dust is mixed with a flux comprising lime, manganese, carbonaceous fuel and heated in a kiln with excess air, the resulting solid is mainly iron oxides. According to this process the carbonaceous fuel reduces the oxides of lead and zinc to metallic forms, which will be volatized and carried away by the exit gases. The sulphur present in the dust combines with excess oxygen to form $SO_2$. The kiln is fired to a temperature range of 1384 - 1440$^{o}$C.

Pyrometallurgical processes involve reactions at very high temperatures. Therefore it consumes a large amount of energy.[23] The equipment required for these processes is expensive to install and operate. All pyrometallurgical processes have to consider the environmental pollution caused by emission of gases which occurs during their operations. High energy cost and stringent environmental controls have caused a severe setback in pyrometallurgical operations to produce low cost metals.

In the metal extraction technology hydrometallurgy is considered as an alternative to several pyrometallurgical operations.

2.1.2 Hydrometallurgical Processes.

Hydrometallurgy has made considerable impact in recent years due to reasons such as improvements achieved in practice and its preferential suitability for the treatment of many low grade ores. Usually results in high extraction rates as reported in the treatment of oxidized ores of gold, uranium, vanadium and copper.[11] Most of the hydrometallurgical operations do not consume a large amount of energy. The equipment needed is relatively simple, pollution free and inexpensive in comparison with equipment required for pyrometallurgical processes.[23] Hydrometallurgy has become an important method of recovering many metals from oxide ores and sulphide concentrates.

All hydrometallurgical processes involve two important stages:

(i) The primary step in this technology is getting the desired mineral from its associated solid ore into solution known as leach liquor, and

(ii) getting the desired metal out of the solution by further processing of the leach liquor.

The technique is fairly recent and it involves reagents and chemical knowledge. The main advantage of these processes is their ability to obtain metals directly in a pure form from the leach liquor by chemical methods such as cementation and electrowinning. Most of the hydrometallurgical operations consume less energy except when preliminary roasting is necessary.[23] However, some difficulty may arise in separating the insoluble fraction from the leach liquor.

The reagents used in chemical leaching processes are acids, alkali hydroxides, alkali sulphides, alkali cyanides and ammonia solution. They are commonly used in oxide or sulphide leaching operations. In some processes the reagent is regenerated by the precipitation operations which bring about a significant saving in the production cost.

Usually hydrometallurgy includes a combination of unit processes whereby the product metal or metal salt is produced from aqueous solution.

In a recent publication Davies[24] discusses the unit operations involved in all hydrometallurgical processes. They are broadly classified into separation and non-separation processes. The separation processes in hydrometallurgy include leaching, filtration, centrifugation, flotation, liquid extraction, cementation, ion exchange, membrane separation and electrowinning. The non-separation processes are usually referred to operations such as crushing, grinding, communition

and conveying. The author[25] also discusses the step-wise processes found for separation and non-separation processes in hydrometallurgy with specific reference to Sherrit-Gordon cobalt/nickel process. The efficiency of a separation process can be described by the equation below. The components i and y are product components in a mixture. Then the separation factor $a_{iy}$ is defined as

$$a_{iy} = \frac{x_{i1}/x_{j1}}{x_{i2}/x_{y2}} \qquad (1)$$

The numbers 1 and 2 refer to the product stream where the mole fractions of $x_i$ and $x_y$ enters.

### 2.1.2.1 Hydrometallurgy for the Treatment of Lead and Zinc Containing Materials.

The high level of iron oxides present in the electric arc furnace dusts makes caustic leaching the best choice for excluding iron from the leach liquor. Summaries of a survey carried out on alkaline leaching of lead and zinc containing materials are given in the following sections.

The caustic leaching of zinc-bearing materials such as roasted zinc sulphide concentrates, and lead containing zinc oxide materials like smelter dusts, drosses, slags, converter oxides are well documented.[26 - 30]

Several investigations on caustic leaching of zinc from oxidized zinc ores and iron-containing zinc sulphide concentrates are reported. Baroch et al[26] carried out

caustic leaching of oxidized zinc ores. The resulting zinc solution was purified with zinc dust (cementation) at temperature 35 - 50°C. Finally the zinc from the solution was recovered by electrowinning.

Winter et al[27,28,29] issued patents to the caustic leaching of zinc bearing ores (oxidized). The extraction was carried out at 93°C where the zinc value from the ores enters the solution as sodium zincate. The solution was purified by cementation using zinc dust at 50°C. The zinc from the solution was obtained as electrolytic zinc powder.

U.S. Bureau of Mines[30] suggested a process for the recovery of zinc from iron-containing zinc sulphide concentrates by caustic leaching. In this process initially the zinc sulphide concentrates are de-sulphurized in a primary roasting which form ferrites. The ferrites are subjected to a reducing roast treatment with reducing agents such as carbon-monoxide, hydrogen, coal and hydrocarbon oils. Following the reduction roast the ore is then leached with sodium-hydroxide solution of strength 20 to 35% (w/w) to dissolve the zinc as sodium-zincate. Finally the solution waspurified with zinc dust which removes the impurities and zinc was recovered electrolytically.

More publications and patents have appeared recently on the caustic leaching of zinc-bearing materials.

Cusanelli et al[31] discovered a process for the recovery of zinc from secondary by-product materials arising from metallurgical processing plants, e.g. smelter dust, lead and zinc-containing fumes from furnaces. The process involves selective lead separation into solution by controlled caustic leaching. During this leaching, the existing conditions depress the solubility of zinc. This is achieved by carrying out the leaching at high temperature of 204°C with an operating pressure of 200 p.s.i.g. for a leaching time of about two hours. The lead will enter the weak alkaline solution used. The solid fraction from the leaching, enriched with zinc, will be leached again with strong caustic solution (ION-NaOH) at 95°C and atmospheric pressure for about three hours. Once again the leach solutions were subjected to cementation with zinc dust at 38°C.

Abbruzzese[32] studied the caustic leaching of lead and zinc ores and recommended alkaline leaching for the low grade ores.

Rinelli and Abbruzzese[33] patented a process for separating lead and zinc from oxidized ore by ammoniacal leaching of the ore in the presence of polycarboxylic acids (sodium tartrate), subsequently applying selective extraction using chelating agents. According to this process the lead (present as carbonate) in the presence of tartrate ions was dissolved as a complex. During this leaching, the evaporation of ammonia was kept to a minimum by conducting the operation at 50°C. The filtrate obtained was then introduced into the

extractor in the organic phase. The selective extraction is carried out by LIX - 64N at a pH of about 9 - 10 ($H_2SO_4$ - used to adjust the pH value). During the organic phase extraction process, the LIX - 64N forms $Pb^{++}$ chelates and zinc does not react which is already dissolved as a stable complex $Zn(NH_3)_4^{2+}$. The lead from the organic phase was recovered by acid stripping followed by electrolysis. The zinc was precipitated from the liquid phase by evaporation.

Merril and Lang[34] investigated caustic leaching of oxidized zinc ores and minerals. Ores containing 21.20% zinc were treated with caustic solutions of strengh ranging from 180 to 240 g/l up to temperatures of boiling point. They reported rapid reactions with increasing caustic strength and temperature.

Kupfer and Vol Roll[35] put forward a technique for separating iron, zinc and lead from flue dust and/or flue sludge. This method involved three reaction stages, all in aqueous phase. The separation of heavy metals involved several stages of filtration. The three reaction stages of the above process were:-

(i) oxidation by $H_2O_2$ of the iron compounds and filtration of the turbid liquid. The residue from the filter was used in the next step.

(ii) acidification of the residue from stage one with 50% hydrochloric acid to form a turbid liquid. The filtration of the scond turbid liquid yields iron sludge.

(iii) neutralization of the filtrate from the second stage with $Ca(OH_2)$ or $Na_2CO_3$ which was followed by another filtration. The resulting filtration residue which gives mainly the precipitated heavy metals.

Stages (ii) and (iii) are pH controlled reactions. The above process involves numerous filtration stages and this alone can cause practical difficulties in achieving good separation. The shortcomings of this method are not discussed in the publication, especially the efficiency of separation, the final yield and purity of products are not known.

Duval [36] discovered a method by which the zinc oxide present in the flue dust from steel making processes can be removed by the use of spent pickle liquor ($H_2SO_4$ or HCl). The major portion of the zinc oxide is converted to zinc salt ($ZnCl_2$ or $ZnSO_4$). The process claims that iron oxide is separated from the mixture as a solid cake with only a small amount of zinc (0.5%) in a form which is acceptable for recharging into the furnace.

Goens et al[37] patented an invention which deals with the chlorination leach of zinc containing materials including sulphide ores, using either ferric chloride or chlorine gas. Following the leaching metals such as magnesium, bismuth and lead are recovered from the solution by cementation with iron. The remaining solution contains only zinc chloride and ferrous chloride. The zinc chloride was separated from the ferrous chloride by sodium chloride stripping. The ferrous chloride from the above extraction step was sent to a chlorination and hydrolysis step, where ferric chloride leaching agent was regenerated and iron removed.

Leaching forms an important step in hydrometallurgy and some of the factors controlling the reactions rate are discussed below.

### 2.1.2.2 Kinetics of Leaching

Several investigators [38,39] assume that the reaction during the leaching processes occurs first at the outermost surface (skin) of the particles. The reaction gradually works its way into the solid leaving behind the product and the unconverted solid fraction. This means that at a certain time during the leaching there will be an unreacted core of material which continues to shrink as the leaching proceeds.

Based on these fluid - particle reactions Braun et al[38,40] put forward theoretical equations which are called the shrinking core model. The reaction rate in the reaction zone is given by an equation which is given as

$$\frac{dn}{dt} = -\frac{4\Pi\, r_{io}^2}{\phi} K\, C_s G \qquad (2)$$

where $K$ = reaction rate constant (cm/sec).

$n$ = number of moles still unreacted in the core

$r_{io}$ = radius of the particle in cm.

$C_s$ = reaction concentration ($mol/cm^3$) in the reaction zone

$G$ = mass fraction of the leachable fraction in the solid particle

$\phi$ = shape factor for the sphericity of the solid particle.

The above model assumes the following conditions:-

(i) there will be full wetting of the solid particle by the surrounding fluid

(ii) the concentration of the leaching reagent in the leach solution should be constant

(ii) both the chemical reaction and the diffusion of effective reagent ions contribute to the reactive model

(iv) the chemical reaction will be dominating near the surface of the unreacted core, and

(v) the diffusion process is rate controlling in the rest of the core.

Levenspiel[40] suggests a three step mechanism during the reaction of a shrinking particle. The three steps occurring in succession are:-

(i) Diffusion of reactants from the bulk of the solution through the liquid film onto the solid surface

(ii) Surface reaction between reactant and solid

(iii) Diffusion of reaction products from the surface of the solid through the liquid film into the bulk of the solution.

The overall process is either chemically controlled or diffusion controlled. When chemical reaction is the controlling resistance, Levenspiel presents the following equation for the time-conversion behaviour of single particles as

$$t = \frac{\rho_B}{b\, k_s\, C_A} (R - r_c) \qquad (3)$$

$\rho_B$ = molar density of solid

b = stoichiometric coefficient for the reaction

$k_s$ = reaction rate constant based on unit surface

$C_A$ = concentration of reactant A

R = radius of particle at t = 0

$r_c$ = radius of unreacted core

In a diffusion controlled reaction the film resistance at the surface of a particle is known to be dependent on several factors such as relative velocity between particle and fluid size of particle and fluid properties.

Froessling[41] developed an empirical equation to represent the mass transfer to free falling solids in a fluid and is given as

$$\frac{k_\ell \, d_\rho \, y}{D} = 2.0 + 0.6 \, (Sc)^{\frac{1}{3}} (Re)^{\frac{1}{2}} \qquad (4)$$

$$= 2.0 + 0.6 \left( \frac{\mu}{\rho D} \right)^{\frac{1}{3}} \left( \frac{d_\rho u \rho}{\mu} \right)^{\frac{1}{2}} \qquad (5)$$

where $y$ = mole fraction of reactive A.

$k_\ell$ = mass transfer coefficient in liquid phase

$d_\rho$ = particle size

$D$ = Diffusion coefficient

$\rho$ = molar density of liquid

$u$ = relative velocity between solid particles and liquid

### 2.2.3 Recovery of Metals from Leach Liquors

The leach liquor containing mostly lead and zinc along with trace amount of silica and other heavy metals is initially treated to recover the lead fraction by the technique of cementation.

The electrochemical series of standard potentials[42] shows that zinc ($E^o$ = 1.22 volts) or aluminium ($E^o$ = 2.36 volts)

will precipitate lead ($E^{o}$ = 0.54 volts) from solutions. Theoretically the cementation efficiency here depends to a large extent on the resulting potential difference between the precipitant metal and the lead in solution. Although aluminium may be better metal for the cementation process, zinc was chosen to stop further addition of foreign ions into the leach liquor.

## 2.2 CEMENTATION

Cementation or contact reduction is the term used to describe the electrochemical precipitation of a metal usually from an aqueous solution of its salts by a more electropositive metal.[23] It is one of the oldest and simplest hydrometallurgical processes. Reactions of this type have been used in industry for a long time as a means of extracting metals from solution. Cementation techniques are also used for the purification of process streams. e.g. the removal of copper and cadmium ions from zinc sulphate electrolyte streams using zinc dust. Another common use of this technique is the precipitation of copper from leach streams and mine water with scrap iron. Further applications are observed in producing smooth, coherent metal coatings by cementation reactions.

The actual yields and process efficiencies are determined by rate factors. A knowledge of the reaction kinetics is essential for the most economic utilization of

the process. Cementation processes differ from other ionic transport processes in two respects. The presence of an adhered deposit which is reported to have a significant effect on the rate of precipitation[39] and any side reactions involving oxygen and/or hydrogen ions can completely alter the course of the reaction.

The general rate equation for dissolution of metals in solution containing ions of more noble metals is given as

$$\frac{dC}{dt} = k. \frac{S}{V}. C \qquad (6)$$

where k is the velocity constant, S is the area of metal in contact. The integral form of this equation gives,

$$k = - \frac{V}{S}. \frac{1}{t} \ln \frac{C}{C_o} \qquad (7)$$

The symbols are defined on the nomenclature. Cementation processes may be diffusion controlled or chemically controlled or sometimes a combination of both to form a mixed controlled reaction.[11,43]

The performance of industrial cementation equipment in existence is not published except for launders[44] and cones.[45] The launders use arbitrary precipitant surfaces (scrap iron) and the cones usually contain iron in particulate form. For any efficient and economical processes it is important in the design stages to be able to predict reaction

rates, conversions and products for any operating conditions. Such a design demands a good knowledge of reaction kinetics, the effects of reactants, products and the operating variables on the reaction rate.

If one considers the cementation reaction in the process design it is still to be established. The existing industrial cementation equipment is designed and constructed purely on past experience and in some cases on the experience gained in the pilot plant work. The operation of such industrial plant tends to function mainly on trial and error.

In the present study cementation reactions for Pb/Zn systems are carried out both for batch and continuous processes

### 2.2.1 Batch Cementation

One of the early studies of metal precipitation was done by Centnerszner and Heller[46] on the rate of copper cementation using zinc as the precipitant metal. They analysed their results by the following equation:

$$k_o = \frac{2.303\ V}{t.A} \log \frac{C_o}{C} \qquad (8)$$

The symbols used in the above equation apply as described for the previous equations. Centnerszwer and Heller studied the effects of stirring speed on the reaction rates and found the following relationship

$$\frac{D}{\Delta x} = k_o \qquad (9)$$

where D is the diffusion coefficient and $\Delta x$ is the thickness of a limiting boundary layer. They made the following conclusions from their investigations

(i) The precipitation of copper from copper sulphate solutions using a zinc surface follows a first order rate equation

(ii) The $k_o$ values were proportional to the rate of stirring in the range 50 to 400 rpm. In the range 400 to 700 rpm the rate constant ($k_o$) did not change

(iii) The rate constant was proportional to the temperature in the range 0 to 50 deg.C (the rate was not proportional to $\frac{1}{T}$ of the Arrhenius relationship)

(iv) The effects of temperature and stirring suggested a pure diffusion control mechanism.

King and Burger[47] extended the above investigation and found their results were in good agreement with those of Centnerszwer and Heller. They observed that for cadmium and zinc as precipitant metal that the rate constant for copper precipitation at different stirring speeds varied with copper sulphate concentrations irrespective of precipitant metal.

King and Mayer[48] put forward a rate equation for diffusion in a rotating cylinder in a turbulent flow experimental system as follows:-

$$\frac{dn}{dt} = 0.010ACV \left(\frac{D}{\upsilon}\right)^{0.83} \qquad (10)$$

In which $\frac{dn}{dt}$ is the equivalent transported per unit time. A is the surface area, V is the peripheral speed of the cylinder. The other symbols are defined in the nomenclature. They studied the rate of dissolution of zinc and cadmium in chromic chloride solutions. In their results certain higher rates than expected were obtained. This they explained as possibly due to the following factors:-

(a) a greater roughness of the surface at certain high concentrations. In such instances a "roughness factor" may be required for equation (6).

(b) the high rates may be due to dissolution with hydrogen evolution in addition to chromic reduction.

Glicksman et al[49] studied the cementation rates of silver onto rotating cylinders of zinc and copper. Using the rate equation developed by King and Mayer for diffusion reactions, they compared it with the normal first order rate equation $\frac{dn}{dt} = -k\,AC$ and found that

$$k = 0.010\ v \left(\frac{D}{\upsilon}\right)^{0.83} \qquad (11)$$

They also concluded that a greatly enhanced rate occurred mainly due to the presence of an abnormally small "effective

diffusion layer" whose thickness is reduced by local cell electrolysis. The thickness of this diffusion layer is normally determined by a balance between the hydrodynamic nature of convection and the diffusivity of the precipitating reagent. The thickness of this layer can be decreased by a potential difference that exists between the metal surface and the solution.

Lee et al[50,51] in 1975 and 1978 published papers on cementation of cadmium onto zinc and co-deposition of copper and cadmium onto zinc respectively. In the study of cadmium ions depositing onto a rotating zinc cylinder from a dilute solution under an oxygen-free, nitrogen atmosphere, they made the following major conclusions:-

(a) The initial rate of cementation is controlled by the rate of diffusion of cadmium ions to the surface.

(b) With the build-up of the initial layer of cadmium, dendrites of cadmium begin to form which increase the reation rate. The mode of reaction for the enhanced period still remains as for diffusion controlled.

(c) Alterations in the deposit morphology can have an effect on the specific reaction rate.

They also investigated the co-deposition of copper and

cadmium onto zinc by the use of rotating disc geometry. Tests were carried out under both inert and oxygen containing atmospheres. Under an inert atmosphere, the rate of deposition of both cadmium and copper is initially limited by the ionic diffusivity of these metals. As in their previous study, once the deposit built up, the overall rate increased. In this period the rate of cadmium deposition was found to be lower in the presence of copper ions, than when cadmium along was present. The rate of copper deposition onto zinc was slightly higher than it would be if no cadmium ions were present. When similar tests were carried out under an oxygen containing atmosphere, the initial and enhanced rates were found to be affected. The reactants became mixed or chemically controlled. This was in the absence of a considerable concentration of zinc ions in solution. They also observed a marked effect on the deposit morphology and the rate of cementation for the experimental conditions was that of mass transfer.

Ingraham and Kerby[52] studied cadmium precipitation with zinc using two experimental techniques - a rotating cylinder and a rotating disc. They evaluated activation energies for the two geometries under similar conditions as 19.60 KJ/mole for the cylinder and 16.70 KJ/mole for the disc.

Episkoposyam and Kokovskii[53] studied the cementation of copper and silver from acidic chloride solutions

using a rotating disc system. They found that the reactions had first order dependence for copper and silver ion concentrations. They used the rate equation including factors for the hydrodynamics of the system.

$$k_o t = (2.303 \frac{V}{S} p^{-\frac{1}{2}}) \log \frac{C_o}{C} \qquad (12)$$

where p is the number of rotations/sec. of the iron disc of surface area S and V is the volume of solution. The other symbols are as defined in equation (6). They obtained very low values for activation energies for copper and silver, and suggested that the two processes are diffusion controlled. At high acid concentrations excess iron consumption occurred and cememtation rate was reduced. This they explained as due to the reduction of hydrogen. The phenomenon of polarization of the iron disc by reduced hydrogen was suggested. The equation below explains the reaction.

$$H^+ + H_{adsorbed} = H_2 - e^- \qquad (13)$$

A paper published by Biswas and Reid[54] predicts a mixed control by diffusion and surface reaction for Cu - Fe system, where the agitation was achieved by using a rotating impeller above a static steel disc in the solution. An activation energy of 8.60 K.cals/mole was worked out and they suggested a chemical controlled reaction. They also investigated the effect of pH on the reation rate.

Drozdov[55] observed the kinetics of copper cementation on nickel powders from nickel plating baths. In the selected pH range of 3.0 to 4.5 it was found that the rate was first order in copper ion concentration. The activation energy varied widely with the activity of nickel. An important observation was the change in kinetics from diffusion control at high temperatures, the relationship betweem Log k and $\frac{1}{T}$ is not linear. Using the Arrhenius equation for determining activation energy values, he reported that the values varied from 22.0 k.cals/mole to 0.735 k.cals/mole depending on temperature and nickel activity.

Paulin and Zlatkovic[56] investigated the kinetics of copper cementation with iron in sulphate and chloride solutions. They found that the characteristics of the precipitated copper on iron in both solutions depends on the initial rate. In this investigation a technique was chosen to eliminate the effect of deposit by removing the deposited copper from the iron surface by friction. The solution was stirred and pumped into the reaction vessel to meet the iron balls fed from the top. The copper from the used solution was removed using a filter and then the copper-free solution returned to the stirred feed vessel. They found that the solution flow rates influenced the rate of precipitation.

Sareyed-Dim and Lawson[57] studied cementation reactions onto particulate precipitants by the use of two separate deposition reactions Cu - Zn and Ni - Fe. Both

reactions were found to be mass transfer controlled under the oxygen pressures used. They described the specific reaction rate constants by the following equation

$$Sh = 2 + 0.75\ Re_p^{\frac{1}{2}}\ Sc^{\frac{1}{3}} \qquad (14)$$

where the particle Reynolds number $Re_p$ is defined in terms of the settling velocity and of arithmetic-mean particle diameter. The rest of the symbols are defined in the nomenclature. The specific reaction rate increases with increasing agitation until a condition of full particle suspension is reached. Thereafter the specific rate constant was independent of any further increase in agitation.

Lawson and Nhan[58] recently published their work on the kinetics of cobalt precipitation from zinc sulphate electrolytes by a rotating zinc geometry. Studies were carried out for the codepositon of cobalt and arsenic onto zinc in the presence of high concentrations of zinc ions in solution using an inert atmosphere. They found that the cementation of cobalt with zinc was chemically controlled. The evaluated activation energy ranged between 40 and 60 KJ/mole. The kinetic data for the codeposiion invariably showed a two-step reaction.

## 2.3 DIFFUSION CONTROLLED REACTIONS

When a reaction is diffusion controlled, it is

expected the mass transfer rate will depend on the rate of stirring. Several previous investigations have tested this phenomenon via degree of stirring, especially where rotating disc geometries were used. The rate of mass transfer to the plane of the disc increased to maximum value in most cases.[42] Such cementation studies include the following systems, Cu - Zn, Cu - Co, Ag - Fe, Cu - Cd, Ag - Zn, Ag - Cu, Cu - Fe and Au - Zn from cyanide solution. In the above studies the controlling step is assumed to be the transport of reactant cations from the bulk of the solution to the solid-liquid interface. The diffusion processes are represented by the solute diffusivity. Usually all diffusion controlled processes will have low value for activation energy.

Galecki et al [59] modified the conventional diffusivity representation to the interactions with other ion species in solution. Strickland considered the co-diffusion of solute cation to the solid surface and the product cation from the solid surface to the bulk of the solution.[60] The ions will diffuse at equal rates (molar basis) resulting in an effective diffusivity which will be a function of both individual diffusivities. The presence of complex ions in the case of the leach liquor will result in incorporating more diffusivities to evaluate an effective diffusivity.

The mass flux (j) to the plane of a rotating disc for laminar flow condition is given by the Levich equation.[61]

$$j = 0.620\, D^{\frac{2}{3}}\, \upsilon^{-\frac{1}{6}}\, \omega^{\frac{1}{2}}(C_B - C_S) \qquad (15)$$

The symbols are defined in the nomenclature. The theory considers the total available area as the surface over which the controlling step (diffusion) occurs. Wadsworth[38] also MacKinon and Ingraham[62] have disputed this assumption, because of the possible modification of the surface area to some extent due to the presence of deposit.

## 2.4 CHEMICALLY CONTROLLED REACTIONS

Sometimes the reactions of this type are referred to as surface controlled reactions. Only a few examples of chemically controlled cementation reactions have been reported.

Ingraham and Kerby[52] also Drozdov[55] studied the cementation reactions of Cu - Ni, Cu - Al, and Ni - Zn. These reactions were found to be chemically controlled only at low temperatures. When tests were conducted for the same systems at temperatures greater than 90°C, the mechanism involved was then reported to be that of diffusion controlled.

Lawson and Nhan[58] reported that cementation of cobalt onto zinc was a chemically controlled reaction. In most chemically controlled reactions higher values of activation energy have been reported.[42]

In some instances the cementation process may involve a combination of both diffusion and chemical rate controlling

steps. Such processes are termed mixed controlled reactions. If one considers the flat plate geometry suspended in flowing fluid, the plane facing the fluid stream will have considerably higher mass flux and it is likely to be a chemically controlled reaction whereas further down the plate it may be diffusion controlled.

## 2.5 EFFECT OF DEPOSIT ON THE RATE OF REACTION

Several investigators[42,52] in the past have reported the presence of deposit effects on the rate of cementation. Sometimes the effect of deposit is one of hindrance[63] and with other reations it is an enhancing effect[60,64] on the overall rate of precipitation. Such effects can be misleading in the interpretation of the experimental results. Miller[65] also Fisher and Groves[66] have observed that the rate constant depends on the initial concentration which is somewhat in contrary for any first order reactions. It may be attributed to the deposit effect. Kabonova and Khan[67] and Hamdorf[68] carried out experiments with high concentrations and did not analyse their results in the light of the deposit effects. However, Miller and Beckstead[69] also reported Cu - Fe cementation studies with wide range of initial concentrations (5 - 2000 ppm), where low initial concentrations had an enhancing effect and high concentrations retarded the cementation rates. These observations once again contradict the usually expected

increase in the rate constant with increasing initial concentrations of the solute ions due to the increased cathodic surface area. Many cementation reactions are reported to follow first order kinetics with either rate reductions or rate enhancements.

### 2.5.1 Rate Reductions

Von Hahn and Ingraham[63] observed rate reductions in the cementation studies of palladium - copper and silver - copper. Sareyed - Dim[57] also reported a similar behaviour with copper - iron system. In all these cases, a continuous smooth deposit was present. Therefore one could relate the rate reduction due to the nature of the deposit. Perhaps another reason may be the presence of undissolving oxide layers built up on the solid surface which did not dissolve as the reaction progressed.

### 2.5.2 Enhancements

The rate enhancement in any cementation reaction is often attributed to an increase in cathodic surface area. Rickard and Fuerstenau[70] on Cu - Fe, Ingraham and Kerby[52] on Cd - Zn, Strickland and Lawson[60] on Cu - Zn, Cd - Zn, Ag - Zn, Cu - Cd, have all reported rate enhancement in their studies.

Strickland[43] postulated a theory that the increased effective area is not simply an increased cathodic area.

This theory relates the enhancement rates to the formation of a dendritic deposit which creates a roughening of the reaction surface, while the reations rate is still controlled by mass transfer processes. The rate of reaction over the entire deposit masses was described empirically by an equation. The theory based on the specific deposit formed was verified by Strickland using a rotating zinc geometry. Further the theory suggests that as the deposit grows, a zero concentration plane is formed on the outer limit of the dendritic growth. Near the precipitant surface the fluid flow maintains a zero velocity plane. As further deposition continues, the zero concentration plane continues to move away from the zero velocity plane.

Strickland et al[43, 50, 51] studied extensively the deposits formed by various cementation reactions, under different conditions. They reported that Cu, Cd, Pb, Ag and thallium all deposited onto zinc in rough, dendritic forms. The important evidence emerged from the above observations is the reactant cat ions will deposit at the precipitant surface area along with further deposition predominantly on the outer surface of the deposit. This phenomenon will continue until the electrical conductivity of the deposit ceases to exist provided that the deposit structure remains porous. This is necessary for the free passage of the cat ions from the active sites of dissolution (anodic sites) and enters the bulk solution. The deposit formed can be smooth as in Ag - Cu

and Cu - Zn systems. The type of deposit formed is dependent on several factors, such as experimental condition and the presence of other ions in the system. It also depends on the reaction temperature, reactant concentration and stirring rate. Therefore, those parameters are imperative in any cementation studies.

Von Hahn and Ingraham[63] along with several others[39] have reported the presence of the precipitant metal in the deposit upto 50%.[43] Power and Ritchie[42] using polarization diagrams showed such behaviour during cementation reactions.

## 2.6 ACTIVATION ENERGY

Most investigations[43,54] have attempted to explain the mode of cementation reaction from the experimentally determined activation energy values. Usually high activation values for chemically controlled and low activation values for diffusion controlled reactions have been suggested.[50,51] Such demarcations are open for discussions. Miller et al[65,69] have shown that it is possible to obtain activation energy of magnitude 7 - 8 k.cals/mole, and for the process still to be mass transfer controlled. According to these studies which used the rotating disc system, the onset of the turbulance at higher Reynolds number at higher temperatures resulted in a reduction of the mass transfer boundary layer thickness. This will cause an apparently high activation energy for the system.

## 2.7 TYPES OF CEMENTATION SYSTEMS

The following section deals briefly with the types of geometries and the systems used in cementation studies.

### 2.7.1 Natural Convection Systems

A typical example of natural convection systems is where strips of metal are used in an unstirred solution. These types of cementation processes carried out under natural convection do not appear to be an effective method. Kabonova and Khan[67] obtained rate plots for the precipitation of cadmium onto zinc surface from sulphate solutions. As one might expect, low conversation rates were reported in these cases. Previously Vandevelde and Wasteels[10] also carried out cementation of Cu - Zn system under natural convection. Such systems are extremely difficult to analyse hydrodynamically and also it is doubtful about the uniform accessibility of solute ions to the surface. The system can be affected by external influences.

### 2.7.2 Forced Convection Systems

A great many cementation studies reported fall within this category. Reactions carried out with forced convections are discussed here under the following headings:

#### 2.7.2.1 Precipitant Plate Systems with Separate Agitators

Much work has been carried out by many investigators using a separate agitator with both a static plate and metal

powder as the precipitant surfaces. Kamecki et al[71] studied the Pb - Zn cementation from chloride solutions using a separate agitator with a precipitant metal (zinc) at low pH 2 - 3. Later Hein[72] reported his investigation of cadmium cementation on zinc plates from technical grade $ZnSO_4$ at very low pH - 1.0. Considerable numbers of publications on the copper cementation on Fe, Ni, Pd are reported in literature[72,73] where separate agitators were used. The mathematical analysis on the use of separate stirrers is difficult.

2.7.2.2 Metal Powder Systems with Separate Agitators

Cementation by metal powders have received considerable attention over the last two decades, mainly using zinc power (dust) as the principle source of precipitant for the separation of Cu, Co, Te, Ni, In, from different solutions. Some of this work and their theories are already discussed in the previous sections.

2.7.2.3 Precipitant Mounted on Stirrers

Centnerszwer and Heller[45] carried out the early work on copper cementation onto zinc strips mounted on stirrer blades. Similar experiments for Cu - Al, Ag - Al systems were adapted by MacKinon and Ingraham.[62]

2.7.2.4 Rotating Cylinder

The use of the cylinder geometry is found in the work of many authors of solid-liquid reactions. The main reason for its selection is its uniform accessibility to the

surrounding liquid. However, the exact mathematical solution for flow about this geometry is yet to be developed. Gabe and Robinson[74,75] put forward a theory based on Prandtl's mixing length to predict the mass transport to a rotating cylinder for both laminar and turbulant conditions. For this geometry the transition from laminar to turbulant flow takes place at very low Reynolds numbers (50 - 200). Gabe and Robinson's solution for turbulent flow is expressed for a concentric cylinder with radius R, and outer stationary cylinder radius $R_2$.

$$St = (2b)^{\frac{1}{3}} Re_c^{-\frac{1}{3}} Sc^{-\frac{2}{3}} \qquad (16)$$

where $St$ = Stanton number ($k/u$)

$Re_c$ = Reynolds number for a cylinder ($ud/\upsilon$)

$(2b)^{\frac{1}{3}}$ = a constant = 0.079

$d$ = $(R_2 - R_1)$ annular gap

They also suggested an empirical correlation for the first order rate constant (k) as

$$k = (2b)^{\frac{1}{3}} u^{\frac{2}{3}} \nu^{-\frac{1}{3}} d^{-\frac{1}{3}} D^{\frac{2}{3}} \qquad (17)$$

where $u$ = peripheral velocity of the cylinder.

The other symbols are as described for equation (11)

2.7.2.5 Flat Plate Geometry

The mass transfer equation for fluid flow under laminar flow conditions across a suspended plate was obtained

by Levich[61] from the continuity equation. The simplified form of this equation is expressed as:

$$j = 0.34D\,(C_B - C_S)(u/\upsilon_x)^{\frac{1}{2}}(\upsilon/D)^{\frac{1}{3}} \qquad (18)$$

where $x$ = distance along the plate from the leading edge

The rest of the symbols are defined in the nomenclature.
This geometry is applicable in any cementation study.
The reason may be due to the complexities encountered by the occurrence of non-uniform mass flux in the system.

2.7.2.6 Rotating Sphere

So far there have not been any studies reporting the possibility of using rotating spheres in cementation work. A theoretical equation for the motion of a sphere by Newman[76] and others suggests

$$Sh = f(\theta)\,Re^{\frac{1}{2}}\,Sc^{\frac{1}{3}} \qquad (19)$$

where $f(\theta) = 0.474$ at $\theta = \frac{\pi}{2}$

$\theta$ = angular coordinate in radians

However, very little experimental work had been carried out to check the validity of the above theories.

2.7.2.7 Rotating Disc

The rotating disc in laminar flow has attracted the attention of many authors in studying the electrochemical

reactions.[77] The rate of mass transfer due to diffusion of ions to the surface of a rotating disc in an agitated system is given by Levich[61] as described in equation (15).

The theory assumes that the system is under laminar flow conditions. The important outcome of Levich's model is that the local mass flux is independent of any position on the disc. This is due to the presence of the hydrodynamic and mass transfer boundary layers both being of uniform thickness on the entire disc surface. Therefore, the use of a rotating disc allows uniform accessibility to the diffusing solute ions. Another advantage is the ability of a rotating disc to maintain the laminar flow conditions in a well stirred system to high Reynolds number[42] up to $3 \times 10^5$ (for smooth disc). Even a disc with rough surface will reduce the above limit only by a small amount.

Riddiford[77,78] has written comprehensive reviews on the theories and uses of rotating discs.

Gregory and Riddiford[79] have showed some modifications required for the constant of the Levich equation for Schmidt number less than 1000. However, the analysis of several experimental works[42, 50,51] by Levich's model have shown excellent accuracy in predicting the mass transfer rates.

Newman and others[75,76] have published further work on Schmidt number and limiting current evaluations for rotating discs.

### 2.7.3 Continuous Cementation

The use of flow through packed bed of precipitant surfaces did not receive much attention. A summary of reported studies on continuous cementation systems are included here.

Strickland and Lawson[43] reported batch and continuous cementation for Cu - Zn system at every low initial concentration of copper of 10 ppm using the rotating disc geometry. The theoretical results were predicted by a complex empirical model.

$$\frac{K - K_s}{K_o - K_s} = \frac{1}{\sqrt{2\pi}} \int_{o}^{\frac{\ell - \bar{\ell}}{\ell}} e^{-\frac{x^2}{2}} dx \qquad (20)$$

where $K$ = first order hererogenous rate constant

$K_o$ = initial rate

$K_s$ = steady state rate constant

$\ell$ = natural logarithm of the specific deposit mass

$\bar{e}$ & $\bar{\ell}$ are respectively the mean and standard deviation of $\ell$

The above equation is merely a mathematical description of the reaction kinetics and does not describe any of the physical processes taking place.

Belberyszki and Ibagos[80] used laboratory scale launders in an attempt to obtain an empirical equation for the design of industrial scale launders. A continuous copper

cementation onto strips of iron was carried out in a series of six launder system. Their suggested model gave poor results when compared with actual industrial plant performance data.

Spedden, Malouf and Prater[44] studied the efficiency of copper cementation for varying flow conditions through a cone precipitation containing scrap iron (usually shredded), where the copper bearing solutions were pumped through a manifold with nozzles injecting the feed into the mass of iron. The cone precipitations consume a considerable amount of iron.[45] The performance of the equipment was reported in terms of the percentage copper recovered.

Hamdorf[68] investigated the precipitation of lead and silver from brine solutions of $CuCl_2$ and NaCl. The solutions were pumped through a packed bed of iron pellets at different flow rates for a range of temperatures (30 - 90°C). The study reported low activation energy for the system and the rate constant was found to be dependent on percentage utilization of precipitants.

Biswas and Reid[54] extended their investigations to test the batch studies to a laboratory scale continuous cementation using a column packed with iron spheres. They found an overall increase in mass transfer rates during the cementation on the iron spheres. The experimental values were found to be much higher than the theoretically predicted values.

Plaskin and Budnikova[81] studied the precipitation of gold by zinc and from cyanide solutions under nitrogen atmosphere at low concentrations of gold (15ppm). They reported the percentage conversion for varying flow rates.

Schrader and Clauss[82] studied the concentration of Cu - Ni in continuous system in $NH_3^+$ and $SO_4^{--}$ ions at pH = 11.0 under notrogen atmosphere. The concentration of copper ions was 1000 ppm and the temperature of the feed solution was at $70^oC$. They observed that the rate depends on the source of nickel.

In the present research a packed column of zinc cylinders was used to study the continuous cementation of a solution containing lead, the results of which can be treated in the light of the few existing theories of mass transfer.

Gupta and Thodes[83] reported a method of evaluating area availability factor for columns with different types of packings which included spheres, cylinders and cubes. Results based on this method were compared with those results published for heat and mass transfer data from packed bed operations. The relationship between the j factor for mass transfer and the modified Reynolds number for different types of packings were established. The modified Reynolds number (Re') for cylinders, spheres and other packings are defined as

$$Re' = \sqrt{A_p}\, G/\mu \qquad (21)$$

where $A_p$ = area of single particle

$G$ = superficial mass velocity

$\mu$ = absolute viscosity.

when the modified Reynolds numbers were plotted against $j_D$ factor for several heat and mass transfer data, the linear relationship was established. They put forward an empirical relationship to evaluate mass transfer modulus using the modified Reynolds number. The equation is given as:

$$\frac{\varepsilon j_D}{f} = \frac{0.300}{(Re')^{0.35} - 1.190} \qquad (22)$$

where $\varepsilon$ = voidage of the packing in the column

$f$ = area availability factor for the type of packing used

Carberry[84] presented a model to predict fluid-particle mass transfer in fixed beds at Reynolds numbers less than 1000. The theory was based on transient molecular diffusion within a boundary layer. Carberry defined the average mass transfer coefficient for diffusion within the boundary layer which is developed and destroyed as the fluid travels through the bed. The average mass transfer coefficient is defined as

$$k = 1.15\, U_a\, Re^{-\frac{1}{2}}\, Sc^{-\frac{1}{3}} \qquad (23)$$

where $U_a$ = average velocity in packed bed.

The other symbols are defined in the nomenclature. Then the average mass transfer coefficients were treated in terms of a boundary layer of $j_D$ factor which is given as

$$j_D = \frac{k}{U_a} \varepsilon Sc^{\frac{2}{3}} = 1.15 Re^{-\frac{1}{2}} \qquad (24)$$

# C H A P T E R  T H R E E

## PHYSICO-CHEMICAL PROPERTIES OF E.A.F. DUSTS

### 3.1 GENERAL PROPERTIES

Electric arc furnace dust supplied by a local steel works (GKN - Tremorfa Steel Works, Cardiff) was characterized in terms of its chemical composition, particle size distribution, surface area, bulk density, compactibility and specific heat values.

The dusts used in the present study are dark brown in colour and consist of very minute particles (average size of 5 microns) and agglomerates of different sizes. The size and shape of the particles of dust are shown by the attached micrographs obtained by scanning electron microscopy.

The dust particles are very light and flow easily. They are magnetic and have high angle of repose which makes handling difficult. The physical and chemical characteristics vary a great deal from one furnace to another. The chemical composition depends upon the types of material (scrap) being charged to the furnace. The chemical composition of the dust was determined by the following method.

A small amount of the electric arc furnace dust sample (0.25 gm.) was treated with 15.0 ml of concentrated nitric acid and perchloric acid mixture (4:1 by volume in a 100 ml. beaker. The mixture was gently boiled on a hot plate until most of the liquid had evaporated. The procedure was repeated with 15.0 ml. of 5M. HCl. Then the mixture was added to de-ionised water. After a thorough mixing the solution

was filtered, washed and the filtrate was made up to a definite volume. The concentration of metals such as Pb, Zn, Fe, Cu, and Mn were determined by atomic absorption spectrophotometer.(Table 1) Table 1A gives analysis of dry e.a.f. dusts by Energy Dispersive Analyser.

The elements present agree well with those detected by the energy-dispersive X-ray analysis. Although the metals in the dust occur mostly as oxides, they are reported here as elements. Other elements such as Ca, Mg, Al, S, F, Cl, Na, Cr and Ni are not determined in this study. The total inorganic carbon analysis of the sample indicated a value of 0.5%. The analysis for other elements by atomic absorption spectrophotometry showed their concentration to be very low.

As can be seen from the results given in Table 1, iron and zinc form the major constituents in the dusts used in the present study. The concentration of elements generally relfects the relative vapour pressures of those elements present and the grades of scrap used.

Figure 1 shows the energy-dispersive X-ray analysis of e.a.f. dusts used in this study. The results confirm the chemical analysis by the atomic absorption spectrophotometry. The X-ray diffraction analysis identifies with strong lines the presence of crystal phases such as $Fe_3O_4$, $\gamma$-$Fe_2O_3$, $SiO_2$, ZnO, PbO, MgO, CaO and graphitic carbon. Some weak lines were observed which appeared to represent $CaF_2$, FeOOH, $\beta$-ZnS and $Mn_3O_4$.

Table 1. Chemical Analysis of e.a.f. dusts

| Element | Chemical Composition % | |
|---|---|---|
| | Batch Sample 1 | Batch Sample 2 |
| Fe | 46.00 | 40.00 |
| Zn | 24.30 | 25.00 |
| Pb | 5.60 | 5.07 |
| Cu | 0.85 | 0.80 |
| Mn | 5.75 | 5.00 |
| C (inorganic) | 0.50 | - |

Table 1.A Chemical analysis of dry e.a.f. dusts by Energy Dispersive Analyser. (S.E.M. S150 Link System 860)

| Element | % of element present (weight basis) |
|---|---|
| Si | 1.862 |
| Cl | 2.779 |
| K | 2.635 |
| Ca | 1.764 |
| Mn | 6.049 |
| Fe | 50.090 |
| Cu | 1.130 |
| Zn | 27.530 |
| Pb | 6.158 |

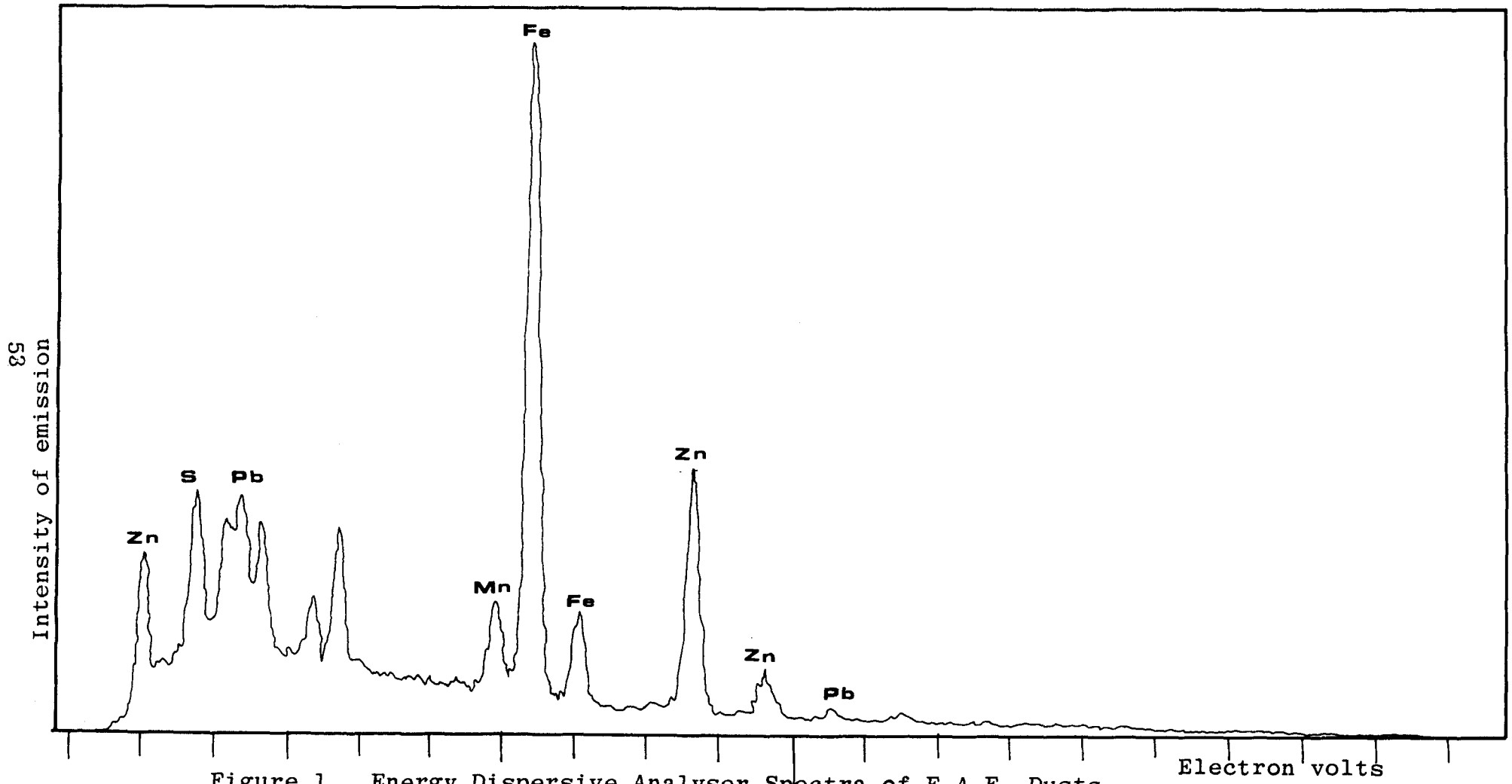


Figure 1. Energy Dispersive Analyser Spectra of E.A.F. Dusts.

## 3.2 PARTICLE SIZE

The particle size distribution was measured using a Coulter Counter-Model TA. The technique uses 1.0 to 2.0 milligrams of the sample sonically dispersed in an aqueous electrolytic solution (5% sodium-chloride - "Isoton II"). The dispersed particles are then made to flow through an aperture supplied with two adjacent electrodes. As each sample volume passes between the electrodes, an electrical resistance is created which produces a voltage pulse proportional to the particle size.(85)

The number of changes per unit time is directly proportional to the number of particles per unit volume of the sample suspension. The voltage pulse produced is then amplified and fed to the threshold circuit, where an actual sizing occurs. The integrator voltages are then fed to a multiplexer card and sampled one by one for differential data and subsequently added for cumulative data. The output of the multiplexer card is converted to electronic signals for plotting on an X - Y recorder presentation relative to 100% for total sample. The overall accuracy is better than 1.0% with low statistical deviations.

The results obtained are shown in Figure 2. and the particle size distribution is presented in Table 2. The average particle size was found to be $4.5\mu m$ in diameter.

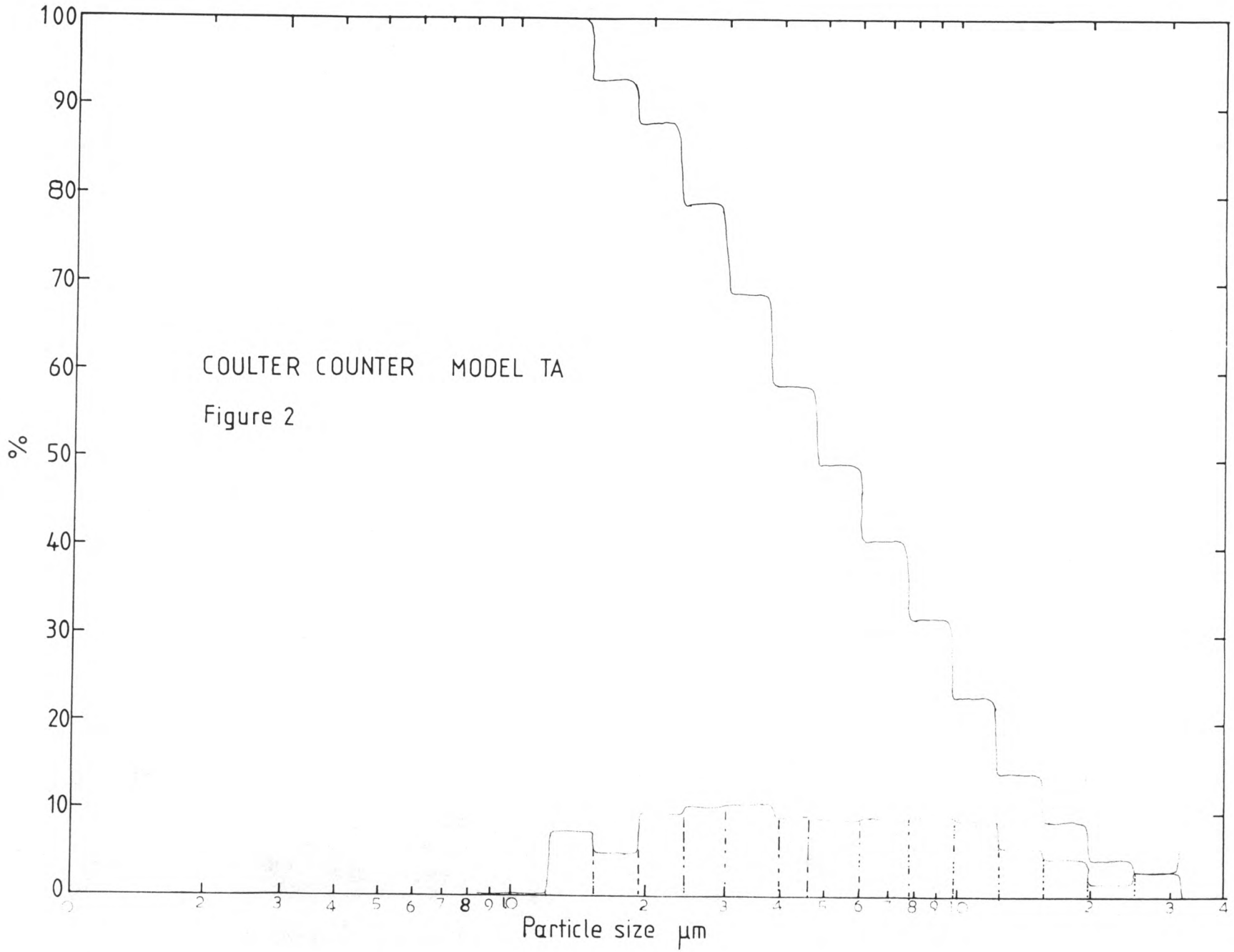
100
90
80
70
60
50
40
30
20
10
0
%
COULTER COUNTER MODEL TA
Figure 2
2
3
4
5
6
7
8
9
10
2
3
4
5
6
7
8
9
10
2
3
4
Particle size µm

Table 2. Particle Size Distriction of E.A.F. Dusts

| Mean particle size = 4.5 μm | |
|---|---|
| Particle size μm | % |
| 1.20 - 1.50 | 7.20 |
| 1.50 - 1.90 | 5.00 |
| 1.90 - 2.40 | 9.50 |
| 2.40 - 3.00 | 10.00 |
| 3.00 - 4.00 | 10.20 |
| 4.00 - 4.70 | 9.00 |
| 4.70 - 6.00 | 8.75 |
| 6.00 - 7.50 | 9.50 |
| 7.50 - 9.60 | 9.00 |
| 9.60 - 12.00 | 8.75 |
| 12.00 - 15.30 | 5.50 |
| 15.30 - 19.20 | 4.25 |
| 19.20 - 24.00 | 1.50 |
| 24.00 - 31.00 | 3.00 |

The micrographs of the dust sample indicate the spherical shape of the particles and they are considered to be mainly due to iron and/or oxides of iron. The fragmented objects usually scattered around appear to be flux additives and traces of slag.

## 3.3 SURFACE AREA

An area meter was used to determine the surface area of the dust sample. The apparatus uses the method based on low temperature nitrogen adsorption. The theory of which is described by Brunauer, Emmet and Teller (B.E.T. method).

The apparatus consists of eight adsorption vessels and the same number of empty adsorption vessels as reference vessels. The vessels are connected to their outlet valves through displacement capillaries.

A weighed sample is introduced into the adsorption vessel, usually the amount chosen to give the differential pressure on the manometer reading between 100 and 300 mm for reliable results. Initially, the weighed sample was dried in the heating block of the apparatus to drive off any moisture present. Nitrogen flow of 45 l/hour was maintained during this drying period.

After the samples had cooled to room temperature the vessels were purged with nitrogen at a flow rate of ten

litres per hour. This will remove all the air from the vessel. The sample and reference vessels were then equilibrated to the room temperature and purging continued to ensure equilibrium state. Then the apparatus was sealed by closing the valves. The two vessels are separated from each other and connected to the manometer.

Then the vessels were immersed in liquid nitrogen for five minutes and the difference in pressure due to the nitrogen adsorbed on the dust sample was observed. The method of calculation is shown below. Such data are useful in the evaluation of kinetic parameters for leaching of e.a.f. dusts.

The surface area ($S_g$) is calculated from the equation

$$S_g = \frac{A.\ \Delta h}{m} \qquad (25)$$

where $S_g$ = specific surface area ($m^2/gm$)

$A$ = apparatus coefficient

$\Delta h$ = pressure difference in manometer (m m)

$m$ = sample weight (grms)

The value of A is obtained from nomogram.

Two different samples of e.a.f. dust were used in the area measurements. Their results were calculated as follows:-

Sample I

$m = 3.72$ grms

$\Delta h = 89.0$ m m

$A = 0.1416$

$\therefore$ Surface area ($S_g$) = 3.41 $m^2$/grm.

Sample II

$m = 3.9873$ grms

$\Delta h = 102$ m m

$A = 0.1419$

$\therefore$ Surface area ($S_g$) = 3.71 $m^2$/grms

## 3.4 DENSITY MEASUREMENT OF DUST SAMPLE

The bulk density of dry electric arc furnace dust (moisture content less than 1.0% w/w) was determined by weighing the amount of dust required to fill a 100 ml. measuring cylinder. Settling of the dust sample was achieved by hand tapping with each addition. The typical measurement gave a bulk density value of 1.0452 gm/$cm^3$.

## 3.5 COMPACTIBILITY TESTS

Primarily the compactibility tests were carried out to determine the density of e.a.f. dusts at different test pressures using a hydraulic/pneumatic press available in the department. The compactibility test results are given in Figure 3.

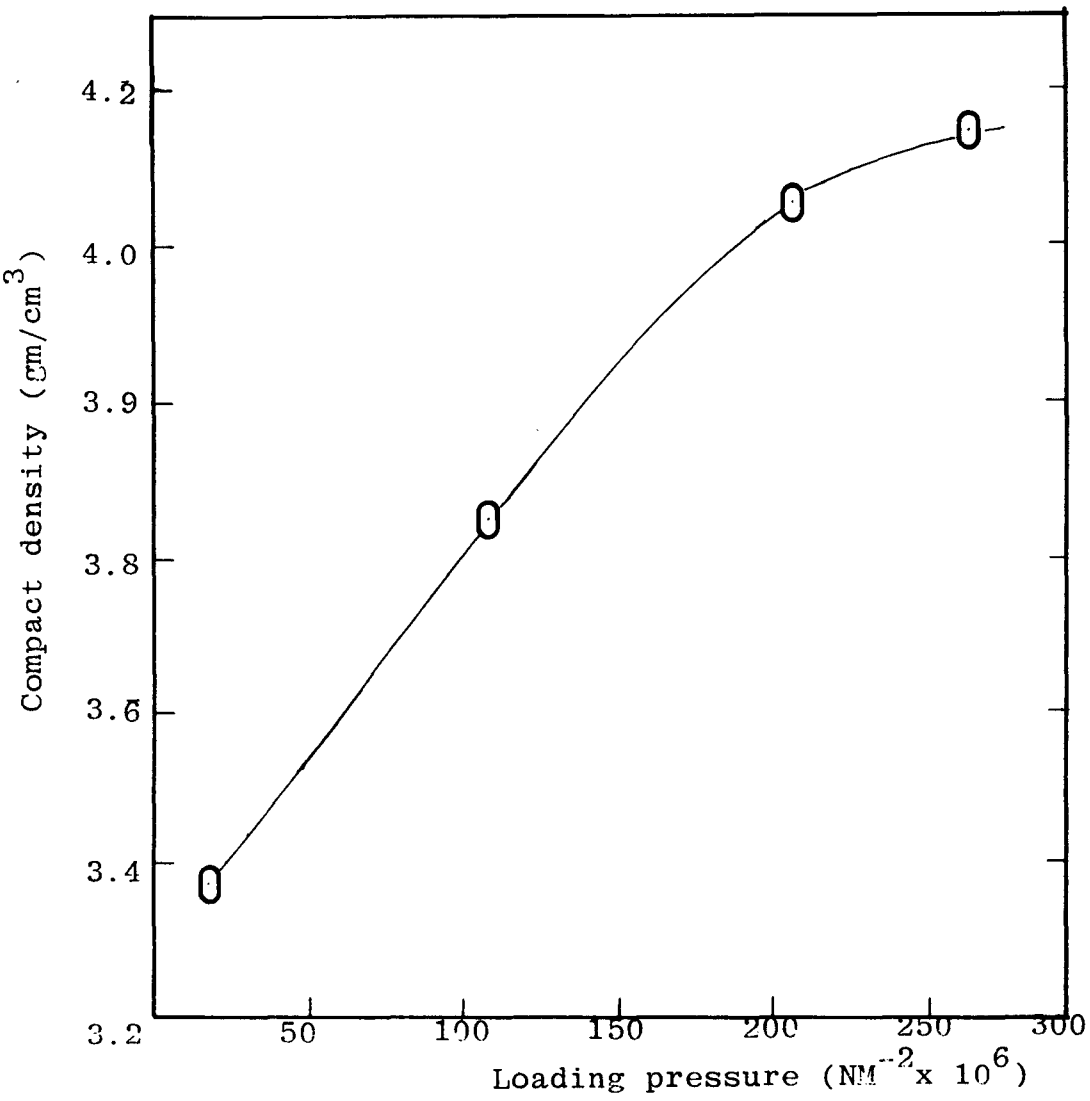


Figure 3. Density-loading pressure relationship of e.a.f. dusts

Such cylindrical compacts were prepared from dry e.a.f. dust and compressed at 10, 30, 50 and 65 p.s.i for approximately two seconds using a 0.15 cm (I.D.) and 1.0 cm high die made of inert alloy. Each die was previously weighed. The cylindrical compacts were of identical size and each die was filled to the brim by incremental addition of the sample. For each pressure, the density was determined by a mean weight from three tests. The procedure was repeated for other pressures. The gauge pressures were converted to loading pressures using a statimeter. The calibration curve is shown in Figure 3.1. The compact density - pressure relationship results are useful in determining the strength of compacts. Generally the dry collected dusts yielded fairly weak compacts. Such results are important in any investigation leading to the strengthening of e.a.f. dust pellets.

## 3.6 SPECIFIC HEAT

The specific heat of e.a.f. dust was determined using Differential Scanning Calorimetry (DSC) equipment (Perkin Elmer DSC-2) which is available in the department. The tecnhique is used for the measurement of heat evolved or absorbed by a physical change or a chemical reaction. It involves the use of the sample and the reference material at a temperature predetermined by the programmed oven. The amount of energy supplied or withdrawn from the sample to have zero temperature differential between the sample and reference is given as the thermal analysis curve.

Table No. 3. Specific heat of e.a.f. dusts.

| Temperature $^{o}K$ | Specific Heat cals/gm/deg) |
|---|---|
| 332 | 0.1590 |
| 334 | 0.1605 |
| 336 | 0.1619 |
| 338 | 0.1636 |
| 340 | 0.1652 |
| 342 | 0.1664 |
| 344 | 0.1679 |
| 346 | 0.1694 |
| 348 | 0.1710 |
| 350 | 0.1725 |

The pans containing the sample and the reference material are separately provided with platinum resistance thermocouple and a heater. Any temperature difference which results between the sample and reference material is automatically balanced to match the programmed temperature

The signal produced is the measure of the rate of energy absorbed by the sample in millicalories per second and is proportional to the specific heat of the sample, since the specific heat at any temperature determines the amount of thermal energy necessary to change the sample temperature by a given amount.

The specific heat values determined for the temperature range from 332$^{o}$K to 350$^{o}$K are given in Table 3. The samples were heated at a uniform heating rate of 10$^{o}$C/min.

## 3.7 DENSITY OF LEACH LIQUOR

The leach liquors obtained from different caustic leaching tests with a solid-liquid ratio of 1:4 were used in the density measurements. A standard 50ml density bottle was used and the following values were obtained for different leach liquors at ambient temperature.

(i) leach liquor with sodium-hydroxide concentration of 400 g/l = 1.4243 gm/ml

(ii) leach liquor with sodium-hydroxide concentration of 200 g/l = 1.3100 gm/ml

(iii) leach liquor with sodium-hydroxide concentration of 100 g/l = 1.1300 gm/ml

## 3.8 VISCOSITY MEASUREMENTS

The viscous properties of the leach liquors were measured at different temperatures in a set of Haake Viscometer.

The coaxial cylinder system was used, which allows viscosity measurements of Newtonian and non-Newtonian substances over an extremely wide range of shear stress and shear rate. The results were read on the indicator. The viscosity values are obtained in poise and centipoise.

The liquid to be measured was contained in the annular gap between a rotating cylinder (called the rotor) and a fixed cylinder (called the cup or beaker). The rotor speed works on defined r.p.m. and the resulting shear stress is an accurate measure for the viscosity of the liquid to be measured.

The rotor is driven by an electronically controlled motor. The torque produced by the test sample was measured by measuring head and transformed into an electrical value by a high precision potentiometer.[86] The voltage output of the potentiometer is linear to the angular displacement of the spring inside the measuring head.

The torque can also be recorded as a function of strain (shear rate) on a X - Y recorder.

The instrument factors M, A and G are used to calculate shear rate, shear stress and viscosity. Shear rate (D) is defined as $D = M.n\ (sec^{-1})$, where m = shear rate factor, depending on sensor system. The value of D depends on the test speed n.

Shear stress ($\tau$) is calculated from equation $\tau = A.S(dyne/cm^2)$ where A = shear stress factor depending on the type of measuring head and sensor system.

The viscosity ($\eta$) is determined from the equation $\eta = \frac{G.S}{n}$ (centipoise).

The measured viscosity of a leach liquor at different temperatures is indicated in Table 4.

## 3.9 COMPOSITION OF LEACH LIQUOR

The leach liquors were analysed by using atomic absorption spectrophotometry. The concentration of lead and zinc ions from different leaching tests are shown in Table 5. The analysis for Fe, Cu and Mn indicated only trace amounts present. The chemical composition of the leach liquor was found to be dependent to a great extent on the experimental conditions of leaching. The results given in Table 6 were obtained for leaching tests carried out at $25^{o}C$ and $60^{o}C$.

Table No. 4. Measurements of Viscosity of leach liquor at different temperatures.

(caustic Conc. = 400 gm/l)

| Temperature $^{o}C$ | Viscosity of leach liquor (centipoise) |
|---|---|
| 21 | 24.650 |
| 30 | 11.738 |
| 40 | 7.042 |
| 43 | 7.747 |
| 50 | 5.860 |
| 60 | 4.450 |

Table No.5. Chemical Analysis of Leach Liquor from leaching with different solid-liquid ratio.

| Leaching of e.a.f. dusts with caustic concentration of 400 gm/l | | | |
|---|---|---|---|
| Solid-liquid ratio % (w/v) | Leaching Temperature $^{o}C$ | Conc of $Zn^{++}$ (gm/l) | Conc of $Pb^{++}$ (gm/l) |
| 15 | 80 | 27.50 | 5.50 |
| 20 | 107 | 47.50 | 9.00 |
| 25 | 115 | 46.00 | 5.80 |

Table 6. Chemical Composition of Leach Liquor from Different Leaching Experiments.

| caustic conc. (gm/l) | Temperature 25°C $Pb^{++}$ (gm/l) | 25°C $Zn^{++}$ (gm/l) | 60°C $Pb^{++}$ (gm/l) | 60°C $Zn^{++}$ (gm/l) | 115°C $Pb^{++}$ (gm/l) | 115°C $Zn^{++}$ (gm/l) | Solid-Liquid ratio % (w/v) |
|---|---|---|---|---|---|---|---|
| 400 | 5.75 | 20.25 | 8.50 | 45.00 | 9.50 | 47.50 | 25 |
| 200 | 6.50 | 9.25 | 13.75 | 30.00 | 8.25 | 32.00 | 25 |

The composition of leach liquors resulting from experiments with varying solid-liquid ratio given in Table 5 was obtained at temperatures corresponding to the boiling point of the slurry.

When the original leach liquors were diluted with excess de-ionised water this often resulted in some of the zinc being precipitated. For a fourfold dilution as much as 40% (w/v) of the zinc present in the leach liquor forms precipitates which can be separated by decantation.

# CHAPTER FOUR

## DESCRIPTION OF APPARATUS

Cementation was attempted using a zinc surface in a solution containing lead ions. In the present study a batch cementation cell and a rig for continuous process were constructed. The overall flow sheet of the cementation cell is presented in Figure 4 and the continuous process apparatus in Figure [6]. The detailed arrangements of the apparatus are considered under the following headings. The apparatus used in this study is also illustrated by the photographs attached.

### 4.1 BATCH SYSTEM

#### 4.1.1 Cementation Cell

The cementation cell consists of a cylindrical pyrex glass beaker of 13.00 cm. internal diameter, 0.30cm. wall thickness and 18.80cm. height with an incorporated rotating disc system. The total volumetric capacity is 2.00 litres.

The vessel was firmly supported within a vertical framework of four cylindrical mild steel rods, each 20.00cm. high and 1.00cm. in diameter. The rods are fixed to the base plate using brass nuts (size 1.30cm.). The steel rods were installed to prevent any rotational movements of the vessel during the experiment. The four rods are bolted to a perspex flange which acted as the lid of the cementation cell. The

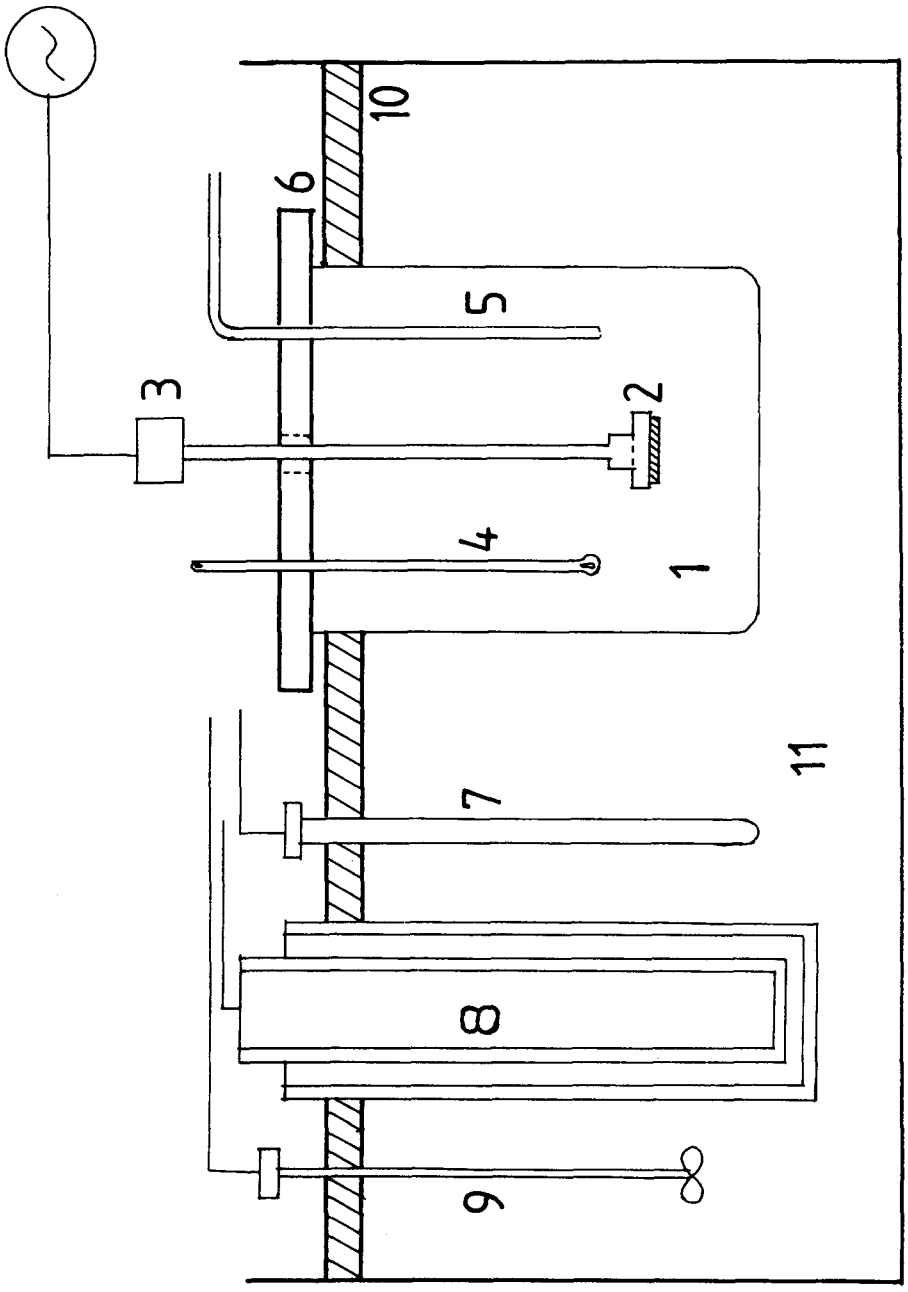


Figure 4. Schematic diagram of the apparatus for batch cementation experiments.

Symbols for Figure 4.

| Symbol | Item |
|---|---|
| 1 | Reaction vessel |
| 2 | Disc |
| 3 | Stirring motor |
| 4 | Thermometer |
| 5 | Sample tube |
| 6 | Flange |
| 7 | Thermostat |
| 8 | Main heater |
| 9 | Bath stirrer |
| 10 | Insulating layer of plastic spheres |
| 11 | Constant temperature bath |
|  | A.C. main supply |

lid contains three parts, namely a central part for the rotating shaft gland and two smaller parts for the sample tube and the thermometer.

4.1.1.1 Dimensions of the Cementation Cell

| | | |
|---|---|---|
| Height | = | 18.70cm. |
| Diameter (I.D) | = | 12.50cm. |
| Wall thickness | = | 0.3cm. |
| Flange diameter | = | 19.00cm. |
| Flange thickness | = | 0.70cm. |

The solution to be cemented is stirred using a variable speed motor (supplied by Voss Instruments Ltd., Essex.). The speed of rotation is controlled with a dial. The degree of agitation is measured in r.p.m. which was accurately determined with a tachometer (supplied by Smith Industries, Ltd.). The scale of the speed control knob is graduated from 0 - 100 and the corresponding range in r.p.m. for the solutions tested is 0 - 2000. The desirable speed of rotation is achieved by the appropriate setting of the knob to its scale. The stirrer is connected to the vertical shaft of the motor via a stainless steel sleeve of internal diameter 0.60cm. and 4.0cm long. Any vibrational movements of the stirrer and disc are reduced to a minimum by the central P.T.F.E. gland fixed to the flange. The assembly of the cementation cell is shown in the photograph attached and also shown in Figure 4.

4.1.1.2 Construction of the Disc.

The dimensions and construction of the disc are shown in Figure 5 (page 74 ) and by the photograph attached.

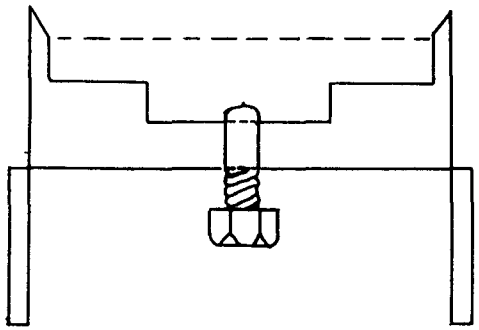

(a) Brass mould

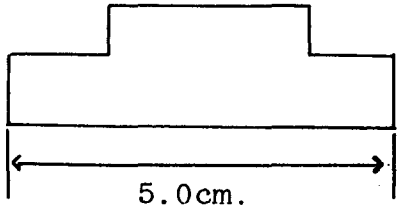


(b) Zinc casting

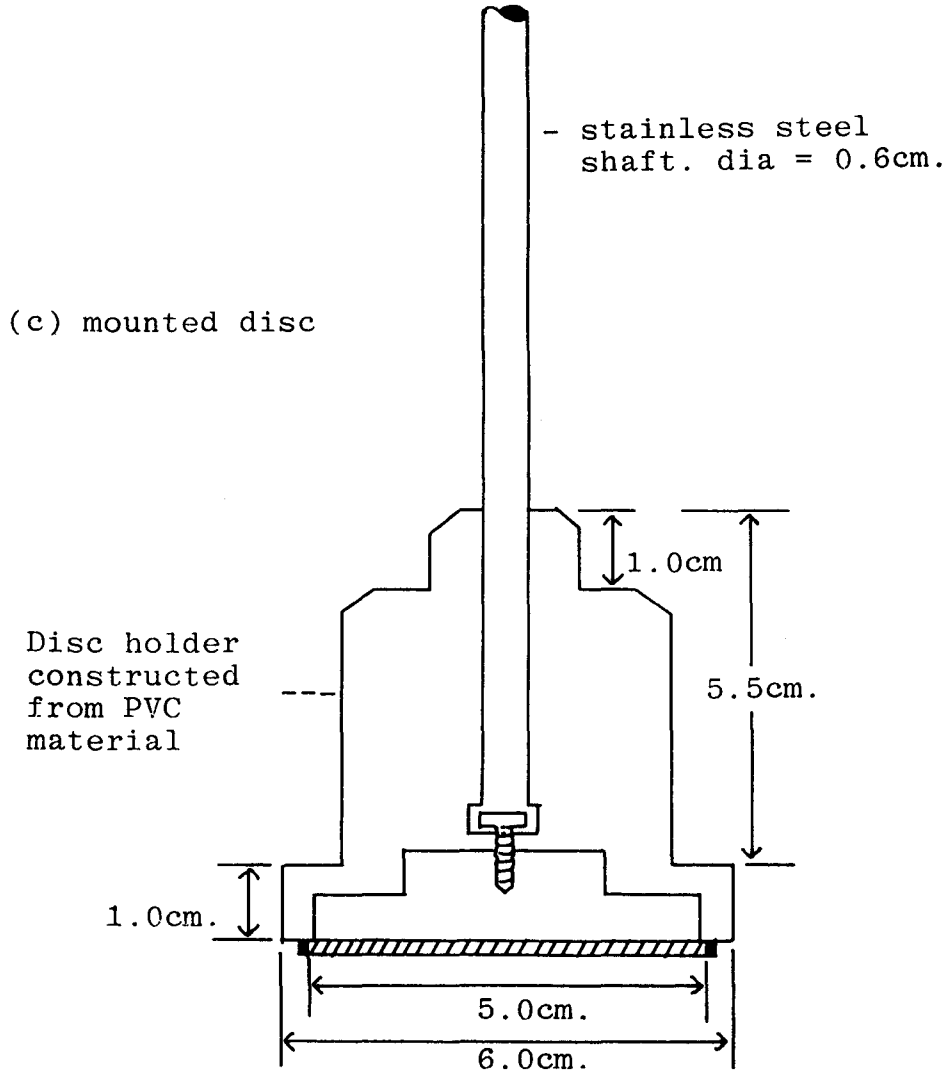


Figure 5. Design and construction of disc

The discs were cast from pure zinc in a brass mould by the following procedure.

Zinc rods (99.9% pure supplied by B.D.H.) were melted in a porcelain crucible under an acetylene-air flame. The molten zinc was then carefully transferred into a brass mould (a) of internal diameter 5.00cm., and depth 1.2cm. in the middle. Prior to the transfer of the molten zinc, the brass mould was sprayed with aerosol based P.T.F.E. to prevent contamination and adherence to the brass surface. The zinc disc cast (b) was then allowed to stand for annealing. Any surface layer formed due to atmospheric oxidation was removed during the disc cleaning operation. After six to eight hours annealing the cast zinc solid was removed from the mould by gentle tapping, the zinc was then machined to the appropriate size to fit the disc holder(c).

4.1.1.3 Disc Holder

The disc holder was constructed from a nylon block of 8.0cm. cube. It is imperative that an inert material is used. An internal plastic screw was used to hold the disc in place. A 6.0mm. diameter hole was drilled through the centre of the block to take the stainless steel shaft. Initially the mounted disc had a projected height of 1.0cm. and this was gradually reduced as several experiments were done using the same disc. The peripheral surface of the disc was

covered by "Araldite" to prevent any electrochemical attack. The resulting overall projected area was 19.6325 $cm.^2$. A stainless steel shaft of diameter 6.0mm. and 22.50cm. long was inserted into the central hole of the disc holder.

4.1.1.4 Baffles

Four baffle plates each 1.25cm. wide (1/10th of the vessel diameter) and 10.0cm. long were used. The baffles were constructed of stainless steel. In order to facilitate the cleaning of the cementation cell, the baffles were fixed to two stainless steel rings of diameter 11.80cm. Each ring passed through a hole drilled in the baffle plate about 3.0cm. from the ends of the plates. The effect on the reaction rate due to use of baffles was investigated.

## 4.2 CONSTRUCTION OF APPARATUS FOR THE CONTINUOUS SYSTEM

The overall flowsheet of the equipment used in the study of continuous cementation system is shown in Figure 6 Since the solutions used are highly corrosive in nature, careful consideration was given to the choice of materials for the construction of the apparatus.

The cementation kinetic parameters for varying flow conditions were studied.

### 4.2.1 Column

It consists of a cylindrical borosilicate Q.V.F. glass tube (P) of 5.10cm. internal diameter and 5mm. wall

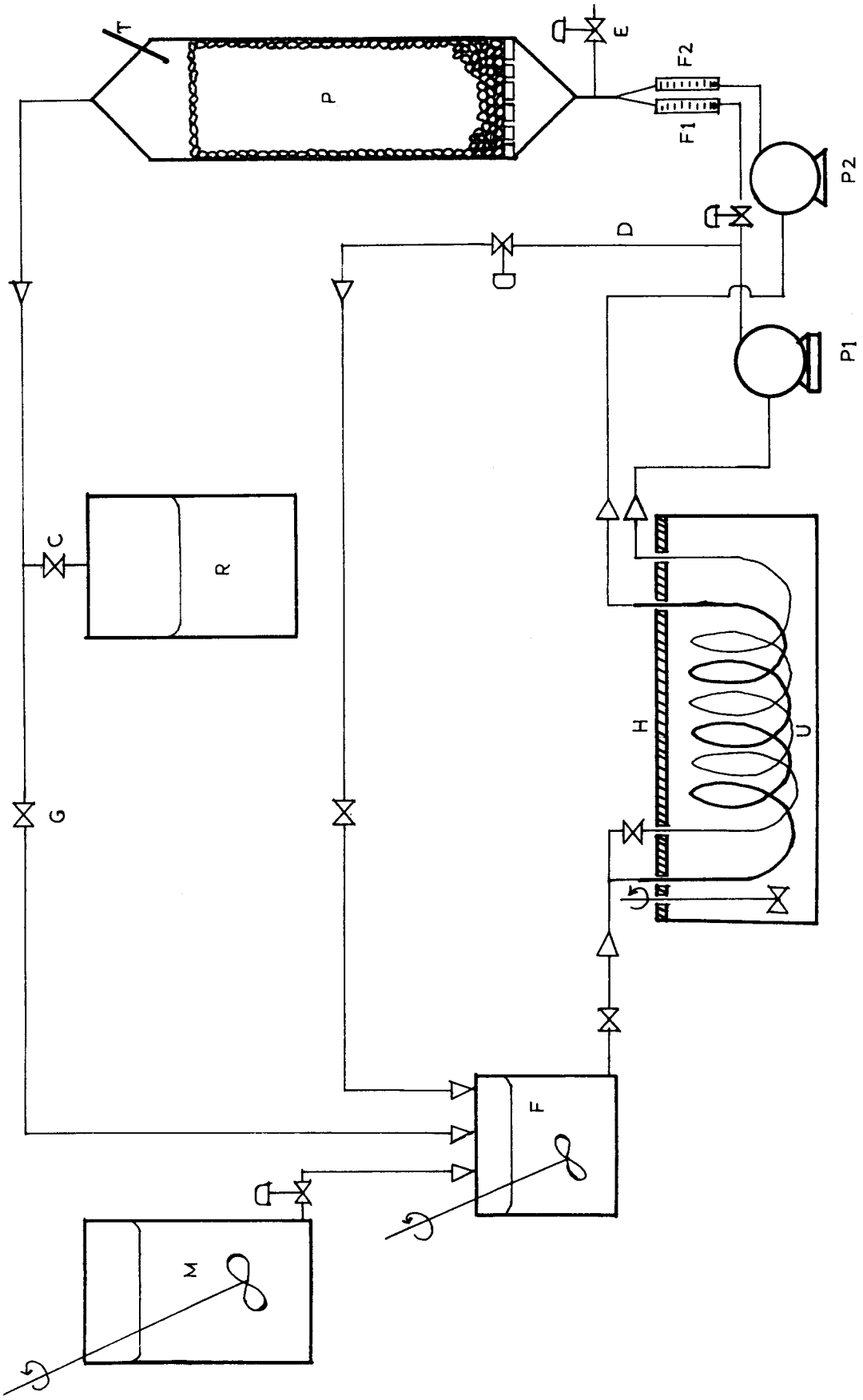


Figure 6. Flowsheet of the apparatus for continuous cementation

Symbols for Figure 6

| Symbol | Item |
|---|---|
| F | Feed vessel |
| M | Make-up reservoir |
| H | Heating unit |
| u | Heating coil (helix) |
| P1, P2 | Peristaltic pumps |
| F1, F2 | Flowmeters |
| P | Packed column |
| E | Drainage valve |
| D | Liquid by-pass line |
| R | Collection vessel |
| ⋈ | On/off valve |
| ⋈ | Control valve |

thickness and 44cm. in height. The bottom tapering end of the column is fixed with the help of two parallel circular metal fittings and five equally spaced galvanized bolts. A circular stainless steel plate (liquid distributor) with perforations (hole size 1.0mm.) was inserted into the space between the vertical column and the bottom tapering piece. The liquid distributor plate along with the tapering end of the column ensured a uniform distribution of liquid into the column. By using a larger pipe for the outlet stream, the pressure drop in the bed was reduced and subsequently the leakages through joints were completely stopped. The occasional reduction in flow rates due to cavitation was minimised by reducing the excess tube length connecting the feed pump and feed vessel. The column was held in position by three horizontal clamps fixed to the supporting framework.

The pressure drop in the column during the operation was measured using a water manometer. Because of the highly corrosive nature of the feed solution, extreme care was taken in choosing materials for the column. The level of erosion of borosilicate glass for 50% w/v sodium-hydroxide solution at $50^{o}C$ is quoted as very low (87) and the use of a borosilicate glass column was accepted in the present study.

### 4.2.2 Packing Material

Non-porous, zinc cylindrically shaped packings were used throughout the experiments. The construction of the packing material is briefly discussed below.

A large number of small flat rectangular zinc plates were cut, originally from a sheet of pure zinc (purity 99.85% supplied by Printers Plates, Ltd., London) of 0.07cm. thickness. Then each small plate was provided with five holes of equal diameter, 3.2mm., which were punched in the centre line of the longitudinal axis using an industrial type drill in the workshop. The rectangular pieces of zinc were then rolled to achieve the cylindrical shape. The dimensions of each rectangular piece and the resulting cylinder are as follows:-

| | | |
|---|---|---|
| Length | = | 4.0cm. |
| Width | = | 1.7cm. |
| Plate thickness | = | 0.07cm. |
| Outside diameter of packing | = | 1.2743cm. |
| Inside diameter of packing | = | 1.1332cm. |
| Diameter of each hole | = | 0.32cm. |

The plate thickness was determined using a micrometer screw gauge. The total area available for each packing is evaluated as 12.7957cm$^2$. The details of the calculation for interfacial area are given later in the thesis.

### 4.2.3 Voidage

The voidage of the packed column was determined by the following method.

The packings were introduced into a 5.10cm. diameter measuring cylinder in such a manner that they were packed in the same was as in the experimental column. The volume of packings

and air ($V_p$) was measured. A known volume of water ($V_w$) was added until the packings were just immersed. Then the total volume after displacing air from the packings ($V_T$) was noted. Voidage 'e' is calculated from the equation

$$e = \frac{V_p - (V_T - V_w)}{V_p} \qquad (26)$$

From the values of $V_p = 250.00cm^3$, $V_w = 232.50cm^3$, and $V_T = 270.00cm^3$, a value of e = 0.85 was evaluated. When the experiment was repeated similar results ranging from 0.83 to 0.875 were obtained. The value of e = 0.85 was used throughout in the calculations for continuous column operations as the voidage of the packed column.

### 4.2.4 Interstitial Velocity

The interstitial velocity was calculated from the total solution flow rate, the cross-sectional area of the column and the bed voidage.

$$u = \frac{Q}{A.e} \qquad (27)$$

where u = interstitial velocity (cm./sec.)

Q = volumetric flow rate (ml./sec.)

A = cross-sectional area of column $cm^2$.

e = bed voidage

### 4.2.5 Effective Interfacial Area

The effective interfacial area 'a' is evaluated from the definition

$$a = \frac{\text{Area of packing}}{\text{Volume of packing}}$$

$$= \frac{\pi d_o h}{\pi(d_o^2 - d_i^2)h/4} \qquad (28)$$

using the dimension given in section (4.2.2) the value of 'a' is evaluated as $4.7406 cm^2/cm^3$. The detailed calculation of which is included in the Appendix.

## 4.3 METHOD OF CLEANING OF PACKING MATERIALS

Initially a large number of the cylindrical packings were made to specification, and the same packings were re-used in a series of experiments. Prior to their use the packings were individually cleaned by following the procedure in sequential steps as described below.

(1) the packings were treated in dilute solution of 5.0% (w/v)$H_2SO_4$for approximately five minutes

(2) thoroughly rinsed in tap water to remove any cement products and excess acid

(3) polished with wet abrasive paper (grade 4/o) (which did not cause any observable scratching of the packing surface)

(4) cleaned with a nylon brish using soap and water

(5) thoroughly rinsed in excess de-ionised water

(6) the packings were treated in a 50% mixture of acetone and de-ionised water for 20 minutes. This removed any greasy materials present.

(7) finally, the packings were washed with de-ionised water and taken into a large beaker filled with more de-ionised water. The beaker with the packings was placed in a thermostatically controlled water bath whose temperature was kept constant at $45^{o}C$.

## 4.4 FEED VESSEL

As shown in Figure 6 it was a closed cylindrical vessel (F) of diameter 20.00cm. and 33.00cm height, whose material of construction was borosilicate glass. The total volumetric capacity was 10 litres. The feed vessel was provided with an electromagnetic stirrer. The solution contained in the feed vessel was continuously stirred at a constant speed. The feed vessel was supplied with an on/off valve. During the continuous operations, the liquid in the feed vessel was kept at a constant level by using a continuous supply of solution fed from the make-up reservoir. The feed tank was also provided with facilities to receive liquids from the pump's by-pass stream and the recycle stream during the recirculation runs.

The level of liquid in the feed vessel was indicated by a sticker graduated to read in volumetric capacity (litres).

## 4.5 MAKE-UP RESERVOIR

The primary objective of incorporating the make-up reservoir was to provide a constant solution level in the feed vessel which gave a constant head of hydrostatic pressure. This ensured a steady flow rate during each run.

The make-up reservoir (M) is a closed rectangular vessel of base 38 x 27cm$^2$. and 50cm. height. The material of construction was PVC with a volumetric capacity of 50 litres. The fresh solution from a mixing tank was usually pumped to the vessel until the level reached the 50 litre mark. The solution was continuously stirred using a variable speed motor with a three-bladed, stainless steel impeller, which was vertically mounted.

The make-up reservoir and the feed tank are connected by a borosilicate pipe with a control valve to regulate the solution flow rate. During the continuous cementation runs the constant level of liquid in the feed vessel was maintained by the flow control through this valve.

## 4.6 TEMPERATURE CONTROL

The temperature for the reactions for the batch experiments were provided by a glass-fronted water bath (supplied by Grants Instruments - Cambridge, Ltd). The temperature of the water bath was thermostatically controlled. The glass

fronted water bath was selected to aid visual observations of the cement product formed during the raction. The constant temperature water bath used in this study controls the solution temperature to within $\pm$ 0.5$^{o}$C, over the temperature range 5$^{o}$ to 95$^{o}$C. Heat loss and evaporation were minimised by covering the water surface with small insulating plastic spheres (supplied by Gallenkamp, Ltd.).

For the packed column operations for both recirculation and continuous runs, the inlet feed temperature which is also the column temperature was achieved by the use of a heating device. This is referred to as the pre-heater (H). As shown in Figure 6 the pre-heater unit was installed between the feed vessel and the pumps. The pre-heater unit essentially consists of two borosilicate helices with nine spirals, each arranged in close proximity. The entire helix was fully immersed in a theromostatically controlled water bath. The temperature of the water bath ranged as stated previously. As in the batch system the surface of the water was covered with plastic spheres.

The feed solution to the column passes through the pre-heater unit prior to its entry to the column. The internal diameter of the tube which makes the spiral was 0.7cm. This pre-heater unit was very effective in the transfer of heat. During its use, the temperature in the column remained constant at the selected value throughout the experiment with an accuracy of $\pm$ 0.5$^{o}$C. This was facilitated by lagging the

the column and the tubings. Some deviations in the temperature in the column were observed at high flow rates greater than 700 ml./min.

## 4.7 FLOW OF FEED SOLUTION

As illustrated in Figure 6 the flow of feed solution was achieved by utilizing two variable speed, two-way flow peristaltic pumps, P1, P2 (supplied by Watson-Marlow, Ltd.) The pumps were installed between the flow meters and the preheater unit. In some instances only one pump was in use. The pump efficiency depended on the rotor speed and the tube size selected. Using a 0.8cm. plastic tubing the flow rate ranged from 60 - 450ml./min. When experiments were conducted with flow rates greater than 450 ml./min., the additional pump which was of similar specification was used.

The use of peristaltic pumps in this study was appropriate and satisfactory mainly because of the highly corrosive nature of the alkaline feed solutions. Unless the mechanical parts of the pumps are fabricated from metals coated with P.T.F.E. or anticorrosive materials the solutions cannot be allowed to come into contact with any parts. For smaller flow rate experiments only pump P1 was used. The flow rate through the pump was regulated by controlling the speed of the rotor.

## 4.8 FLOW RATE MEASUREMENT

The flow rate of the feed solution entering the packed column was carefully controlled and measured by the use of two identical flow meters. The flow rate of each pump ranged from 0.06 to 0.45 l./min. The flow meters (supplied by Meterate G.P.E.) with plastic coated glass floats, were used. As shown in Figure 6 the flow meters F1, F2, together with control valves, were fixed to the pipes joining the feed vessel and the packed column.

Whenever the second pump was in use the temperature setting of the pre-heater unit was slightly increased to compensate for the increase in flow rate of the feed solution. Then the entire solution contained in the feed vessel was recycled until the steady state temperature was attained in the column. This procedure wss adopted for both recirculation and continuous runs.

### 4.8.1 Pressure Drop Measurement

Attempts were made to measure the pressure drop due to fluid flows through the packed column. A u-tube water manometer was connected to a point near the liquid distributor plate via a small tube of internal diameter 0.03cm. The tube in turn was connected to a 'perspex' ring whose internal diameter and wall thickness were similar to those of the column. The ring was sandwiched between the liquid distributor plate and the bottom of the column.

As expected, an appreciable pressure drop was observed for feeds with high solute concentrations and high flow rates. However, in most cases the maximum pressure drop observed was approximately 2.0cm. of water. The small change in pressure drop observed during the reaction was unreliable to correlate to the cementation process.

# C H A P T E R  F I V E

## EXPERIMENTAL STUDY

### 5.1 REAGENTS

The leaching experiments were carried out using different strength caustic solutions which ranged from 100gm/l to 400gm/l. Because of the low cost and the presence of trace amounts of impurities, the industrial grade of sodium-hydroxide solution (supplied by Kernick and Son) was used. When caustic solutions of concentration less than 400gm/l. were required the necessary dilutions were performed using de-ionised water. The chief impurity present in the industrial grade caustic solution was found to be zinc (12ppm.) a level which was acceptable in the present work. The chemical analysis for iron, manganese, copper and lead by atomic absorption spectophotometry showed their presence only in trace amounts (<0.1ppm).

### 5.2 SAFETY PRECAUTIONS

Extreme care was taken in handling the strong caustic solutions and the leach liquor. The highly corrosive nature of the strong alkaline solutions can cause severe burns. The surface of the skin must be washed thoroughly with boric saline solution for not less than 15 minutes. During the handling of the solution protective clothing was worn. An anticorrosive apron, gloves and goggles were also used.

## 5.3 PREPARATION OF LEACH LIQUOR

Electric arc furnace steel making dust supplied by G.K.N. Tremorfa Steel works, Cardiff, was used. A typical chemical composition of the dust is shown in Table 1.(page51). In the preparation of the batch leach liquor the following procedure was adopted.

A known amount of dust sample was dispersed in a fixed volume of solution of sodium-hydroxide of strength 400gm/l, contained in an open stainless steel vessel. The slurry was then heated on a gas burner to the boiling point. This temperature depended on the solid-liquid ratio which ranged from 15 - 25%(w/v). The boiling point of the slurry for the maximum solid-liquid ratio was approximately 115$^{o}$C, while the slurry was stirred at 600 r.p.m. by a three-bladed stainless steel impeller. A reaction time of approximately 40 minutes was found to be sufficient to dissolve most of the non-ferrous metals present in the sample. The solid-liquid separation was achieved by decantation followed by vacuum filtration. The flowsheet of the apparatus is shown in Figure 7.

The slurry was extremely difficult to filter under atmospheric pressure due to the combined effect of both viscosity and the colloidal silica present. Therefore, a vacuum filtration unit was set up to handle a total filtrate volume of two litres per run. The highly corrosive properties of the leach

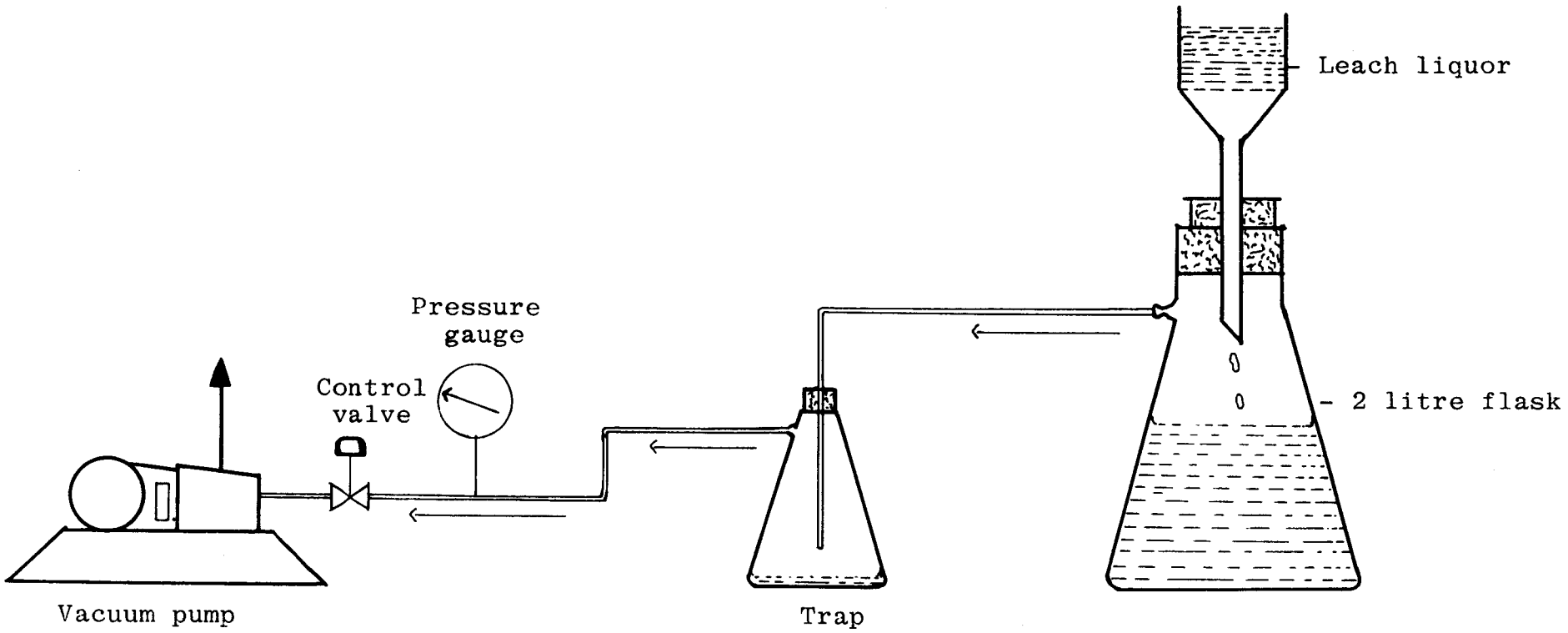


Figure 7. Flowsheet for filtration of leach liquor

slurry attacks ordinary filter papers. Thus the filter papers of glass microfibre filters type GF/A (Whatmann, size 9) were used throughout the solid-liquid separation work.

The operating vacuum was measured using a 'gauge' and a reading of 20.02 - 25.40 cm. of mercury was maintained during the filtration. Under these operating conditons a filtration rate of 15.62ml. per minute was achieved. However, the filtration rate can be increased by several fold if the temperature of the leach slurry is raised to approximately $50^{o}C$.

Leaching parameters such as concentration of sodium-hydroxide, temperature and dissolution time were studied with small scale tests carried out under atmospheric pressure. The tests were carried out in a 250ml. 'pyrex' beaker. A weighed quantity of the dust sample was dispersed in a vigorously stirred excess caustic solution. The stirring rate and the heating were provided by the thermostatically controlled hot plate/magnetic stirrer (supplied by Griffin and George, Ltd.). The solid - liquid ratio of 1:4 was maintained throughout the tests and a 3.0mL sample was taken at regular 10 or 20 minute intervals. The degree of dissolution of lead and zinc was measured by analysing the samples by atomic absorption spectrophotometer.

## 5.4 EXPERIMENTAL PROCEDURE

The study of cementation of lead consists of batch and continuous systems using zinc as a precipitant surface.

### 5.4.1 Batch Cementation

In each experiment the surface of the disc to be used was prepared in the following manner.

(1) the machined surface of the disc was treated with 5.0% (w/v) $H_2SO_4$ for 5 - 8 minutes to dissolve any zinc oxide layer formed.

(2) then the disc was polished with fine wet emery paper (grade 4/o).

(3) finally the disc was rinsed with excess de-ionised water to remove any impurities present.

Each batch experiment was carried out using 1500ml. solution. The solution was equilibrated at the appropriate temperature by immersing the cementation cell in the water bath. The temperature of the water bath was thermostatically controlled. When the desired temperature of the solution was reached the dry zinc disc was transferred to the cementation cell. Only the flat circular face of the disc was exposed to the solution under investigation. The disc was mounted at a distance of 5.0cm. from the base of the cementation cell. The disc was spun at a pre-selected speed by the variable speed motor for

approximately three hours. The rotational speed of the disc was measured using a tachometer. The temperature of the liquid was measured accurately with a laboratory thermometer whose scale ranged from 5 to 100°C with each division equal to 0.5°C.

The progress of the lead cementation onto the zinc surface was followed by withdrawing a 1.0ml. sample at regular 20 minute intervals. The samples were neutralised with 2.3ml. of 5M.HCl. diluted with a standard pH solution of 2.5 and analysed by atomic absorption spectrophotometer for lead and zinc contents. The analytical procedures for lead and zinc measurements are given in Section 5.5.

### 5.4.1 Continuous Cementation

#### 5.4.1.1 Recirculation

Prior to the study of the continuous cementation process, attempts were made, using the constructed rig. (Figure 6 page 77) to follow the reaction kinetics on a semi-continuous basis. The advantage of this operation was in its ability to control packing and column temperature more accurately.

In each recirculation run a fixed volume of leach liquor (4 litres) was introduced to the feed vessel (F) and stirred. The liquid was pumped into the column at the selected flow rate, with valve C in a closed position while valve G was opened to allow the liquid to re-enter the feed

vessel. The liquid from the feed tank was recirculated until the solution in the column reached 45°C. Then the required number of packings were introduced into the column. The control of flow rates, temperature and cleaning of packings were carried out in the manner described in sections 4.3 - 4.8.

5.4.1.2 Continuous system

The equipment used for recirculation was modified. The major alteration was the incorporation of the make-up reservoir tank and the required tubing for the system.

The rate of lead separation from the alkaline leach solutions by continuous cementation was studied in a packed column. The parameters such as the effect of apparent mass transfer coefficient in the liquid phase on bed height, flow rates, initial solute ion concentrations and nature of deposit were investigated.

The flow of leach liquor from the feed vessel was heated by allowing the solution to flow through the pre-heater unit. This provides a constant temperature of $45 \pm 0.5$°C in the entire apparatus. The flow rate was measured from the flow meters. Each flow meter was graduated from 0 to 150mm. Prior to the series of experiments, each flow meter was calibrated using the feed solution. The calibration curve is shown in Figure 6.1 (page A.20).

Initially, the solution was recycled through the column by closing valve C and opening valve G as shown in Figure 6 (page 77). The circulation was maintained at the desired flow rate until the column thermometer indicated the operating temperature. When the solution had attained the required temperature, the valve C was opened while valve G was closed, so that the outlet stream from the column could be collected in the container R. Immediately the required number of packings were introduced from the top of the column, until the column was filled to a mark which indicated the working height. Because of the nature of the random packing there were some difficulties in reading the exact height. The height of the packing ranged from 7.5cm. to 43.0cm.

The outlet concentration of lead and zinc ions from the bed was determined from 1.0ml. samples taken at 10 minute intervals. The samples were then prepared for analysis as described in the section below, and the concentrations of the metal ions were determined by atomic absorption spectrophotometer.

At the end of each run the entire equipment was flushed with tap water followed by de-ionised water.

## 5.5 ANALYTICAL PROCEDURE

The samples obtained from the cementation experiments were analysed for their lead and zinc ions using Atomic Absorption Spectrophotometry. This is an effective instru-

mental technique for metal level estimations. Most metal ions can be detected at trace levels even in the presence of much higher concentrations of other elements. The technique is also so specific that chemical separations are rarely necessary.(88)

The major components of an atomic absorption spectophotometer are as follows

(1) a light source, emitting the sharp resonance line of the element to be determined. This is usually a hollow cathode lamp made of the element to be determined;

(2) a flame system (air-acetylene or air-nitrous oxide) which provides sufficient temperature to generate atomic vapour when the solution is aspirated;

(3) a monochromator which isolates the resonance and focuses it upon a photomultiplier;

(4) a photomultiplier which detects the intensity of light energy falling on it.

The emission from the lamp is modulated so that its radiation only, and not that emitted from the flame, is recorded in the galvanised signal.

The technique is accurate, reproducible and rapid. In order to produce constant, reliable results, the mechanical,

optical and electronic conditions are maintained in proper working conditions.[89] Prior to any analysis a meter is adjusted to read zero absorbance and 100% transmittance when a blank solution is atomised in the flame system. During the atomisation of a solution containing the element to be detected, part of the light is absorbed, thus reducing the light intensity falling on the photomultiplier. This produces a deflection of the meter results.

Using standard solutions of the element to be determined, a calibration curve is constructed from which the concentration of the metal in the sample solution can be estimated.

The standards used in the analysis were prepared to resemble chemically the samples taken from the cementation experiments. Working standards of lead concentrations 5, 10, 20, 30 and 40ppm. were prepared by dissolving accurately weighed amounts of lead-nitrate salt - Analar grade (BDH - supplied) in 100ml. of sodium hydroxide solution of concentration 400gm/l. The weight of lead nitrate used in making the master stock solution ranged from 0.0799gm. to 0.6394gm., which resulted in lead concentrations of 500ppm. and 4000ppm. respectively. The fresh working standards were obtained by diluting the master stock solution by 100 fold in each case using a standard pH 2.5 solution.

The following dilution procedures were involved for both samples and working standards:

(1) 1.0ml of each solution was transferred to a 100ml. volumetric flask using a clean 1.0ml pipette.

(2) each 1.0ml.aliquot of the solution was then neutralised with 2.30ml of 5M.HCl.

(3) finally, each flask was made up to the 100ml. mark with the pH 2.5 stock solution

5.5.1 Lead Analysis

The diluted samples were analysed for their lead ions by an atomic absorption spectrophotometer Varian-Techtron - model 1100.

When a solution containing a metallic species is aspirated into a flame (air-acetylene) an atomic vapour of the metal is formed. Some of the metal atoms are raised to an energy level sufficiently high to emit the characteristic radiation of the particular metal. These atoms of the particular element can receive light of their own specific wavelength. Therefore, if light of this wavelength is passed through a flame containing the atoms of the element, a percentage of that light will be absorbed.[86] The absorption is proportional to the density of the atoms in the flame. The above principle is exploited in the design of the instruments.

Figure 8 shows the major components of the instrument. Using the set of working standards of lead solutions a calibration curve was obtained as shown in Figure 8.1 The operating instrument conditions (fixed) for lead were as follows:-

| | | |
|---|---|---|
| Lamp current | : | 6 mA |
| Fuel | : | acetylene |
| Support | : | air |
| Flame stoichiometry | : | oxidising |

The lead ions can be measured at two wavelengths

(1) at 217/nm and spectral band pass 1.0 for optimum working concentration range of 5 - 20 µg/ml (sensitivity 0.11 µg/ml; and

(2) at 283.3 nm and spectral band pass 0.2 for optimum working concentration of range of 10 - 40 µg/ml. (sensitivity 0.23 µg/ml).

In obtaining the calibration curve for lead from the working standards, each absorbance value for its concentration was a mean worked out from several repeated readings. It is important in cases where the sample solutions contain excess sodium that the working standards are prepared to match the compositions of the test samples as regards sodium content.

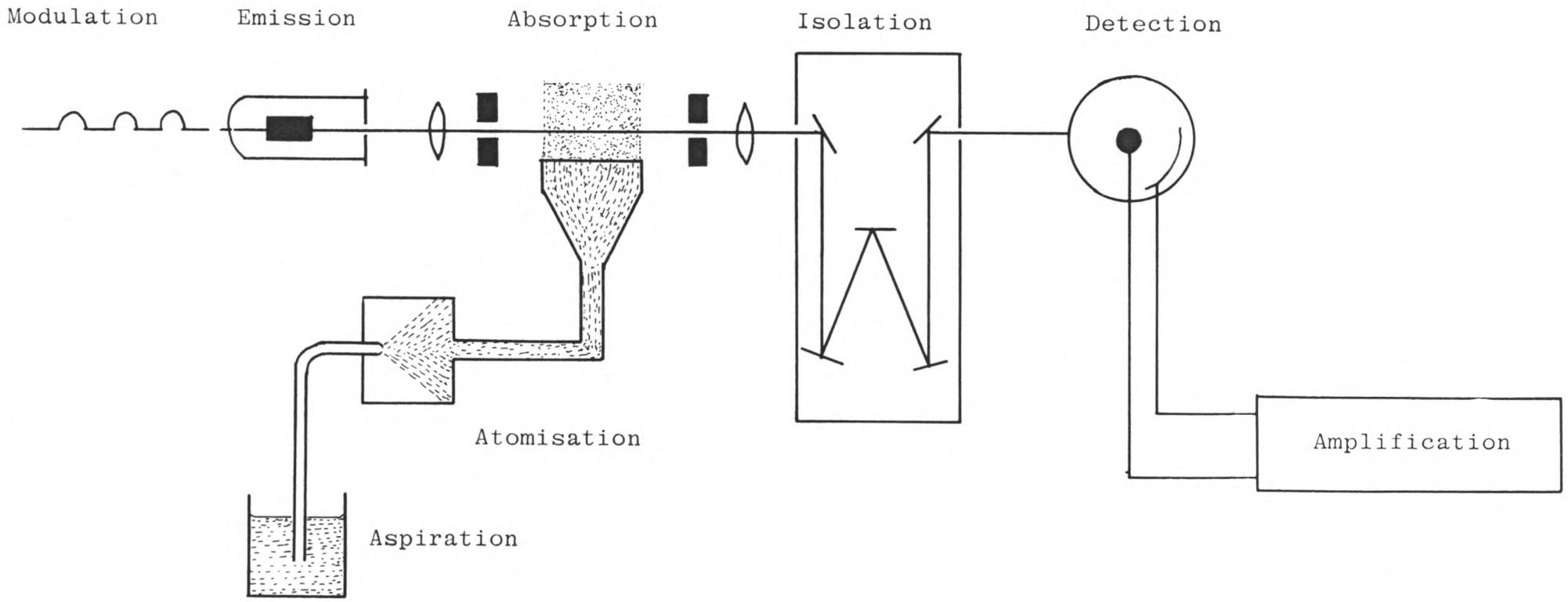


Figure 8 Atomic Absorption Spectrophotometer

### 5.5.2 Zinc Analysis

The determination of zinc by the atomic absorption spectrophotometer was comparatively easy. The presence of a large excess of many other metals in the solution did not affect the zinc response.[88]

The working standards for zinc of concentration 0.5, 1.0, 1.5 and 2.0ppm were freshly prepared from a standard stock solution. Initially an intermediate standard solution of 100ppm. of zinc was prepared from standard stock solution using the pH 2.5 solution as the diluent. The working standards of zinc solutions were prepared from this by further dilutions. The calibration curve obtained is shown in Figure 8.2.

Unlike in lead analysis, the sample for zinc analysis required a further 100 fold dilutions.

The solubilities of both lead and zinc indicated[88] that a pH of 2.5 in the final solution was suitable for accurate measurements in aqueous solutions. If pH was not duly controlled during the sample preparation, it could lead to erroneous results. For pH range 4.5 - 9.0 lead and zinc tended to form white colloidal precipitants, which had to be avoided at all times. Therefore, a stock solution of pH 2.5 was made up using de-ionised water and concentrated hydrochloric acid (approx. 1.75ml/litre). A fresh solution of this was used throughout the dilutions of samples and standards.

# C H A P T E R  S I X

## INTERPRETATION OF DATA

### 6.1 MECHANISM OF CEMENTATION PROCESS

The process of cementation is regarded as electrochemical reactions. The overall cementation reactions can be summarised by the equation

$$nM^{m+} + mN \rightarrow nM + mN^{n+} \qquad (29)$$

where M is the noble metal which reacts with the more electropositive metal N to form precipitation. This is a heterogeneous reaction in which the ions of the precipitating metal are reduced to zero valence at a solid surface (cathodic) while the dissolving metal is ionised and enters the solution from separate (anodic) areas. Thus it involves the reduction of a more noble species(M).

$$M^{m+} + m\bar{e} \rightarrow M \qquad (30)$$

and the oxidation of the less noble species (N)

$$N \rightarrow N^{n+} + n\bar{e} \qquad (31)$$

This makes cementation process essentially a redox reaction. The oxidation and reduction reactions do not occur at the same locality, instead the oxidation transfer electrons to site where reduction reaction occurs.

Cementation process is known to occur in several steps and the possible steps can be represented by a schematic diagram as shown in Figure 9.

The possible steps are

1. Transport of the depositing ion ($M^{m+}$) to the surface from the bulk of the solution

2. Electron transfer to the depositing ions by the conductance of electrons from the precipitant metal through the deposit.

3. Adsorption of M ions.

4. Dissolution of $N^{n+}$ ions into the solution possibly from sites where electron transfer initiated step 2.

5. Transfer of $N^{n+}$ ions to the deposit-solution interface

6. Transport of $N^{n+}$ ions into the bulk of the solution

The overall cementation reaction will depend on all six steps mentioned above. In most cementation reaction steps 1 and 6 are slow, hence rate controlling. Since these two steps involve transportation of components the reaction can be termed diffusion controlled. If steps other than these two are slow it can be said to be chemically controlled.

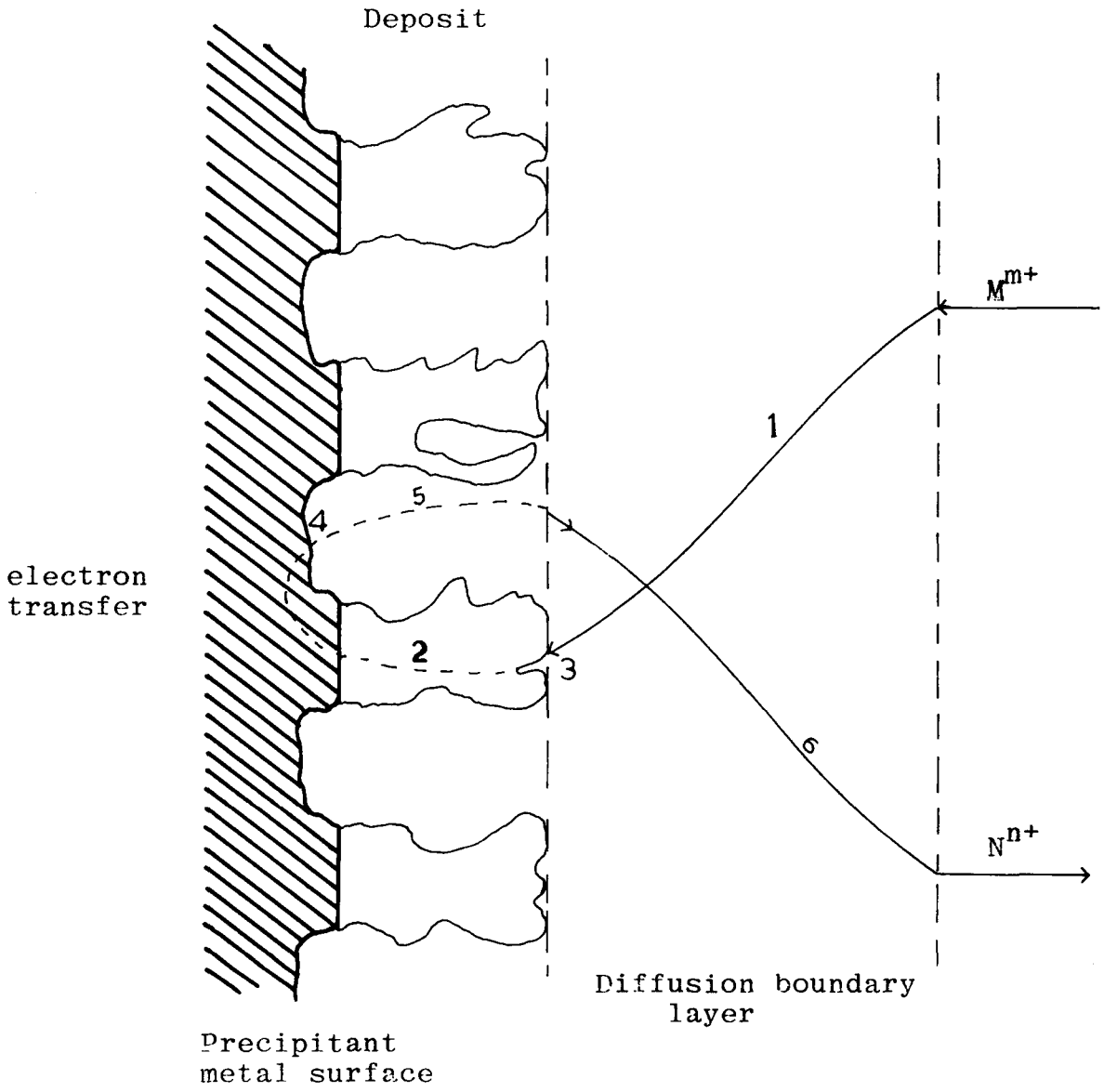


Figure 9. A schematic diagram of the cementation process

## 6.2 TYPES OF REACTIONS

Most cementation process are classified either as chemical controlled or as diffusion controlled reactions. The rate equation for chemical controlled reactions can be described as

$$\frac{dC}{dt} = k_c S \left[C_o\right]^n \qquad (32)$$

where $k_c$ is the rate constant, $C_o$ is the concentration of solute, S is the surface area and n is the order of reaction.

When the rate of chemical reaction at the surface is very much faster than the rate of diffusion of solute ions to the surface (or the diffusion of product ions from the surface) the overall process becomes diffusion controlled. The rate of mass transfer due to diffusion can be written as

$$J = k_T S (C_o - C_i) \qquad (33)$$

where $J$ = mass flux

$k_T$ = rate constant for diffusion

$C_o$ = bulk concentration of reactant cation

$C_i$ = surface concentration of reactant cation

If both diffusion and chemical reaction are prominent, the process is of intermediate type.

The following equations are obtained for diffusion through a boundary layer and for a first order reaction.

since $J = \frac{dC}{dt}$ and combination of equations (32) and (33) gives

$$k_T S\ (C_o - C_i) = k_c S\ (C_i)$$

from the above equation, the solute concentration at the interface can be derived as

$$C_i = \frac{k_T \quad C_o}{k_c + k_T}$$

and the rate becomes

$$\frac{dC}{dt} = \frac{k_c \cdot k_T}{k_c + k_T} S\ C_o$$

## 6.3 BATCH CEMENTATION

The experimental data obtained in the batch cementation studies are treated with the following equations. In cementation processes if diffusion mechanism is the rate determining step, first order kinetic behaviour is expected, and the rate equation can be written as

$$j = k\ C_B \qquad (34)$$

where $j$ = apparent mass flux based on the initial exposed precipitant area

$k$ = apparent mass transfer coefficient or rate constant

A material balance on the batch system gives

$$j = \frac{dm}{dt} \qquad (35)$$

where $m$ = mass of deposit at time t per unit area

$$\frac{d(V\ C_B)}{dt} = -S\frac{dm}{dt} + C_B\frac{dV}{dt} \qquad (36)$$

and $$\frac{dm}{dt} = -\frac{1}{S}\left[\frac{d(V\ C_B)}{dt} - C_B\ \frac{dV}{dt}\right]$$

where $V$ = volume of solution at time t

$C_B$ = bulk concentration of reactant ion at time t

For a first order reaction and constant volume equation (36) becomes

$$-\ S\ k\ C_B = \cancel{\frac{dV}{dt}}\ C_B + V\ \frac{dC_B}{dt} - \cancel{\frac{dV}{dt}}\ C_B$$

i.e. $$-\ S\ K\ C_B = V\ \frac{dC_B}{dt} \qquad (37)$$

Rearranging and integrating this equation for a constant specific rate gives

$$-\int_{C_o}^{C_B}\frac{dC_B}{C_B} = kS\int_{O}^{t}\frac{dt}{V}$$

$$\ln\left[\frac{C_o}{C_B}\right] = kS\int_{o}^{t}\frac{dt}{V} \qquad (38)$$

Assuming the constant volume for the solution the equation (38) can be written as

$$2.303\ V \log \left[ \frac{C_o}{C_t} \right] = kSt \qquad (39)$$

Equation (39) is used to present the results of batch cementation.

## 6.4 CONTINUOUS CEMENTATION

The mechanism of the cementation process is diagramatically illustrated in Figure 9. For a given point in solution, the velocity components parallel to the x, y and z are $u_x$, $u_y$ and $u_z$ respectively. The rate of change of concentration at that point is given by the equation of continuity.

$$\frac{\partial C_A}{\partial t} + \left(u_x \frac{\partial C_A}{\partial x} + u_y \frac{\partial C_A}{\partial y} + u_z \frac{\partial C_A}{\partial z}\right)$$

$$= D \left(\frac{\partial^2 C_A}{\partial x^2} + \frac{\partial^2 C_A}{\partial y^2} + \frac{\partial^2 C_A}{\partial z^2}\right) + R_A$$

where $\frac{\partial C_A}{\partial t}$ is the sum of the rate of change due to diffusion and convection and for steady state condition $\frac{\partial C}{\partial t} = 0$ and $R_A$ is the rate of disappearance of A.

Considering the diffusion in the axial direction and for fluid velocity to be constant in x, y co-ordinates, the above equation reduces to the form.

$$\frac{\partial C_A}{\partial t} + u_z \frac{\partial C_A}{\partial z} = D \frac{\partial^2 C_A}{\partial z^2} + R_A$$

In this equation the term containing the second order differential can be neglected as the change of $\frac{\partial c}{\partial z}$ with respect to z is negligible. Therefore the equation becomes

$$u_z \frac{dc}{dz} = R_A$$

Considering the surface reaction and the diffusion process based on film theory, a $Pb^{++}$ balance for a first order reaction gives

$$u_z \frac{dc}{dz} = k_\ell a(C - C_S) = k_c C_S \qquad (40)$$

The concentration of lead ions ($C_S$) at the stagnant film interface can be defined from the rate equations

$$k_\ell a (C - C_S) = k_c C_S$$

$$C_S = \frac{k_\ell a C}{k_\ell a + k_c}$$

substituting $C_S$ into equation (40)

and $u_z = u_i$ (measured interstitial velocity)

$$u_i \frac{dc}{dz} = k_c \frac{k_\ell a C}{k_\ell a + k_c}$$

which on integration for the following boundary condition

when $z = O \qquad C = C_{in}$

$z = L \qquad C = C_{out}$

$$\int_{C_{in}}^{C_{out}} \frac{dc}{C} = \frac{k_c \, k_\ell a}{k_\ell a + k_c} \int_{o}^{L} \frac{dz}{u_i}$$

Since $C_{in} > C_{out}$

$$\frac{C_{out}}{C_{in}} = \exp \left[ - k_\ell a \times \frac{L}{u_i} \times \frac{k_c}{k_\ell a + k_c} \right] \qquad (41)$$

For conditions where the rate of surface reaction is much faster than the rate of diffusion $k_c >> k_\ell$ then equation (41) becomes

$$\frac{C_{out}}{C_{in}} = \exp \left( -k_\ell a \times L/u_i \right)$$

which can be written as

$$\text{i.e.} \quad \ln \frac{C_{in}}{C_{out}} = k_l a \times \frac{L}{u_i} \qquad (42)$$

From this equation the apparent mass transfer coefficient ($k_\ell$) can be calculated from the known experimental values of dimensionless concentration, effective interfacial area, bed height and the interstitial velocity.

## 6.5 CORRELATION OF MASS TRANSFER COEFFICIENT

The apparent mass transfer coefficient calculated using equation (42) can be transformed into a dimensionless $j_D$ factor, which is defined by the equation

$$j_D = \frac{k_\ell}{u_i} \times Sc^{\frac{2}{3}}$$

The $k_\ell$ value determined for varying flow rates is correlated with a modified Reynolds number defined by

$$Re' = \sqrt{Ap}\,\frac{G}{\mu}$$

The correlation between $j_D$ and Re' is compared with Carberry's model (84).

## 6.6 PRECIPITATION EFFICIENCY

From the equation developed for continuous cementation an equation for precipitation efficiency can be derived as follows from equation (42)

$$\text{i.e.} \quad \frac{C_o}{C_t} = e^{(k_\ell a \frac{L}{u})} \qquad (43)$$

If $k_\ell a \frac{L}{u} = x$

equation (43) can be written as

$$\frac{C_t}{C_o} = e^{-x}$$

$$(e^{-x} - 1) = \frac{C_t - C_o}{C_o}$$

Since, precipitation efficiency (E) $= \frac{C_o - C_t}{C_o}$

$$E = 1 - \frac{1}{e^x}$$

$$\therefore \quad \frac{C_o - C_t}{C_o} = 1 - \frac{1}{e^{k_\ell a \frac{L}{u}}} \qquad (44)$$

# C H A P T E R  S E V E N

## RESULTS AND DISCUSSION

### 7.1. LEACHING

The extraction of metal contents from the e.a.f. dusts was studied by the hydrometallurgical process of leaching using sodium-hydroxide as the solvent. The degree of extraction was investigated for the following parameters; caustic concentration, temperature, leaching time and solid-liquid ratio.

#### 7.1.1. Effect of Caustic Concentration

The effect of caustic concentration on the degree of dissolution of lead and zinc expressed as percentage recovery is shown in Figures 10 and 11. This was studied for caustic concentration ranging from 100 to 400 gm/l at temperatures of 25°C and 60°C.

It is seen from Figures 10 and 11 that the recovery of lead was always higher than zinc for all caustic concentrations. For concentrations up to 200 gm/l, the percentage recovery of lead gradually increased to reach a maximum value around 90% (Figure 10). The extraction of zinc for the same leaching condition was seen to increase only on a limited scale for concentration up to 400 gm/l where a maximum recovery of 55% was obtained. The results compare favourably with those reported by Merrill and Lang[34] for the leaching of lead and zinc ores.

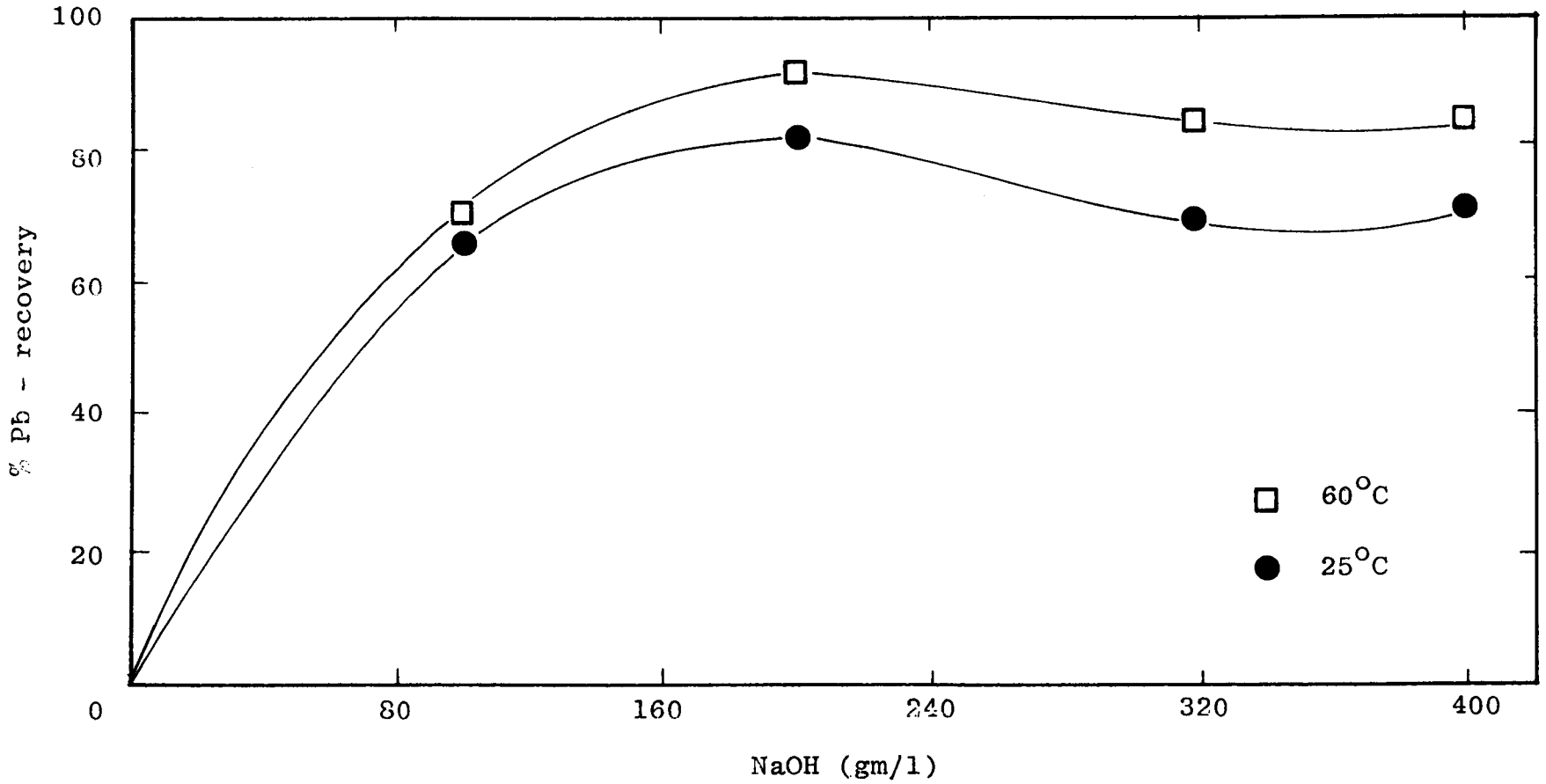


Figure 10. Percentage recovery of lead with varying caustic concentrations. Solid-liquid ratio 1:4

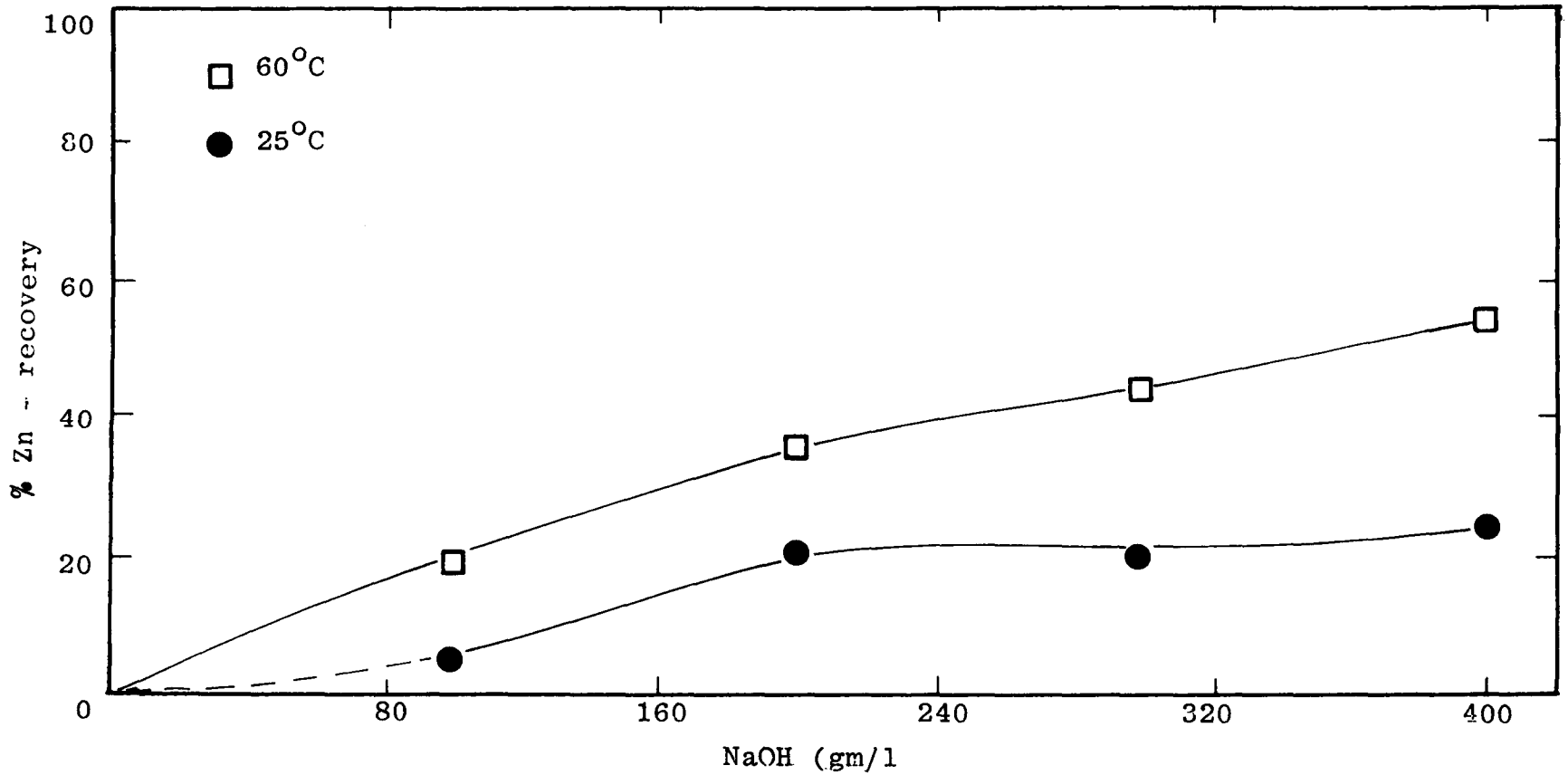


Figure 11. Percentage recovery of zinc with varying caustic concentrations. Solid-liquid ratio 1:4.

The results indicated that a maximum yield of lead and zinc from the e.a.f. dusts can be achieved for caustic concentration in the region of 400 gm/l. One of the factors which seemed to control the degree of dissolution of metals from the e.a.f. dust leaching was the chemical behaviour of lead and zinc. A brief description of the chemical reaction involved in the leaching of the dusts is given below.

When oxides of lead and zinc are treated with caustic solution, the products in solutions are often referred to as soluble plumbates and zincates respectively. The chemical reactions involved in the leaching of e.a.f. dusts can be stated in stoichiometric terms as:-

$$PbO_{(s)} + 2NaOH \rightarrow Na_2PbO_2 + H_2O$$

$$2NaOH + ZnO \rightarrow Na_2ZnO_2 + H_2O$$

The presence of an excess amount of caustic solution is essential for the above reactions. The exact form of the oxides of lead and zinc in the e.a.f. dusts are difficult to determine. The general behaviour of lead and zinc is expected to be somewhat similar.

A comparatively low extraction of zinc during the leaching can be explained as due to the presence of some of the zinc as zinc silicates. Usually zinc oxide combines with silica to form a zinc silicate mineral. The chemical form of

of this mineral is not established in the present study. However, all zinc silicates are difficult to dissolve due to the strong chemical bond that exists between the silica and zinc.[32]

The X-ray diffraction analysis of the dust sample indicated the presence of some silicates besides the zinc oxides. Therefore the degree of dissolution of zinc seemed to be dependent not only on the leaching conditions but also on their chemical form. Leaching carried out at elevated temperatures could favour the breaking down of the zinc silicate bonds.

### 7.1.2. Leaching Time

The rate of extraction of lead and zinc from the e.a.f. dusts are shown in Figures 12, 13 and 14. As shown in Figures 12 and 13 a leaching time of approximately 80 minutes resulted in about 32% zinc and 81.50% of lead. The extraction of the metals indicated a gradual upward trend as leaching time was increased from 10 minutes to 2 hours, after which the percentage extraction remained practically constant. However, the recovery of lead as shown in Figure 13 gave a sharp increase in the rate of extraction and then reached a value of 80% at a leaching time of 40 minutes. The extraction of lead with caustic concentration of 100gm/l showed that a leaching time as short as 10 minutes was sufficient to extract about 75% of the lead.

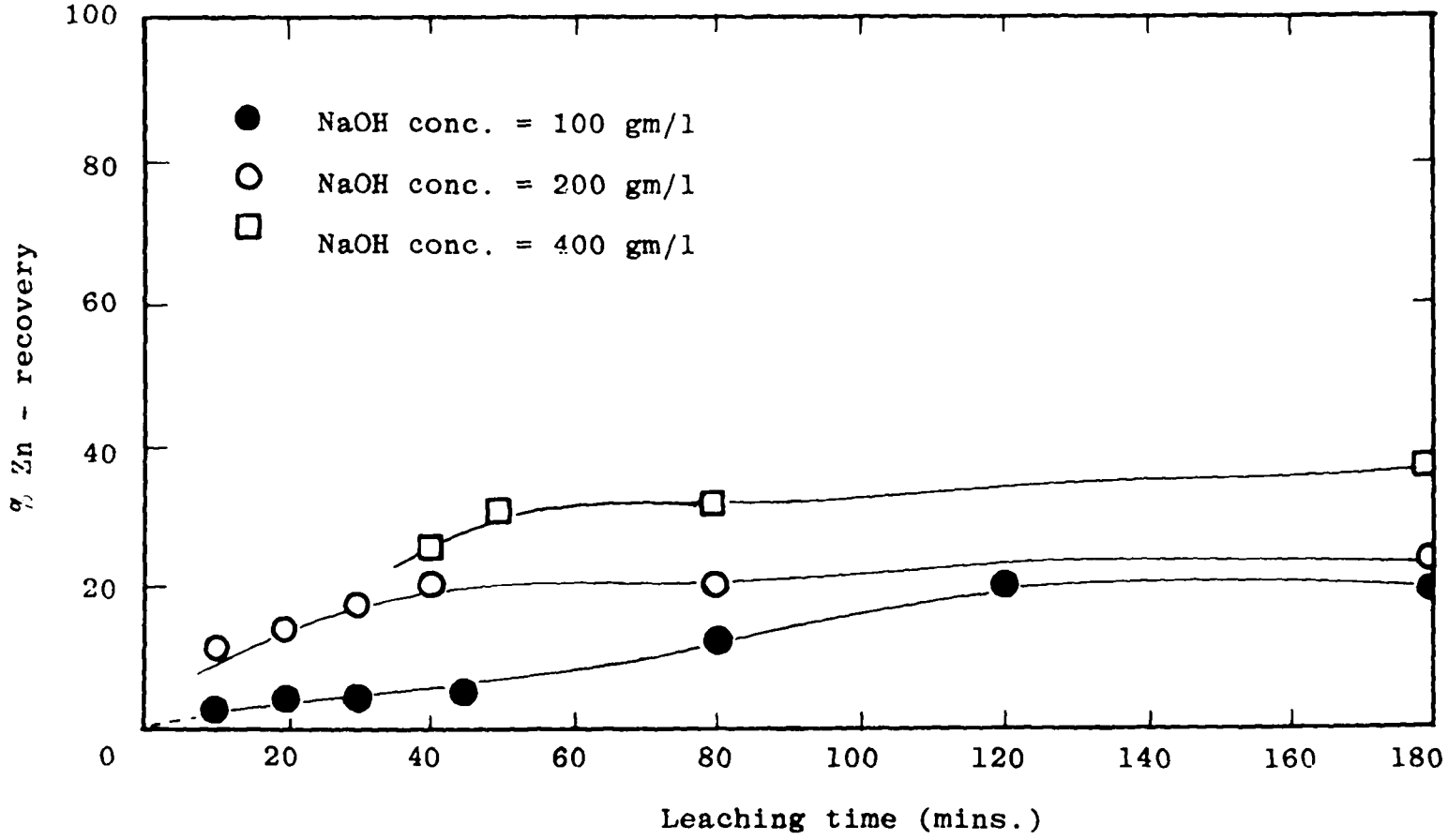


Figure 12. Extraction of zinc with different leaching time. Temperature 25°C, solid-liquid ratio = 1:4.

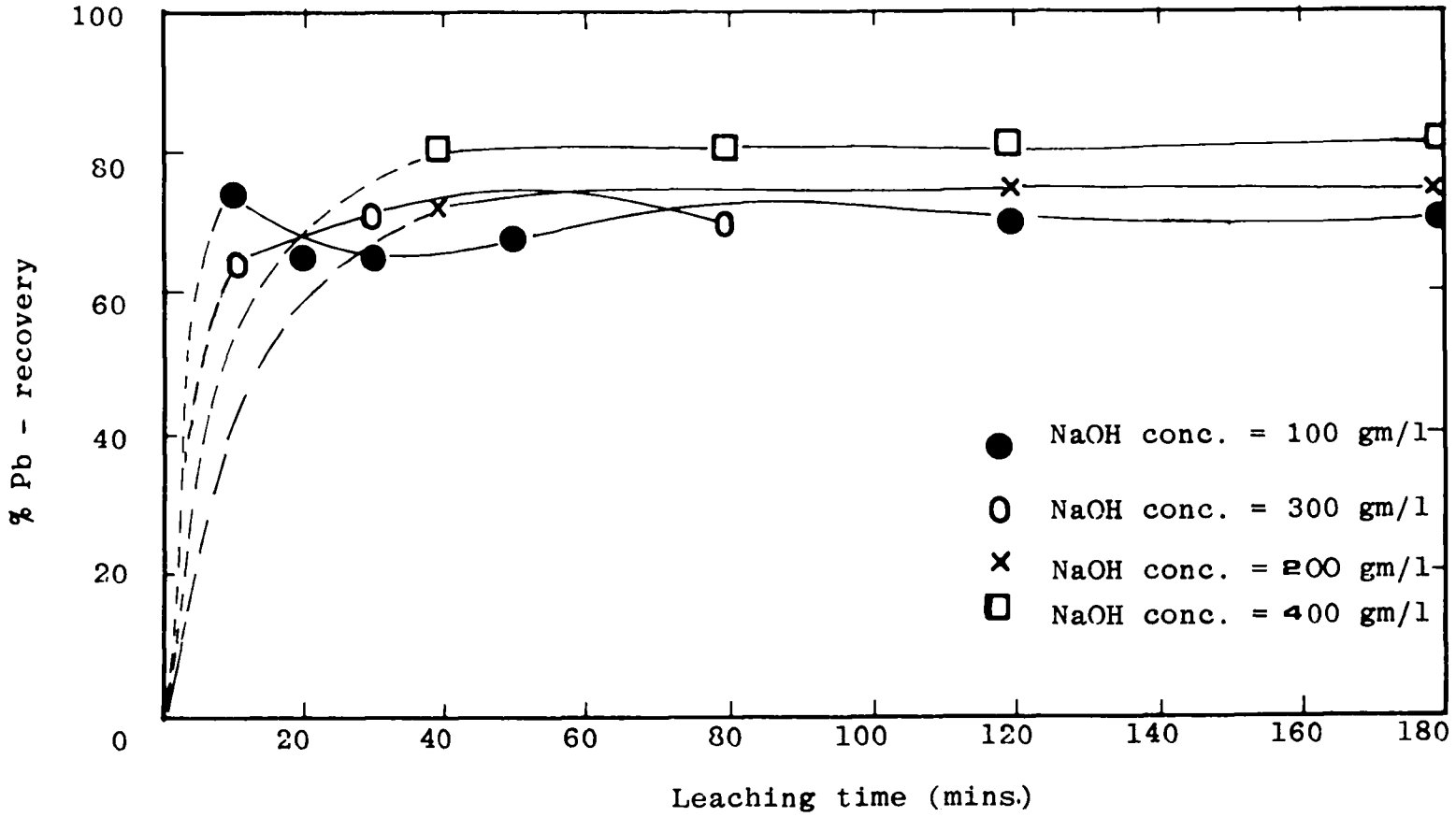


Figure 13. Extraction of Lead with different leaching times. Temperature = 25°C. Solid-liquid ratio = 1 : 4.

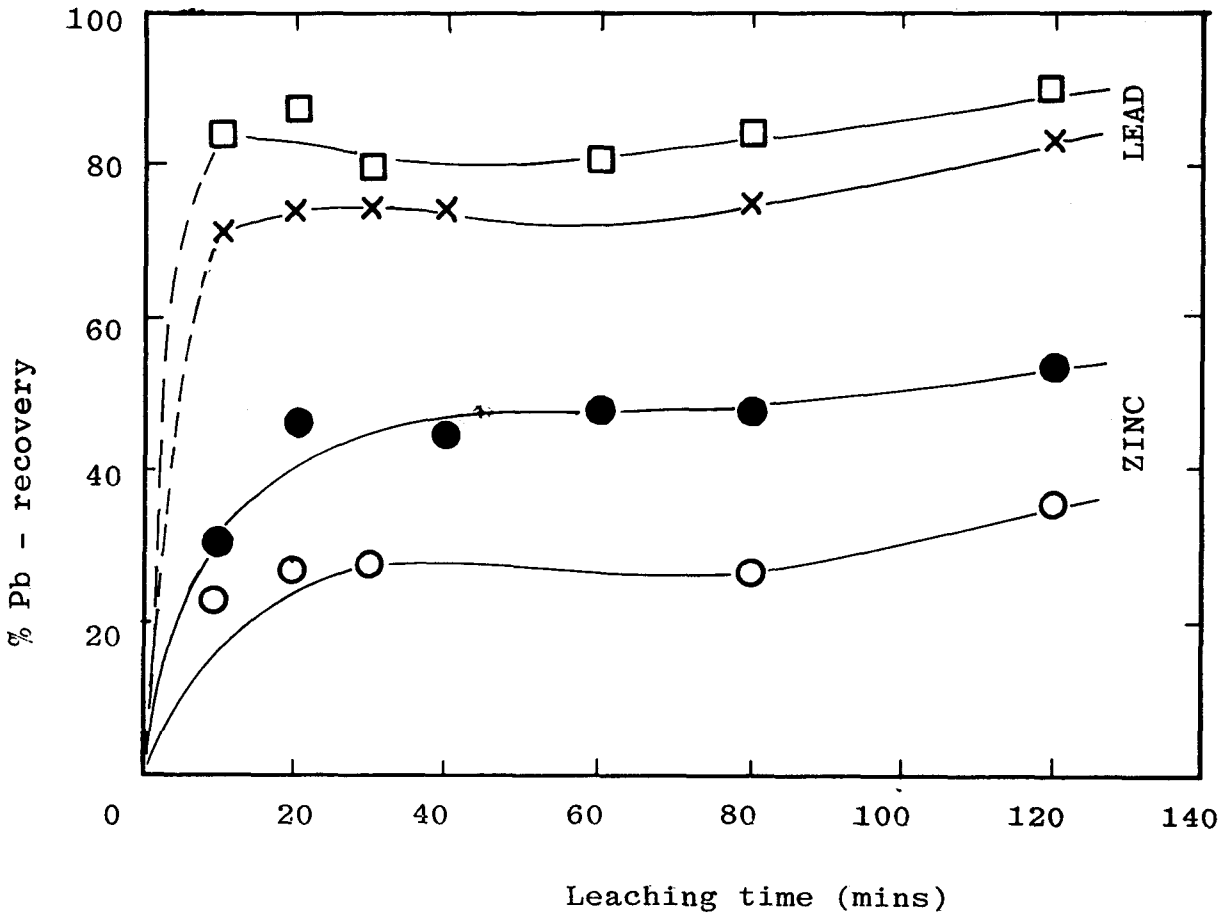


Figure 14. Percentage Lead and Zinc recoveries at 60°C. Solid-liquid ratio 1:4.

The effect of leaching time on the percentage recovery of the metals at 60°C is shown in Figure 14. The result indicated significant reduction in leaching time for both metals. It also shows that for a leaching time of 20 minutes, the recoveries of lead and zinc were in the region of 85% and 40% respectively.

The above investigation shows that the leaching time was dependent on the strength of the caustic solution used and the other leaching conditions. A short leaching time could be used with strong caustic solution (>200 gm/l) at temperatures above 25°C.

### 7.1.3. Effect of Temperature

The study of the effect of temperature on the metal recovery was carried out at temperatures of 25°C and 60°C. The results expressed as percentage recovery can be seen in Figures 12, 13 and 14. The results show a characteristically high lead recovery even at ambient temperature, irrespective of caustic concentrations used. This can be seen in Figure 13 which shows that the lead recovery rapidly reached a constant value in the range of 70 - 80%. The recovery of zinc at this temperature was about 34%.

Leaching at ambient temperature was encouraging for the lead recovery, but the level of zinc extraction remained comparatively low (about 34%). Leaching processes carried out at higher temperatures are preferred in industrial operations

and it is expected to improve the solute contents in the final leach liquor. The results of leaching of e.a.f. dusts at 60°C are shown in Figure 14. As the figure indicates, the leaching at this temperature resulted in recoveries of both lead and zinc, 90% and 54% respectively. On comparison with the metal extraction obtained at ambient temperature, the leaching at 60°C increased the lead recovery marginally by 10% whereas the zinc recovery was increased by 20%.

### 7.1.4 Effect of Solid-Liquid Ratio

The effect of solid-liquid ratio on the metal recovery from the e.a.f. dusts was studied with six large scale leaching tests. In each case, a total volume of five litres of slurry with a solid-liquid ratio ranging from 15% to 25% (w/v) was used. The recovery of lead and zinc for different solid-liquid ratios are shown in Figure 15. The dissolution of lead and zinc were determined for a leaching time of 40 minutes. For a solid-liquid ratio of 20% (w/v) the percentage recovery of lead and zinc from the dusts increased to a maximum value of 99% and 80% respectively. The yields decreased when the solid content was increased to 25% (w/v). Further increase in solid was not possible because the mixture became a thick viscous slurry.

Caustic leaching seemed to be quite effective for the extraction of lead and zinc from e.a.f. dusts. The optimum

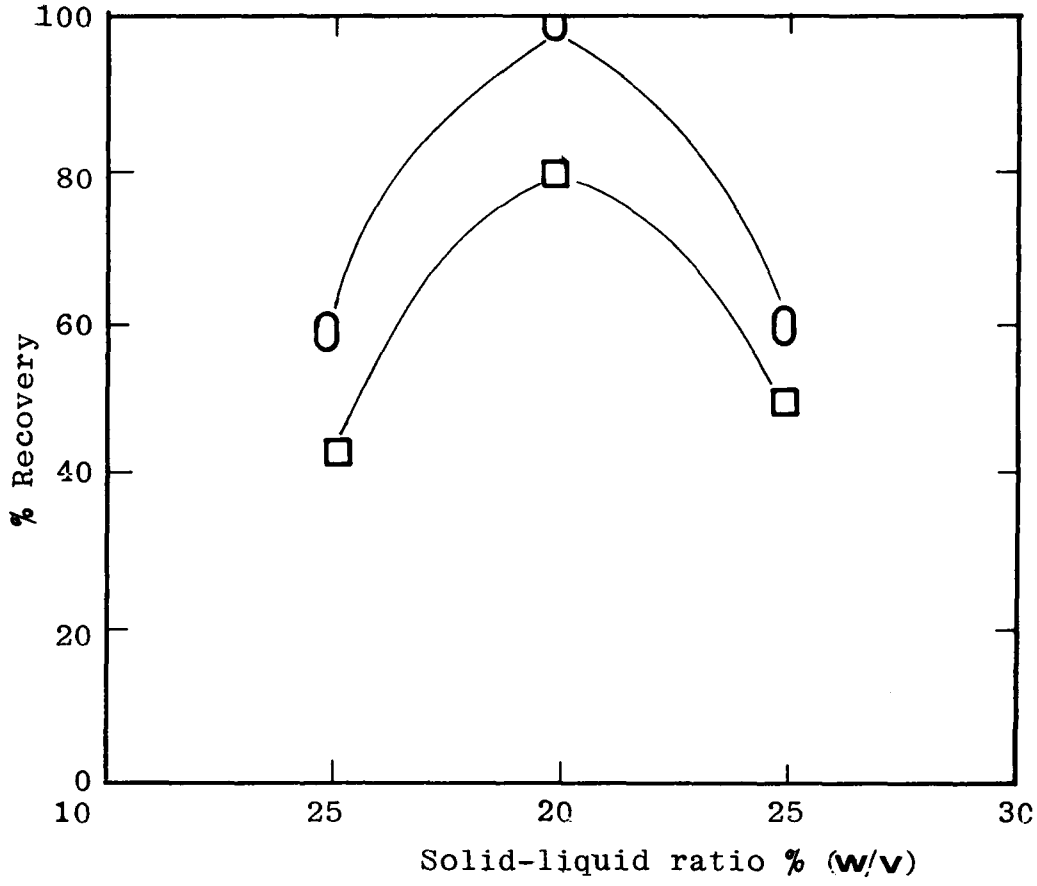


Figure 15. Relationship between solid liquid ratio and percentage recovery of metals from e.a.f. dust leaching: leaching time, 40 mins, temperature ~ 115°C

experimental conditions for obtaining the leach liquor with the highest lead and zinc can be summarised as follows:-

(i) caustic concentration around 400 gm/l dissolved .. the highest amount of zinc along with the entire lead content of the e.a.f. dusts.

(ii) atmospheric leaching at the boiling point ($\sim 115^{o}C$) gave the maximum yield of the metals in the leach liquor with a leaching time of approximately 40 minutes.

(iii) an optimum solid-liquid ratio of 20% (w/v) was found to yield the highest amount of lead and zinc in the final leach liquor.

## 7.2 BATCH CEMENTATION

The study of batch cementation consisted of two separate investigations

(i) with simulated system, and

(ii) with leach liquor of e.a.f. dusts

### 7.2.1. Studies with Simulated System

With the simulated system experiments were carried out to study the nature of lead cementation reaction on a zinc surface in the absence of other cations.

The effect of temperature and stirring speed on the rate of cementation was investigated. Solutions containing

3.60gm/l of lead ions in caustic strength of 400 gm/l were used.

The order of cementation reaction was determined by measuring the lead concentration with time in a stirred solution kept at constant temperature. The data obtained were analysed according to kinetic equation 39. If the process of lead cementation can be represented by this equation, the data should fall on a straight line when 2.303 Log $(\frac{C_o}{C_t})$ V is plotted against time. Figure 16 shows such a plot, which indicates that experimental data falls on a straight line, supporting first order kinetics for the lead cementation.

7.2.1.1 Effect of Temperature

Several experiments were conducted to study the effect of temperature on the rate of cementation. It was also an attempt to confirm the type of rate control.

The kinetic data obtained for a series of runs at temperatures ranging from 22.50°C to 79°C are shown in Figure 17. The specific rate constant values (k) calculated for the experimental temperatures are shown in Table15. There are definite trends in the results. The value of k increases about six fold from a value of $0.822 \times 10^{-2}$cm.sec$^{-1}$ at 22.50°C to $4.98 \times 10^{-2}$cm.sec$^{-1}$ at 79°C.

The specific rate constants can be related to absolute temperature by Arrhenius equation

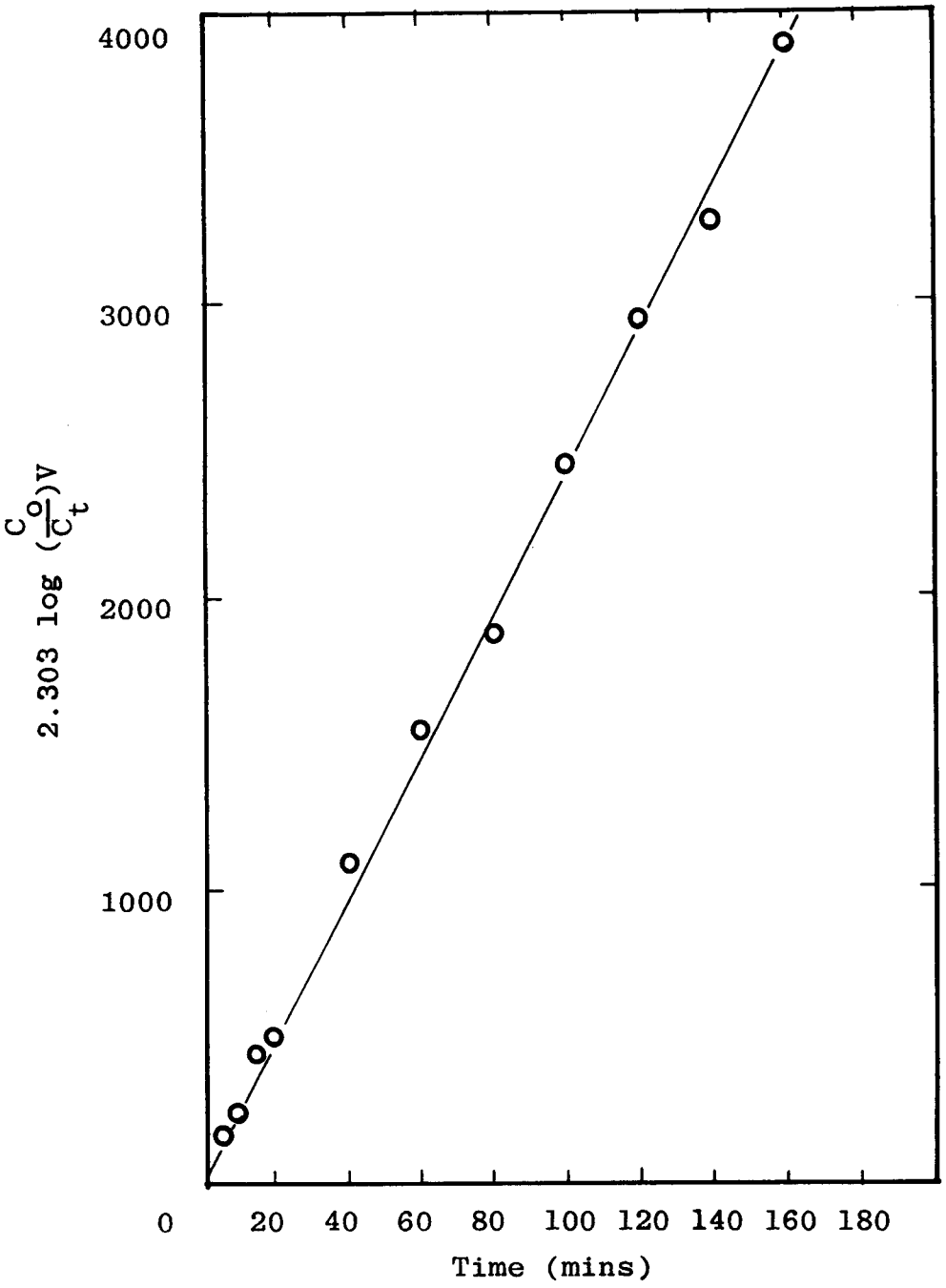


Figure 16. Kinetic plot of 2.303 log $(\frac{C_o}{C_t})V$ against time (mins) r.p.m. = 800, temperature = 45°C, $Pb^{++}$ conc. = 3.6 gm/l.

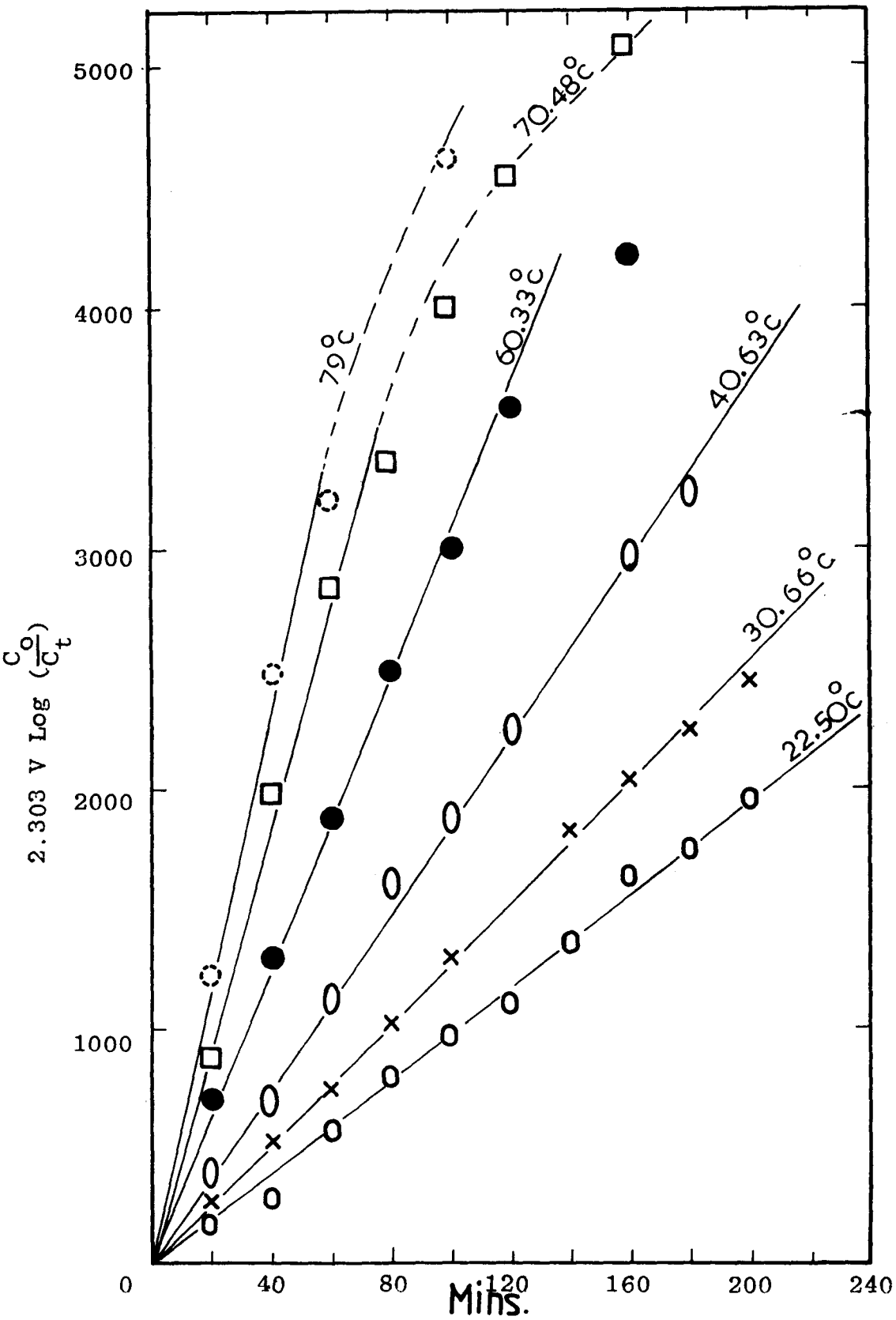


Figure 17 Cementation data at various temperatures for the simulated system: r.p.m. = 250, initial lead ion concentration = 3.60 gm/l

$$k = A \exp (E_a/RT)$$

where $E_a$ is the activation energy and the other symbols are as described in the nomenclature. If the controlling mechanism remains unchanged during the course of the reaction, the value of $E_a$ is constant. Then a plot of log k against $\frac{1}{T}$ (temperature in absolute scale) should result in a straight line, such a straight line is obtained as shown in Figure 18. The experimental data ggrees well with the theory. The slope of the straight line gives an activation energy ($E_a$) of 6.50 K cals/mole. A reaction with an apparent activation energy of this magnitude is an indication of a diffusion controlled reaction.

Ingraham and Kerby[52] reported an activation energy value of 4.0 K cals/mole for similar experimental conditions for the cementation of cadmium onto zinc. They suggested diffusion as the rate controlling step for their system. This was later confirmed by Lee et.al[50]. The value of $E_a$ obtained in the present study compares favourable with those values suggesting a diffusion controlled process.

7.2.1.2 Effect of Stirring Speed

A series of experiments in which the disc rotational speed ranged from 30 to 1600 r.p.m. was carried out, and the results are shown in Figure 19. The specific rate constant for each stirring speed was calculated from the slope of the straight lines obtained in this plot.

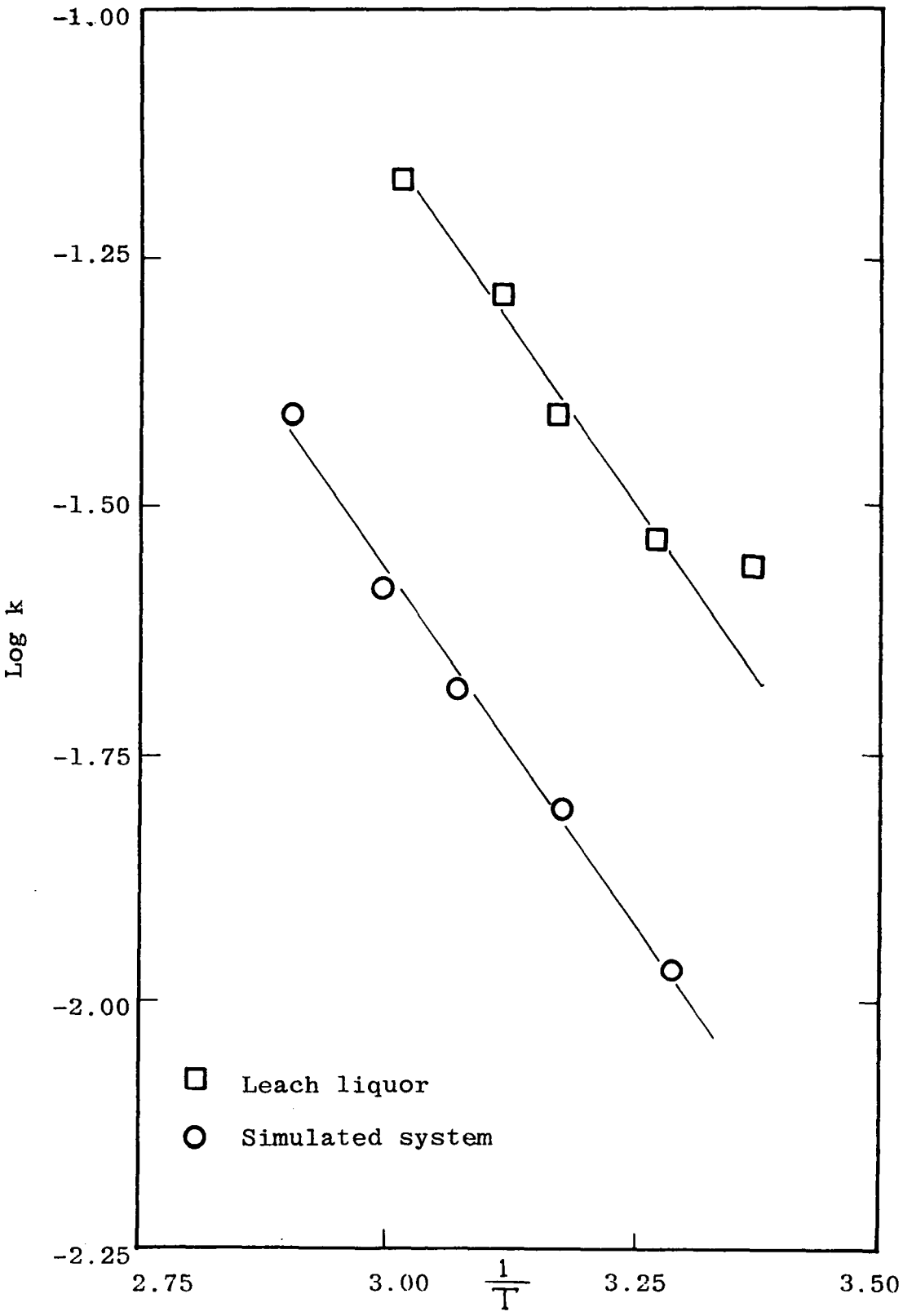


Figure 18 Arrhenius relationship for lead cementations.

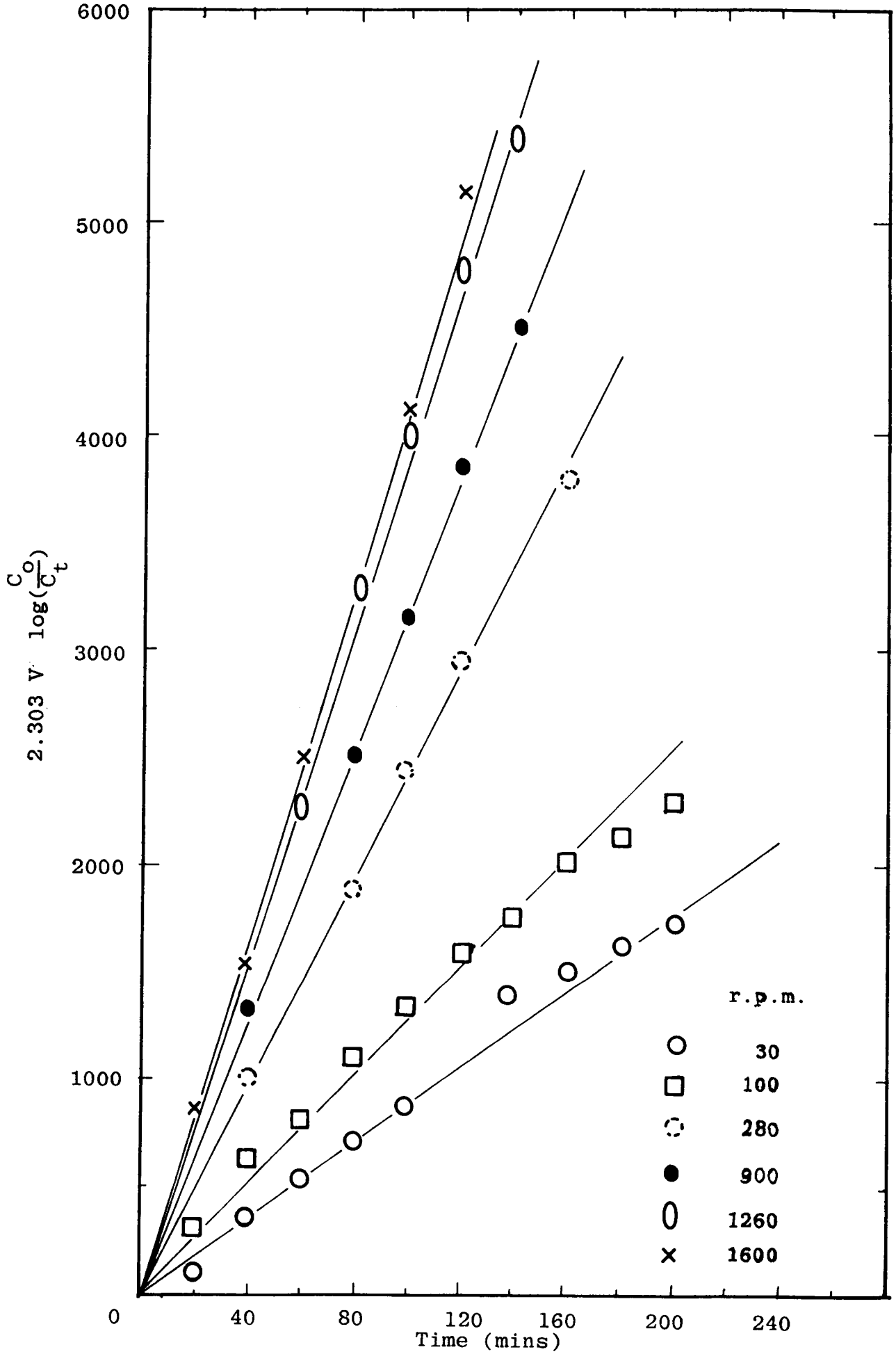


Figure 19. Cementation Data at different stirring speeds
Simulated system, temp.= 45°C, $Pb^{++}$ conc=3.60gm/l

A plot of the specific rate constant versus stirring speed is shown in Figure 20. Usually increase in specific rate constant with stirring speed is expected for any diffusion controlled process. In the above plot the specific rate constant increased with the stirring speed until a value of 1300 r.p.m. was reached. Further increase in stirring speed showed that the specific rate became independent of the stirring speed. The deviations observed at high stirring speed (> 1300 r.p.m.) could be explained as due to the diffusion boundary film formed on the surface of the disc.

The effective diffusion film thickness ($\delta$) could be calculated by

$$\delta = \frac{D.C_B}{j} = \frac{D}{k} \qquad (45)$$

According to Nerst's theory (24), the thickness of the film ($\delta$) varies with stirring speeds until a limiting value is reached. From the equation (45) the thickness of the diffusion layer could be calculated for any experimental conditions. The film thickness calculated in this work at 60°C was approximately 0.027mm., which was within the range of values given (0.020-0.039mm) for different systems by Bircumshaw and Riddiford[78]

The effect of stirring speed on the reaction rate could be analysed in the light of the Levich equation (15). According to this theory if a simple counterdiffusion process of Cations is the controlling step, then a linear relationship between the specific rate constant and the square root of the stirring speed is expected.

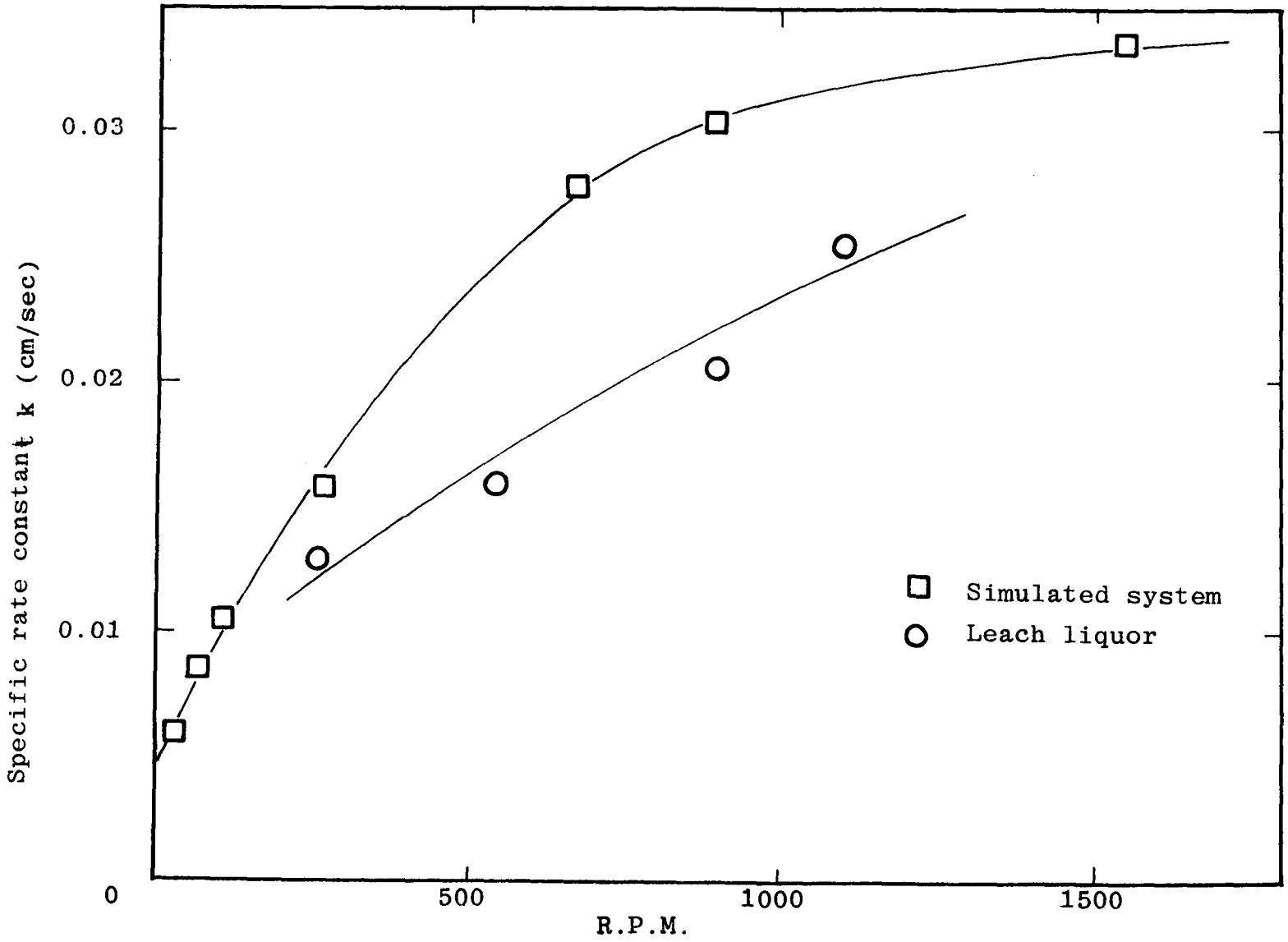


Figure 20 Relationship between specific rate constant and disc-rotation speeds : temperature=45°C.

Under conditions of laminar flow about a rotating disc, the steady state diffusion process could be described by the Levich equation as

$$k = 0.62\, D^{\frac{2}{3}}\, \upsilon^{-\frac{1}{6}} \omega^{\frac{1}{2}} \qquad (46)$$

According to the above equation a plot of the specific rate constant or apparent mass transfer coefficient (k) against the square root of the stirring speed ($\omega^{\frac{1}{2}}$) is shown in Figure 21. The experimental data shown in this figure are in good agreement with the Levich theory of diffusion.

Further evidence emerged when the k values calculated from the experimental data were compared with those predicted by the Levich equation. If the process is diffusion controlled, the two sets of k values should be equal. The results are presented in Table 7 for a range of stirring speeds used. The two sets of values are in very good agreement as expected for a diffusion controlled process.

7.2.1.3 Nature of Deposit

The deposits were rinsed with excess de-ionised water and dried in an over at 110$^{o}$C for 8 - 10 hours. The chemical composition of the dry products were determined by dissolving the solid according to the procedure described in Section 3.1. The metal contents were measured using atomic absorption spectrophotometer and the results are shown in Table 8.

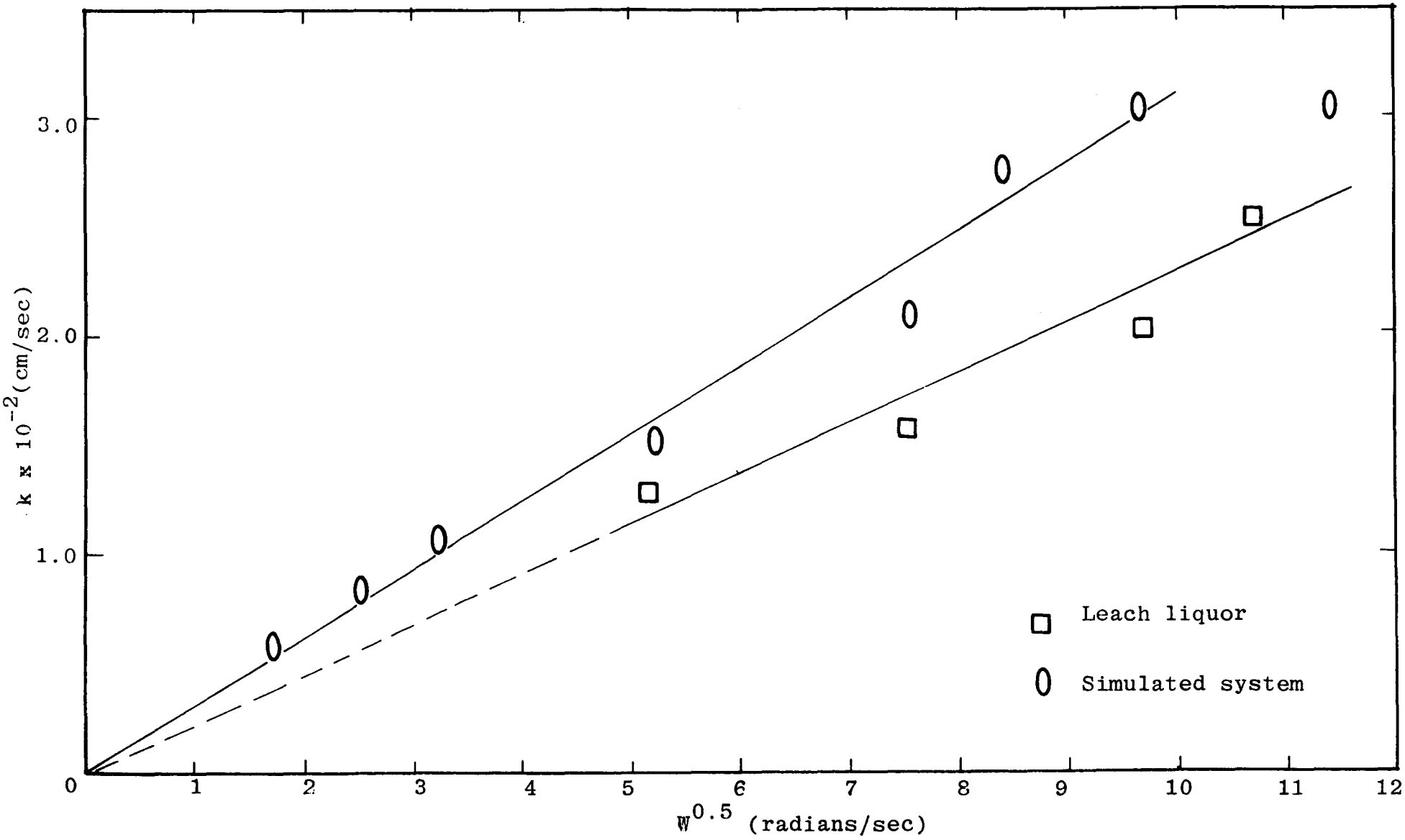


Figure 21 Relationship between the specific rate constant and $W^{0.5}$, temperature=45°C

Table 7. Comparison of specific rate values for different speeds of stirring

| R.P.M. | Specific Rate constant k x $10^{-2}$ cm/sec. | |
|---|---|---|
| | Experimental value | Calculated value from Equation (46) |
| 30 | 0.59 | 0.54 |
| 60 | 0.86 | 0.77 |
| 100 | 1.06 | 0.95 |
| 280 | 1.55 | 1.66 |
| 680 | 2.80 | 2.95 |
| 900 | 3.03 | 2.98 |
| 1260 | 3.10 | 3.53 |
| 1600 | 3.37 | 3.98 |

Table No. 8. Analysis of Cement Products

| Cement Product | Pb % | Zn % | Calculated Moisture Content % |
|---|---|---|---|
| A | 60.00 | 2.00 | 18.00 |
| B | 80.00 | 3.25 | 16.75 |
| C | 75.00 | 2.75 | 22.25 |
| D | 99.50 | 0.50 | - |
| E | 87.50 | 4.50 | 8.00 |
| F | 91.00 | 2.50 | 7.50 |
| G | 98.70 | - | 1.30 |
| H | 75.00 | 7.20 | 17.80 |
| I | 86.00 | 3.25 | 10.75 |
| J | 80.00 | 2.50 | 17.50 |
| K | 80.00 | 4.75 | 15.25 |

The X-ray diffraction analysis of the deposits showed that the products were predominantly in the form of lead and lead(11) oxides. The presence of lead oxide was not surprising as the experiments were carried out in the presence of dissolved oxygen in the solution. During the cementation process a certain amount of the zinc ions from the solution were also deposited on the surface. The zinc level in the dry cement products ranged from 0.5 to 7.2% (w/v), which was very low in comparison to values quoted in some of the other cementation studies.[42,51] Thus the product obtained in the present study was comparatively pure.. The energy dispersive X-ray analysis (Cambridge Instruments S.E.M. S.150, Link Systems 860) of a deposit product is shown in Figure 22, , which indicates the highest peak for lead.

Several factors are known to influence the deposit structure formed during any cementation reaction. Often factors such as the initial solute ion concentration, degree of agitation, precipitant metal surface and also dissolved oxygen are considered to have a major influence on the deposit structure. The deposit can occur in crystalline or dendrite form. The deposit formed on the disc system used in the present study was a dark grey, bulbous mass. The deposits formed usually peeled off from the disc surface. The deposit could occur in crystalline or dendritic form. The appearance of the deposit mass depended on the experimental conditions used. In the present study the observations made under a microscope revealed a bulbous mass containing several dendrites.

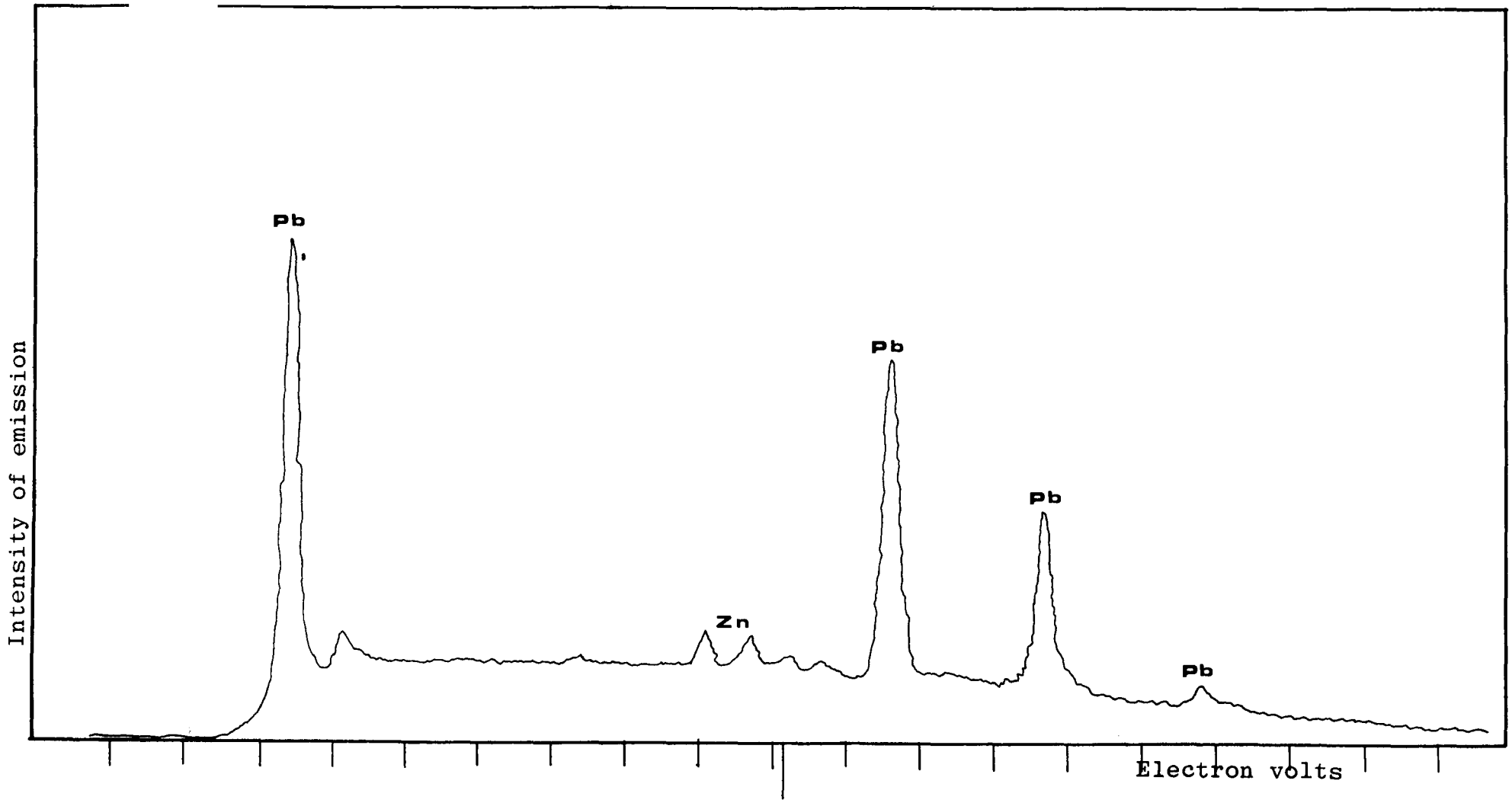


Figure 22. Energy Dispersive Analyser spectra of a cement product.

Strickland[43] reported that copper cementation on zinc surface under nitrogen atmosphere formed dendrites which were open and tree-like in appearance.

The deposit originated at certain sites on the disc surface with the formation of tiny dendrites as shown in Figure 9,(p105)Although dendrites appeared to be continuous, they are assumed to be separated from one another with some empty space between them to allow the diffusion of Cations. The dendrites in this case are basically the formation of metallic lead and its oxide on the zinc surface. The inter-space between any two protrusions usually acts as the anodic site and the locality where the oxide deposit formed is termed the cathodic site. The exact reason for one site to become anodic and another to act as cathodic remains unknown.

7.2.2. Studies with Leach Liquor of e.a.f. dusts.

The leach liquor of e.a.f. dusts contained lead and zinc ions along with trace amounts of manganese, mangnesium and copper.

In addition to the parameters investigated with the simulated system, the study was further extended to determine the effect of

(i) hydroxide concentration
(ii) initial lead concentration, and
(iii) surface area on the rate of cementation.

Prior to the investigation of the above parameters, the nature of lead cementation reactions from the leach liquor was established. During the cementation process the change in lead concentration with time was measured from a system whose temperature and stirring speed were kept constant. The experimental data were plotted according to kinetic equation 39. The results as shown in Figure 23, give a straight line relationship indicating a diffusion controlled process.

7.2.2.1 Effect of Temperature

The effect of temperature on the rate of cementation process was studied for a temperature range of 23 - 60°C. The specific rate constant values were calculated from the kinetic plot shown in Figure 24. The measured specific rate constant increased with temperature as shown in the plot. The values of the specific rate constant (k) increased from $2.8190^{-2}$ cm./sec at 23°C to $6.790 \times 10^{-2}$ cm/sec. at 60°C.

The Arrhenius plot of log k against $\frac{1}{T}$ is shown in Figure 18. The slope of the straight line in the plot gave an activation energy ($E_a$) of 5.62 K cals/mole. This value compares favourably with that of simulated system with an activation energy of magnitude which is indicative of a diffusion controlled mechanism.

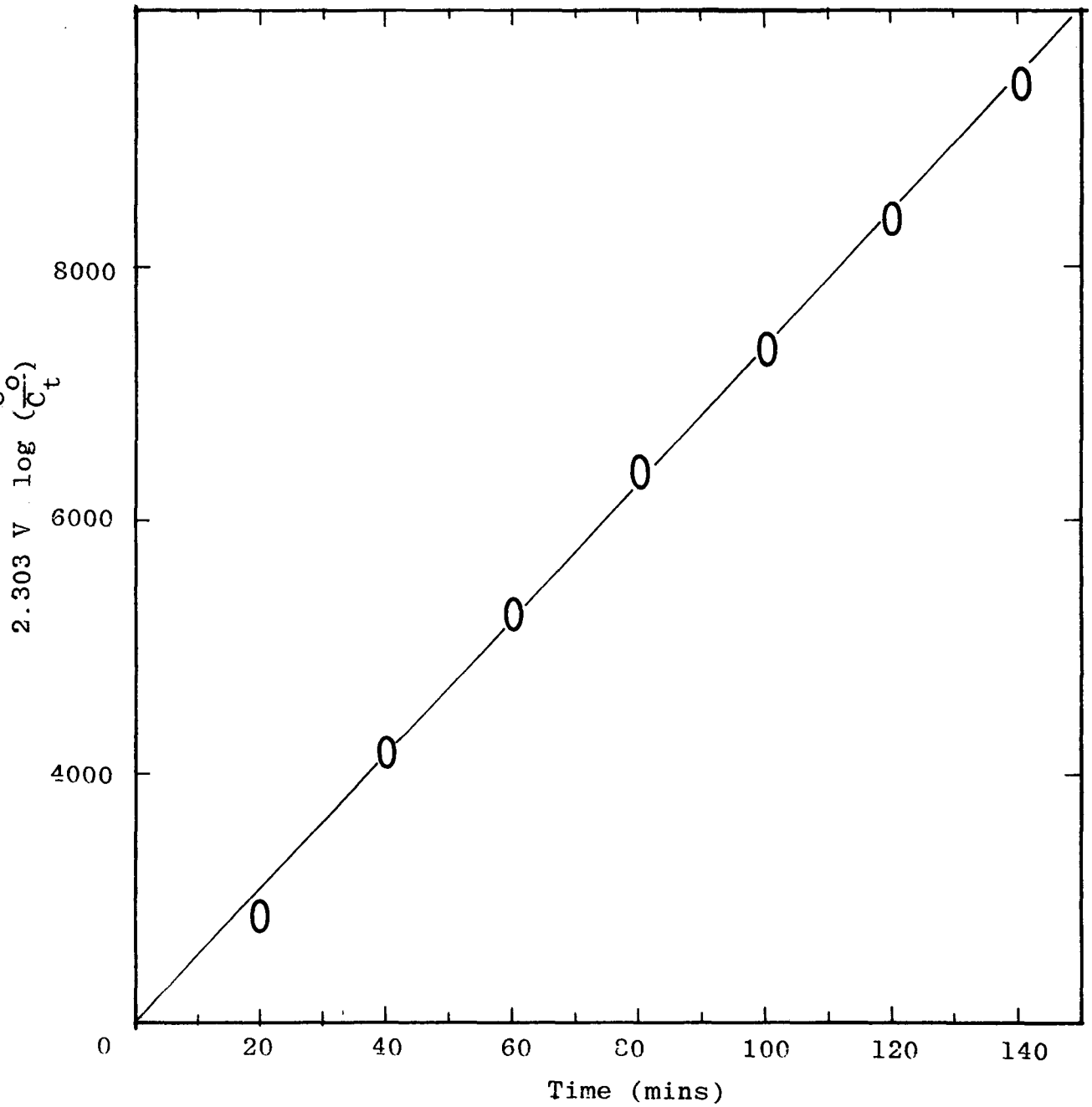


Figure 23. Plot of 2.303 V log ($\frac{C_o}{C_t}$) vs. time for lead cementation from leach liquor. T = 45°C, r.p.m. = 800.

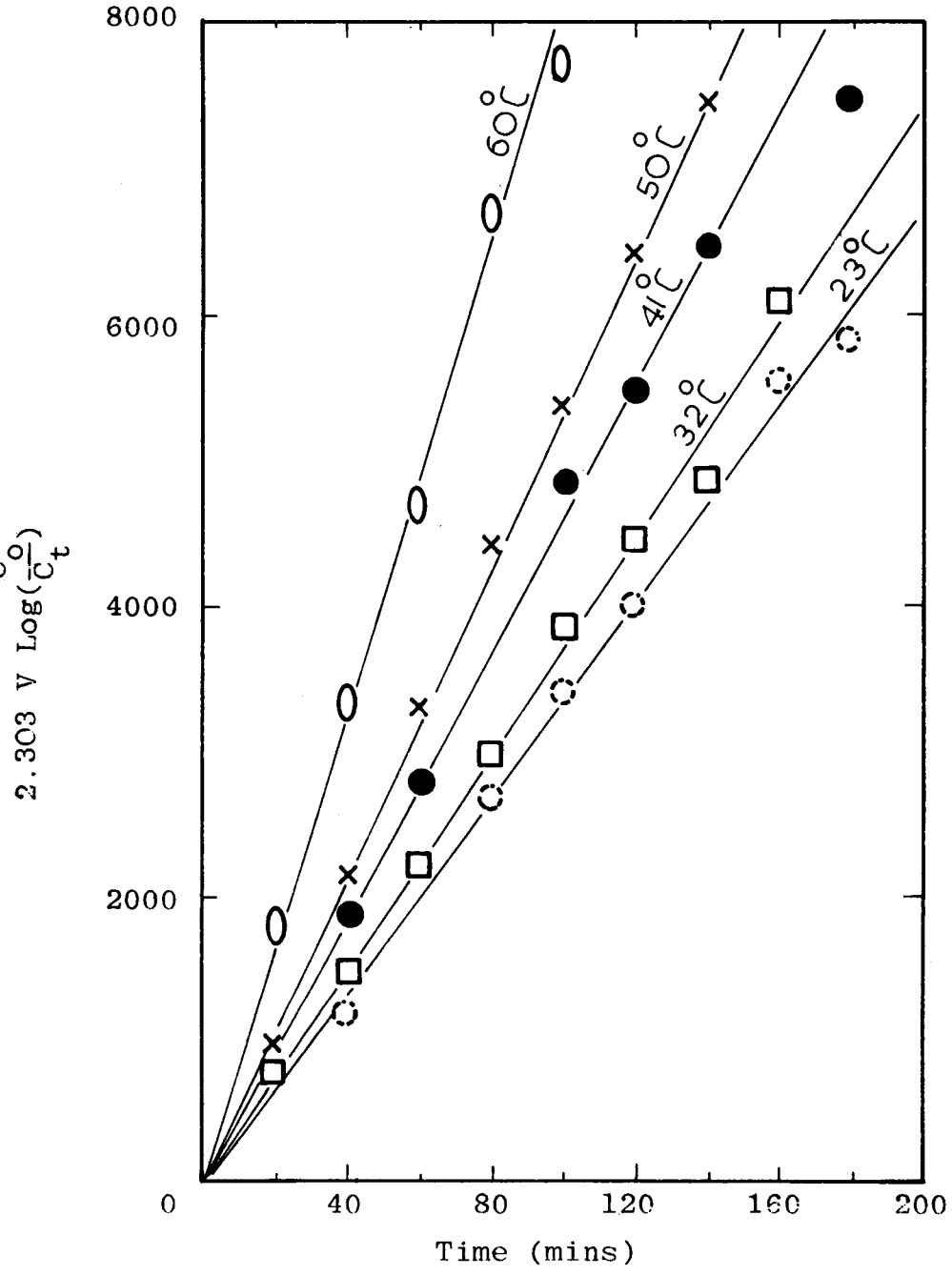


Figure 24. Lead cementation data at various temperatures from leach liquor of e.a.f. dusts: r.p.m. = 800 initial lead ion concentration = 3.86 gm/l

7.2.2.2 Effect of Stirring Speed

The effect of stirring speed on the rate of lead cementation was investigated for rotational speeds ranging from 250 to 1100 r.p.m. The specific rate constant (k) obtained from the kinetic plot of Figure 25 for different stirring speeds is presented with that obtained for the simulated system in Figure 20. The figure indicates that k increases with the rate of stirring and at low stirring speeds the values of k compare reasonably well with those of the simulated system. The deviations observed at high stirring speed may be attributed to the presence of zinc ions in the leach liquor. Such deviations have been reported by Miller[65] for cadmium cementation on a zinc surface in the presence of zinc ions.

Following equation (15) the specific rate values were plotted against the square root of the stirring speed as shown in Figure 21, where a straight line relationship indicating a diffusion process for lead cementation has been obtained.

The mass transfer rate constant for diffusion to a rotating disc surface on a laminar flow can be described through a dimensionless equation of the form[61]

$$Sh = 0.62\ Re^{\frac{1}{2}}\ Sc^{1/3} \qquad (47)$$

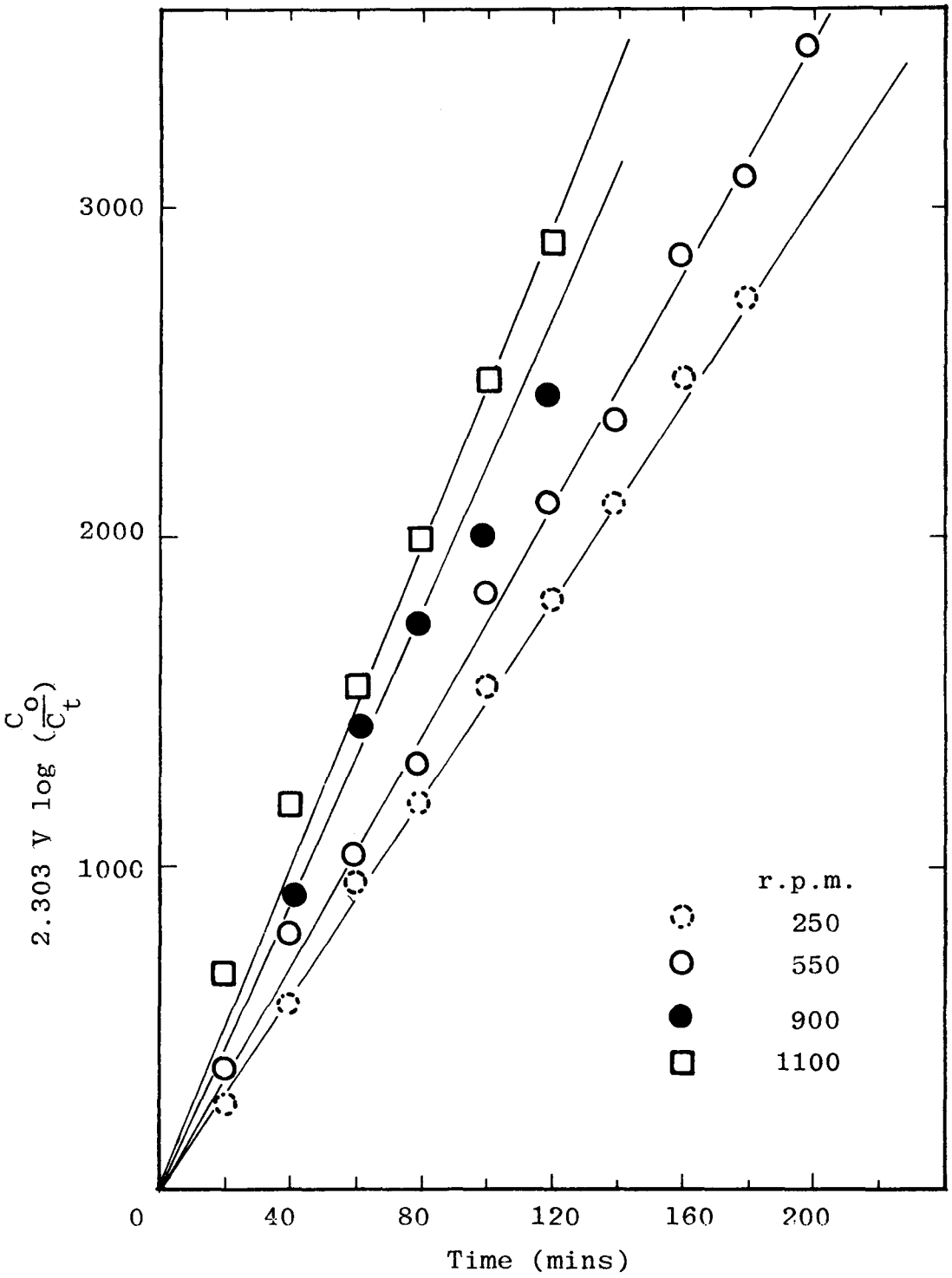


Figure 25. Effect of stirring on the rate of cementation of leach liquor.
Temperature = 45°C
$Pb^{++}$ conc. = 3.60 gm/l.

The results for both simulated and leach liquor cementations are compared with equation (47) by plotting Sh versus $Re^{\frac{1}{2}}Sc^{\frac{1}{3}}$. As can be seen from Figure 26, the simulated and the leach liquor systems show a close agreement with equation (47) by slopes of 0.66 and 0.55 respectively

7.2.2.3 Effect of Baffles

Experiments were carried out to determine whether the rate of cementation is effected by the introduction of baffles into the cementation vessel. In a situation like this the use of baffles is expected to increase the mass transfer rate through intensive mixing. However, when baffles were used in the batch cementation study approximately 10% or more reduction in the cementation rate was observed. It thus appears that an intensive mixing condition in this process is not beneficial.

7.2.2.4 Effect of Caustic Concentration

The experimental results of tests in which the caustic concentration of the leach liquor was varied from 200 to 400 gm/l are shown in Figure 27. The experimental data indicate a significant reduction in specific rate constant values (k) with increase in caustic concentration.

The reduction of k values with increase in caustic concentration can be explained as being due to the rate of

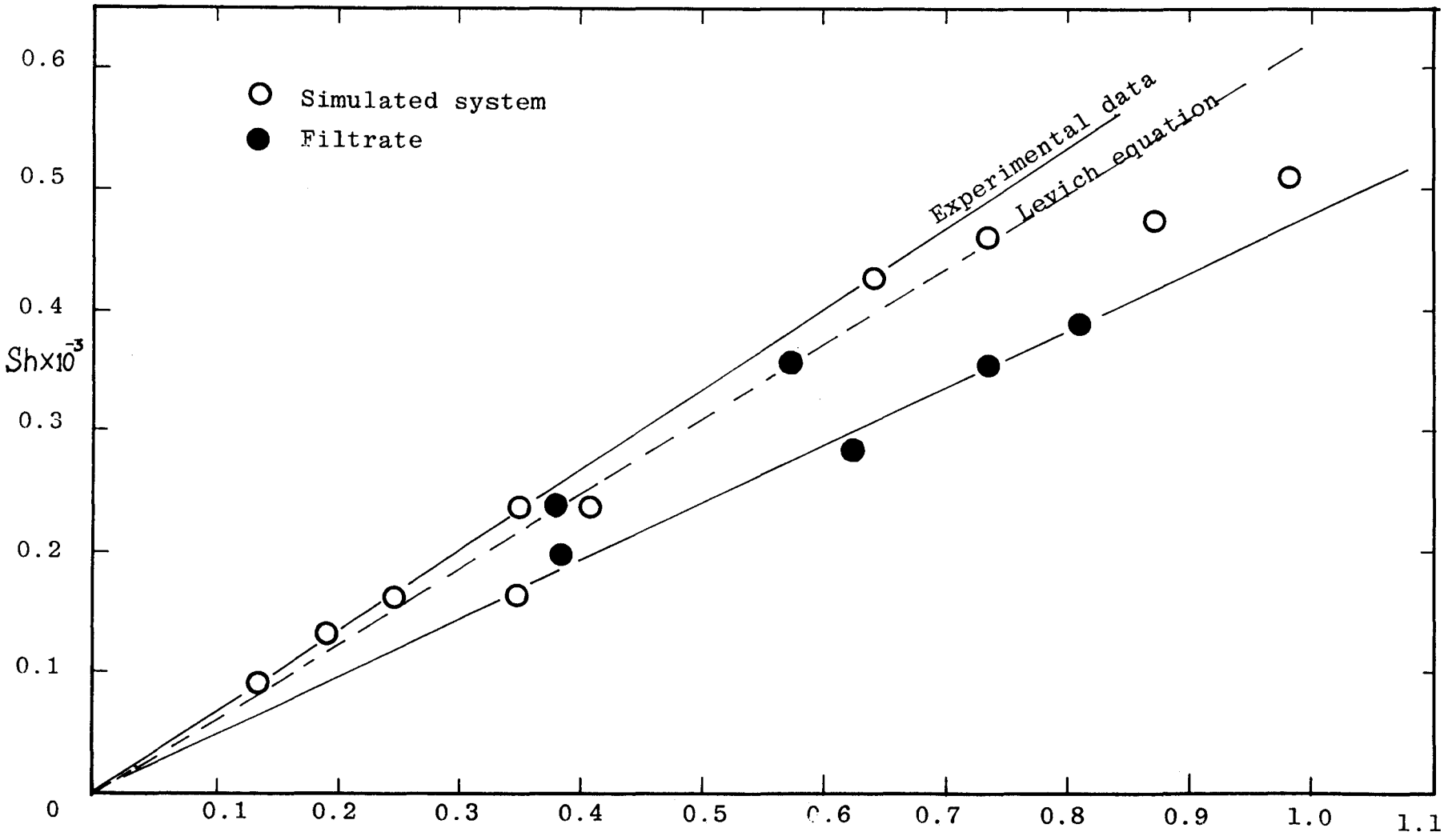


Figure 26 Plot of Sh versus $Re^{\frac{1}{2}}Sc^{\frac{1}{3}}$

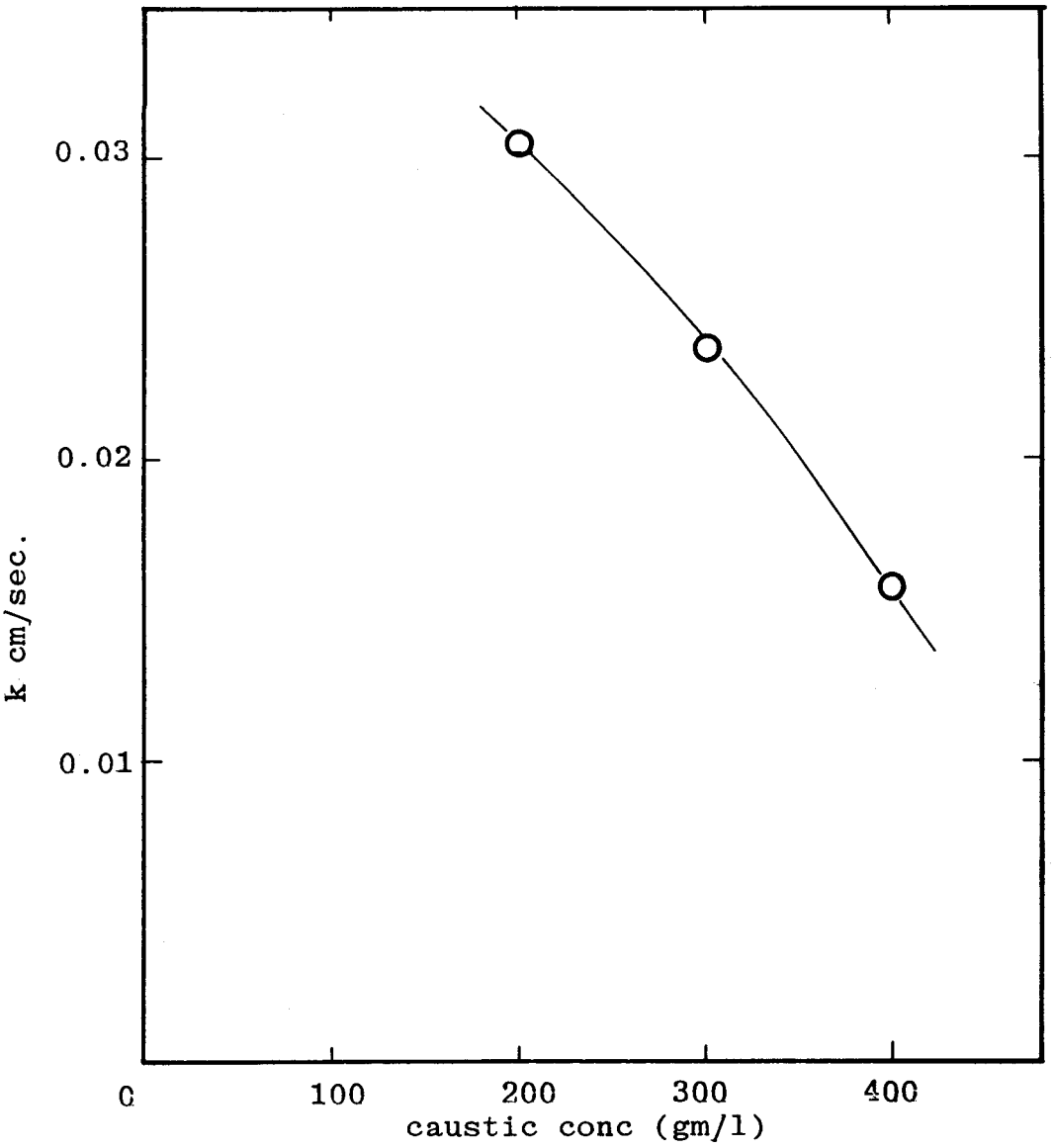


Figure 27. Effect of Hydroxide concentration
Temperature = 45°C
$Pb^{++}$ conc. = 3.60 gm/l
r.p.m. = 550

ionic transport through the diffusion layer. The inonic transport depends on the electric field produced by all ions present, particularly those moving. In this case the diffusivities of hydrogen and hydroxide ions in the solution are much greater than those for sodium and other ions present. The simultaneous transport of either can strongly influence the rate of lead diffusion. Therefore it is possible with greater hydroxide ion concentration the flux of the lead ions was diminished.

7.2.2.5 Effect of Initial Lead ion Concentrations

The relationship between the specific rate constant and the initial lead ion concentration of the leach liquor were studied at 45$^{o}$C and a stirring speed of 550 r.p.m. The data obtained for the initial lead ion concentrations ranging from 0.762 gm/l to 5.50 gm/l are presented in Figures 28 and 29. The measured specific rate constant values were plotted against initial lead concentrations and are shown in Figure 30. It can be seen that with the increasing lead ion concentrations, the rate of cementation increased to a maximum and then decreased. This effect is possibly due to the nature of the lead deposit formed. With low initial lead ion concentrations a loose, bulbous deposit, which was periodically detached from the disc surface, was found to form. This kind of deposit can facilitate the counterdiffusion of cations to and from the surface. Where, as with high initial lead ion concentrations

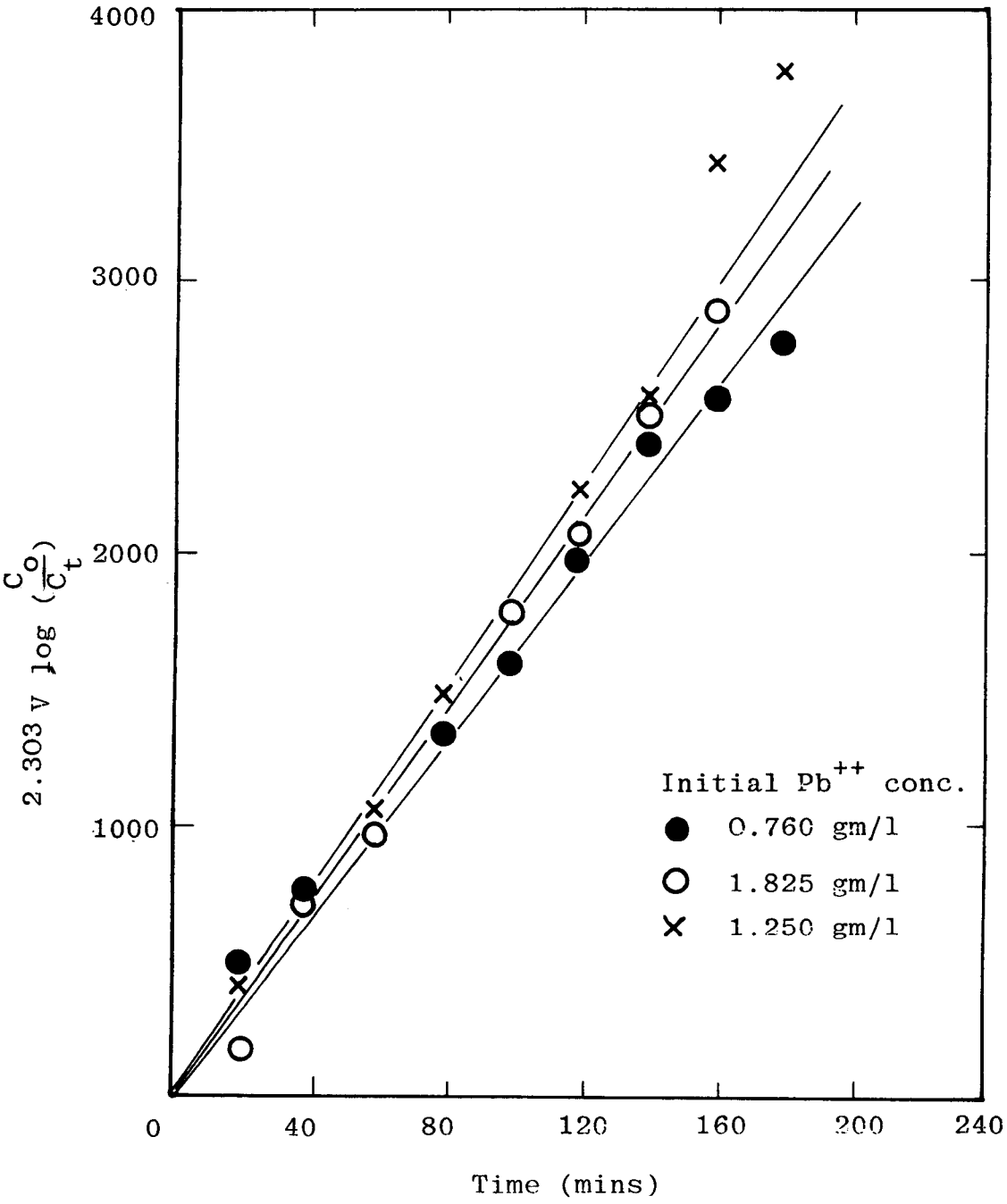


Figure 28. Effect of initial lead ion concentration on the rate of cementation: r.p.m. = 550 T = 45 ± 1°C

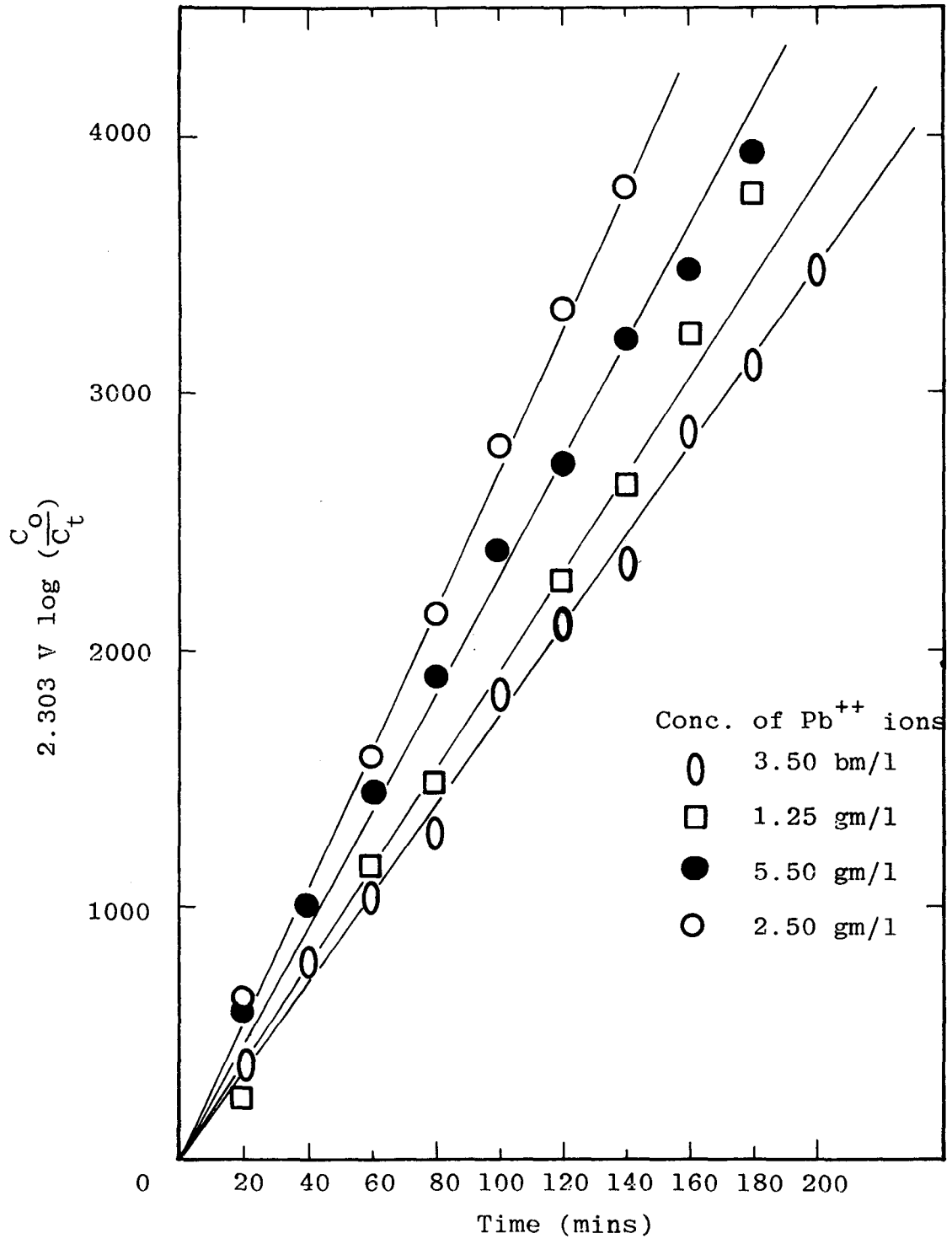


Figure 29. Effect of initial lead ion concentration of leach liquor on the rate of cementation r.p.m. = 550, T = 45 ± 1°C.

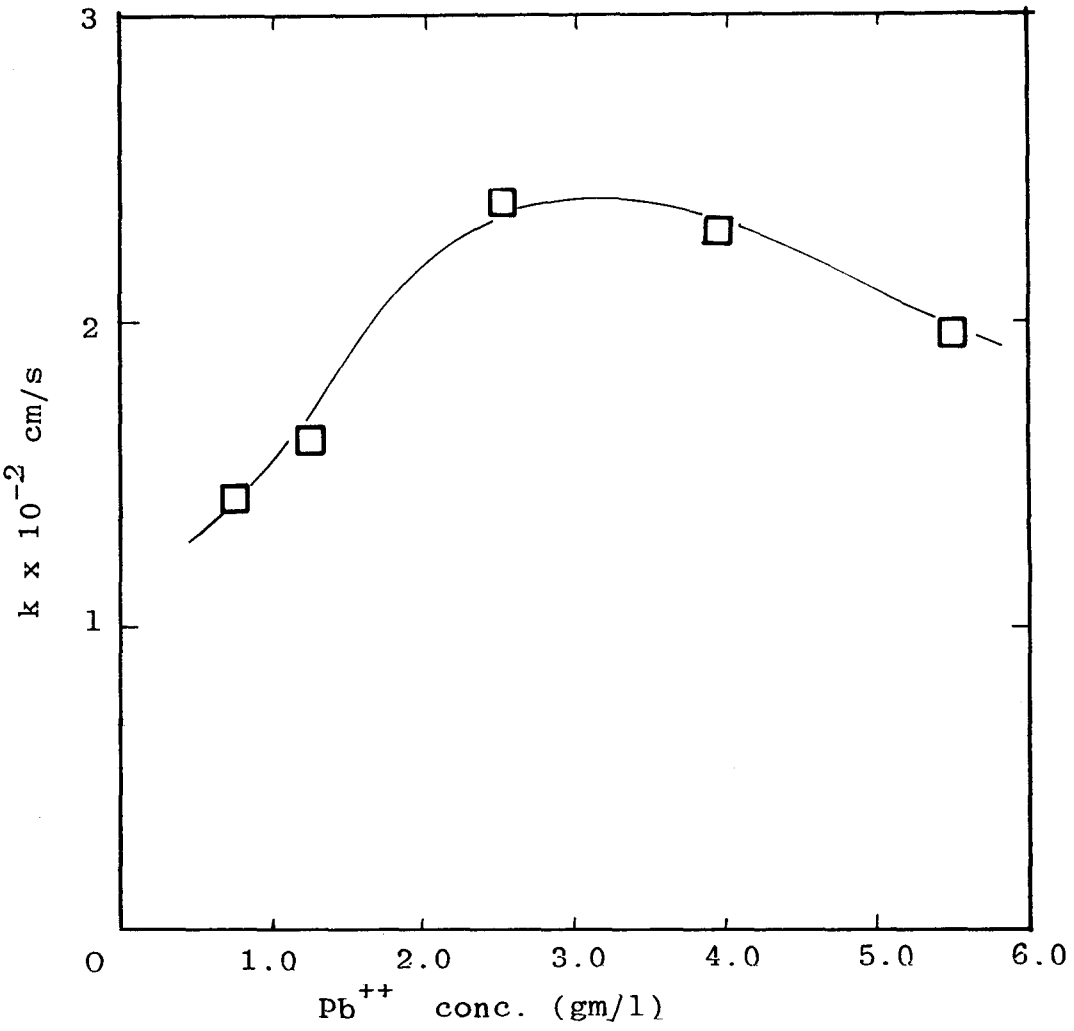


Figure 30. Effect of initial lead ion concentration on the reaction rates for cementation with leach liquor, temperature = 45$^{o}$C; r.p.m. = 550

(> 2.55 gm/l) the precipitate formed were found to be of a relatively smooth and non-porous type which could prevent the counterdiffusion of cations to a certain extent.

In the system under investigation the surface reaction is reasonably fast. However, with high initial lead ion concentration which result in high mass flux, some lead ions from solution will be left unreacted at the exterior of the deposit. These will diffuse into the deposit mass probably through the pores of the precipitate. Such a process would tend to cause a considerable reduction in the porosity of the deposit and consequently restrict the diffusion of the zinc ions from the anodic sites.

#### 7.2.2.6 Effect of Surface Area

In this study several discs of different diameters ranging from 2.50 to 4.00 cm. were used and the results are shown in Figure 31. This plot shows that the rates are directly proportional to the exposed surface area verifying the process is diffusion controlled.

## 7.3 STUDIES WITH RECIRCULATION COLUMNS

The apparatus constructed for the study of continuous cementation was initially used to study the cementation process on a recirculation basis. The objective of this study was to gain further knowledge of the kinetics of the process and to ascertain the factors which influence them.

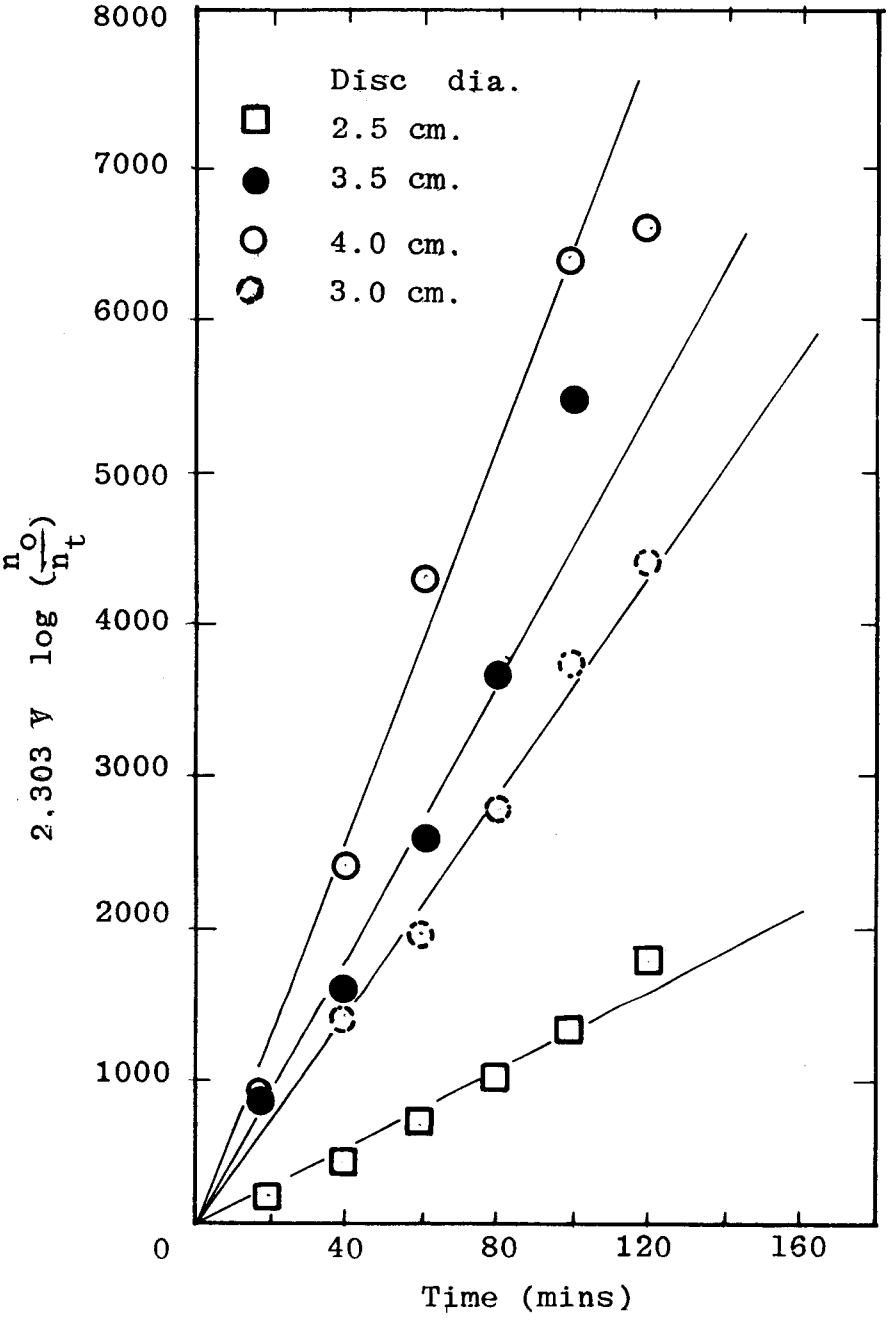


Figure 31. Effect of surface area on the rate of cementation
$Pb^{++}$ conc. = 2850 ppm,
rpm = 550
temperature = $45^{o}C$

The recirculation study was carried out using four litres of leach liquor per run at a constant temperature of $45 \pm 0.5^{o}C$. The rate of cementation was investigated in terms of the surface area of packings, flow rates and initial lead ion concentration.

The data obtained for different parameters were analysed by the rate equation (39) developed previously.

### 7.3.1 Influence of Surface Area

The study of batch lead cementation indicated that larger surface area will result in considerable increase in the specific rate constant. However, such increase in surface area was limited in the batch system and this limitation was overcome by the use of a column packed with zinc cylinders. The effect of surface area on the rate of cementation was studied by using different number of packings in the column while keeping the initial lead ion concentration, the flow rate and liquor temperature constant.

The rate of cementation with the total surface area of the packing material ranging from 63.97 to 319.85 $cm^2$ was investigated. The results show that the rate of cementation increases with increase in surface area by a factor of 4.0. The trend was similar to the one observed during the lead diffusion process in the batch system.

### 7.3.2. Effect of Caustic Concentration

The rates of cementation in the recirculation column were compared for leach liquor caustic concentrations of 100 and 200 gm/l. The results are shown in Figure 32, where the rate constant was halved when the caustic concentration was doubled. The results confirm the earlier observations made in the study of batch cementation that reduction in the cementation rate was mainly due to the hydroxide ions present. This is in line with the theory of fast ionic diffusivities. Another possible reason for the decrease in the cementation rate could be the increase in viscosity of the leach liquor.

### 7.3.3. Influence of Flow Rates

A series of experiments were conducted with a surface area of 319.89 $cm^2$ (bed height of 7.50 cm) for flow rates ranging from 0.25 to 1.0 l/min. The specific rate constant values were calculated from the measured slopes of the kinetic plot shown in Figure 33.. The effect of flow rate on the rate constant is shown in Figure 34, which shows an increase of k values for the range of flow rates 0.25 to 0.60 l/min., and then a decrease from 0.60 to 1.0 l/min.

The variation of k with flow rate can be analysed in terms of the diffusion layer formed on the surface. The increase in the rate of mass transfer obtained with initial flow rates of up to 0.60 l/min was found to be proportional to the

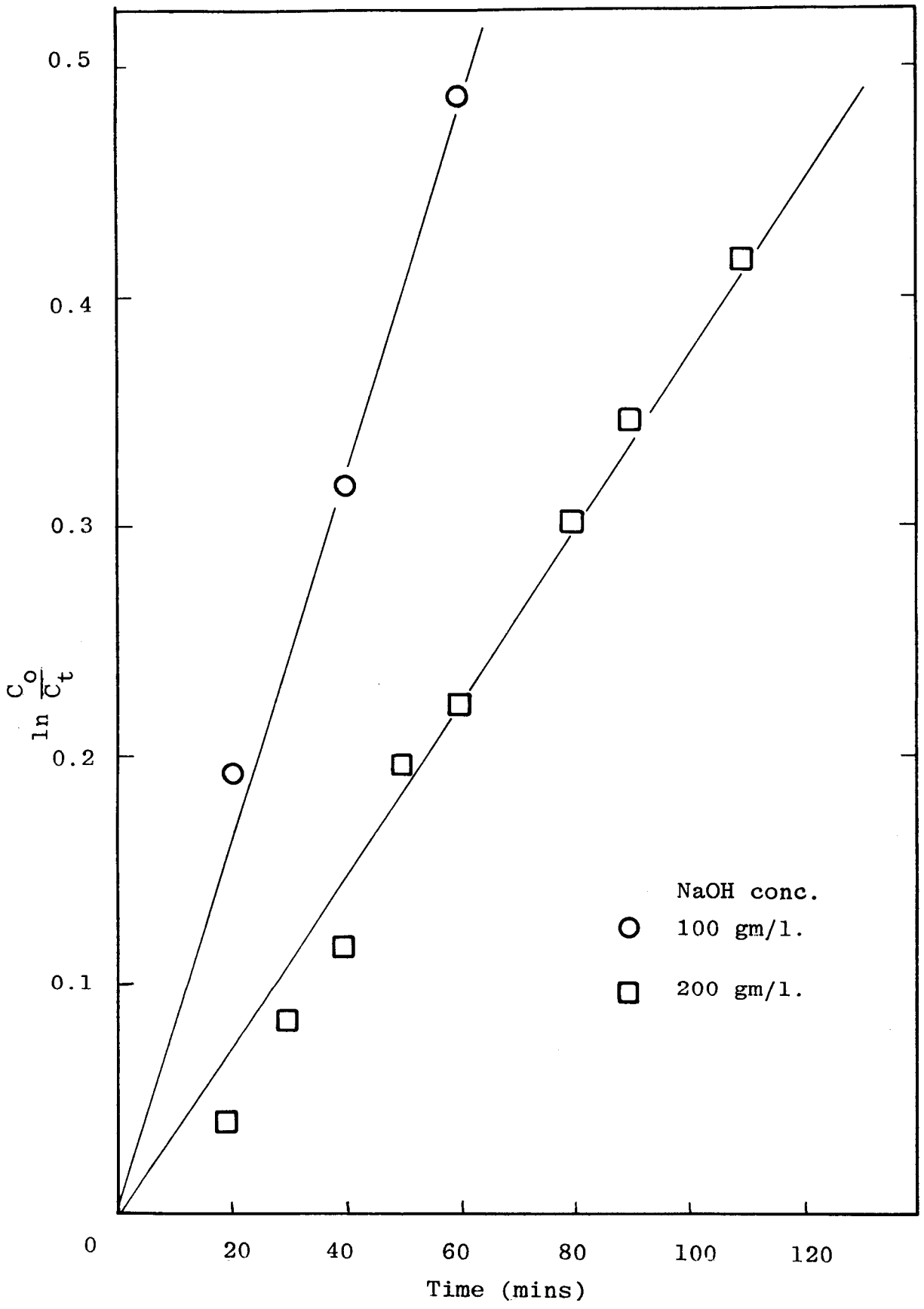


Figure 32. Effect of caustic concentration on the rate of cementation.

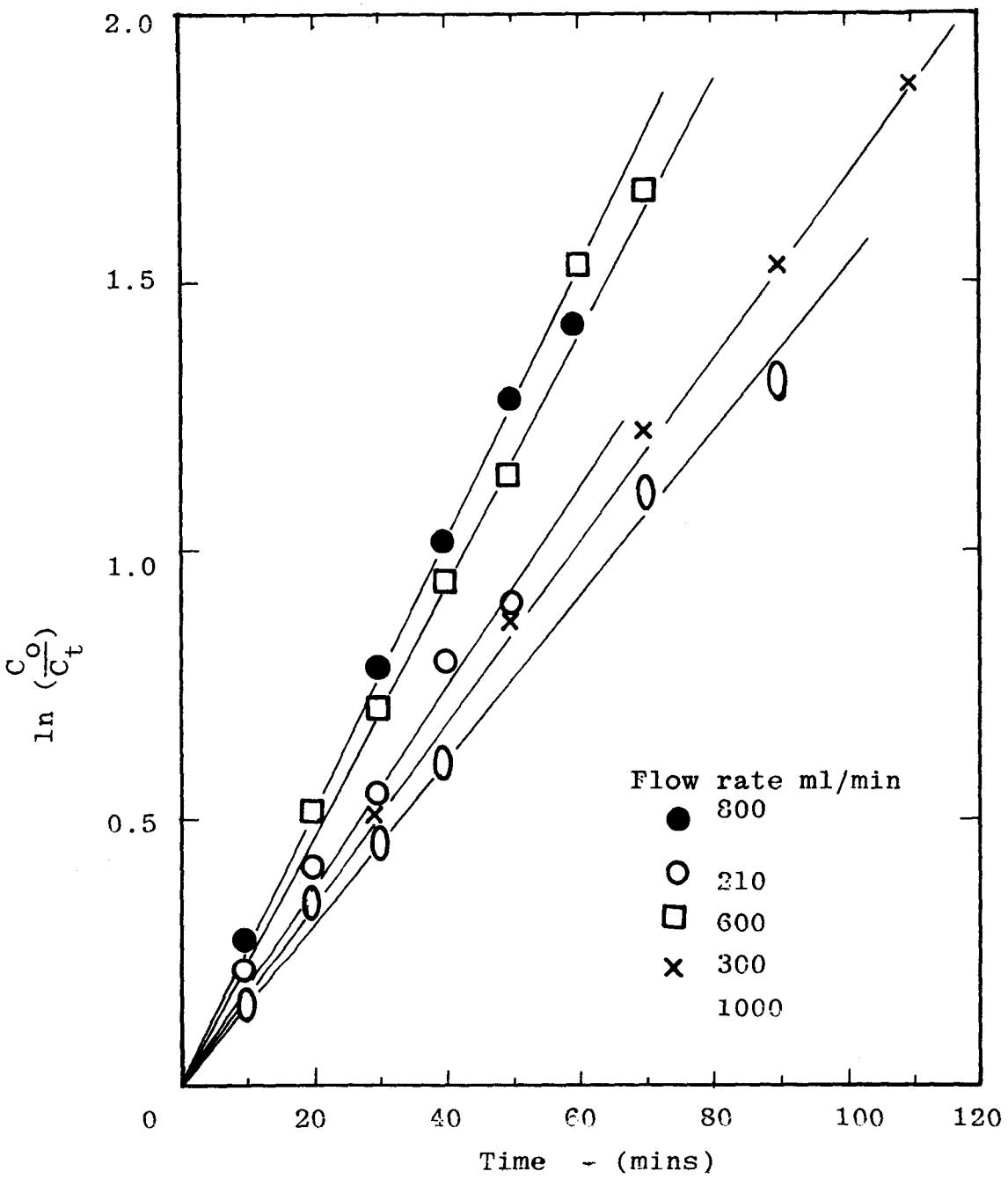


Figure 33. Lead cementation at different flow rates in the recirculation columns: bed height 7.5cm., $Pb^{++}_i$ = 1.80 gm/l, T = 45 ± 0.5°C.

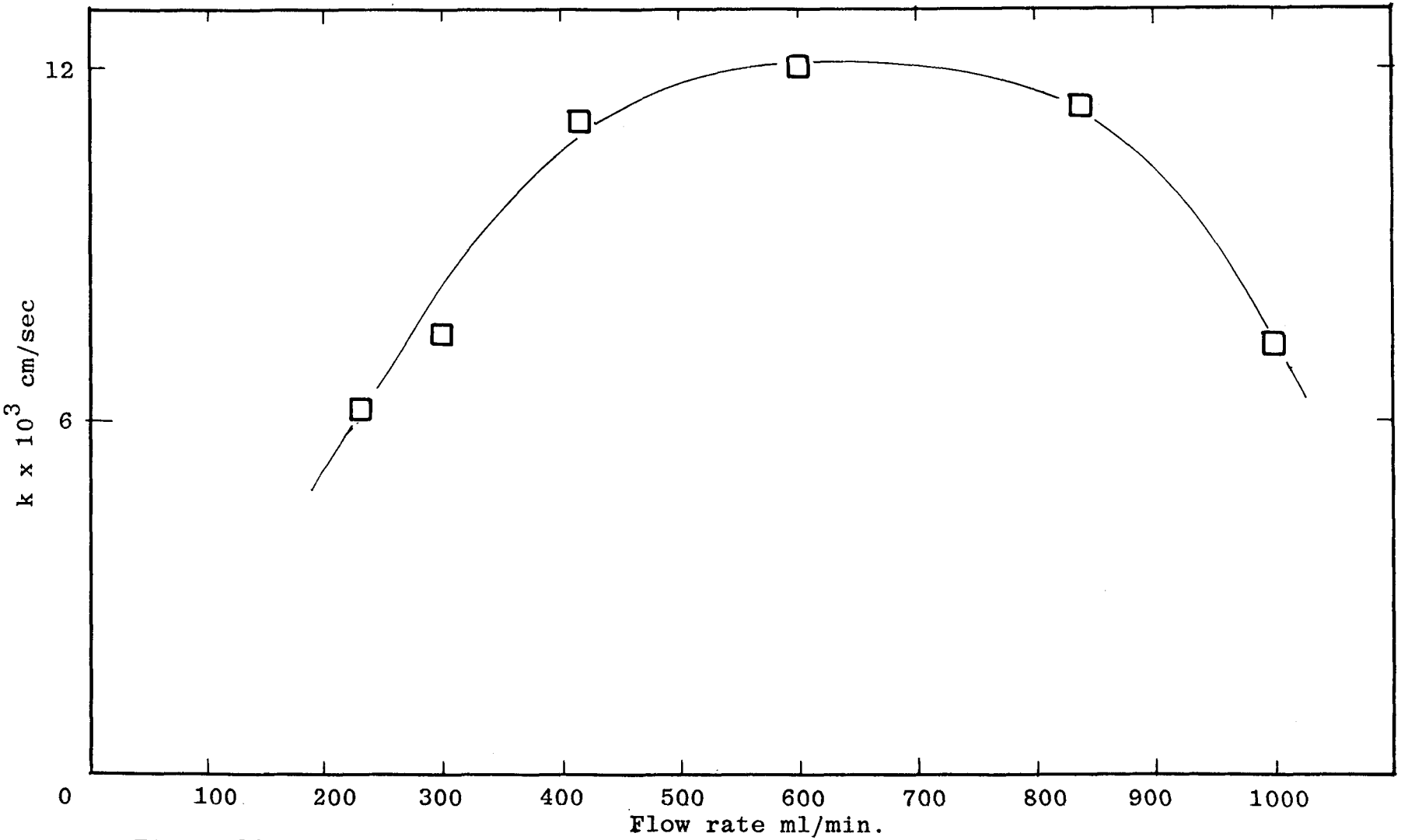


Figure 34 Effect of flow rates on the specific rate constant for cementation in the recirculation column.

$Pb^{++}$ conc. = 1750 ppm. Temperature = 45°C, packing height 7.50 cm.

flow rate. With the above flow rates the controlling step was the diffusion of lead ions through the diffusion layer, where the thickness decreases with increase in flow rate. Since the decrease in thickness of the layer resulted in reduced diffusion path length, an overall increase in mass transfer was observed. Experimental results showed that the doubling of the leach liquor flow rate increased the cementation rate by a factor of 1.70. It can be seen that within experimental error such an increase in the rate suggested that diffusion was the rate controlling step. The results were in good agreement with the theory of Higbie[84] which relates the average mass transfer coefficient ($\bar{k}$) to the diffusivity (D) and the "exposure time" ($t_{exp.}$) for boundary layer diffusion by

$$\bar{k} = 2\sqrt{\frac{D}{\pi t_{exp.}}} \qquad (48)$$

This theory indicates that the mass transfer rate is directly proportional to the square root of the diffusivity and inversely proportional to the square root of the exposure time. However, an optimum rate value was obtained for the flow rate of 0.60 l/min. and further increase in flow rate from 0.60 to 1.0 l/min. produced a decrease in the rate of mass transfer. The reduction in the rate of mass transfer could be due to the combined effect of the diffusion layer reaching a limiting thickness and the intensive mixing that occurs at high flow rates.

### 7.3.4 Influence of Initial Lead ion Concentration

The influence of lead ion concentration on the rate of cementation was studied by using leach liquors with varying lead concentrations. The solutions of low initial lead ion concentration were prepared by adding a required amount of caustic solution to the original leach liquor. A series of experiments were carried out with initial lead ion concentration ranging from 275 p.p.m. to 1100 p.p.m. keeping the temperature, the surface area of the zinc packing material and the flow rate constant. The specific rate constant was calculated from the kinetic plot shown in Figure 35. A plot of the specific rate constant as a function of the initial lead ion concentration is presented in Figure 36. As indicated by the plot the rate constant increased with initial lead ion concentration up to approximately 800 p.p.m. $Pb^{++}$ thereafter a decrease in specific rate was observed. A similar observation with variation of the initial lead ion concentration was made in the batch process of both simulated and leach liquor systems. However, the reduction in the rate with initial lead ion concentration greater than approximately 800 p.p.m. $Pb^{++}$ could be due to the diffusion of lead ions into the pores of the deposit, as the reaction proceeded the porosity of the deposit would tend to be reduced. Hence the outward diffusion of the dissolved zinc ions would become restricted. Therefore, the overall cementation process at high lead ion concentration would be controlled by the extent of the diffusion of the zinc ions from the surface of the packings to the bulk of the liquid.

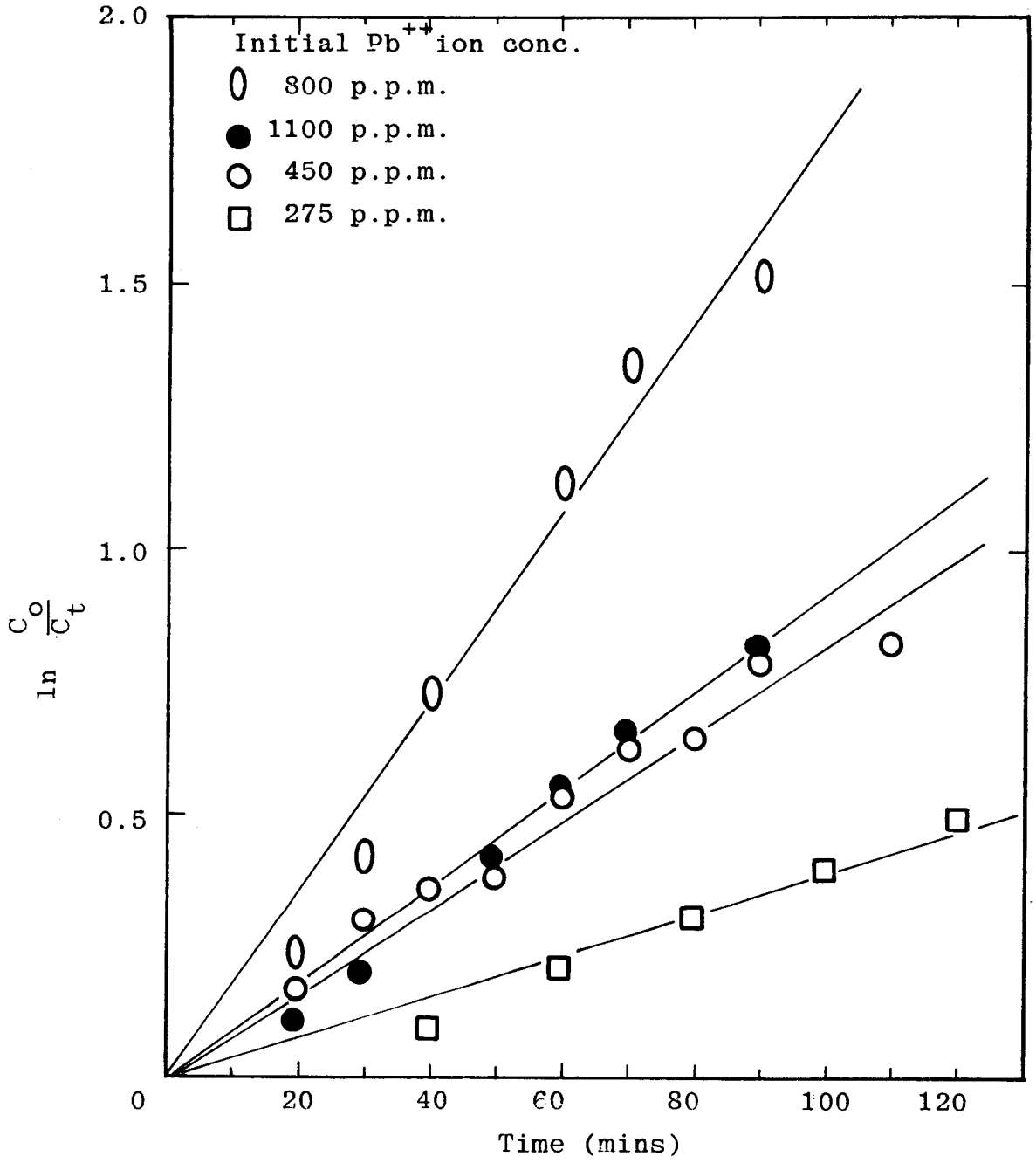


Figure 35. Cementation data with different initial lead ion concentrations in recirculation experiments: flowrate 600 ml/min; temperature 45 ± 0.5°C.

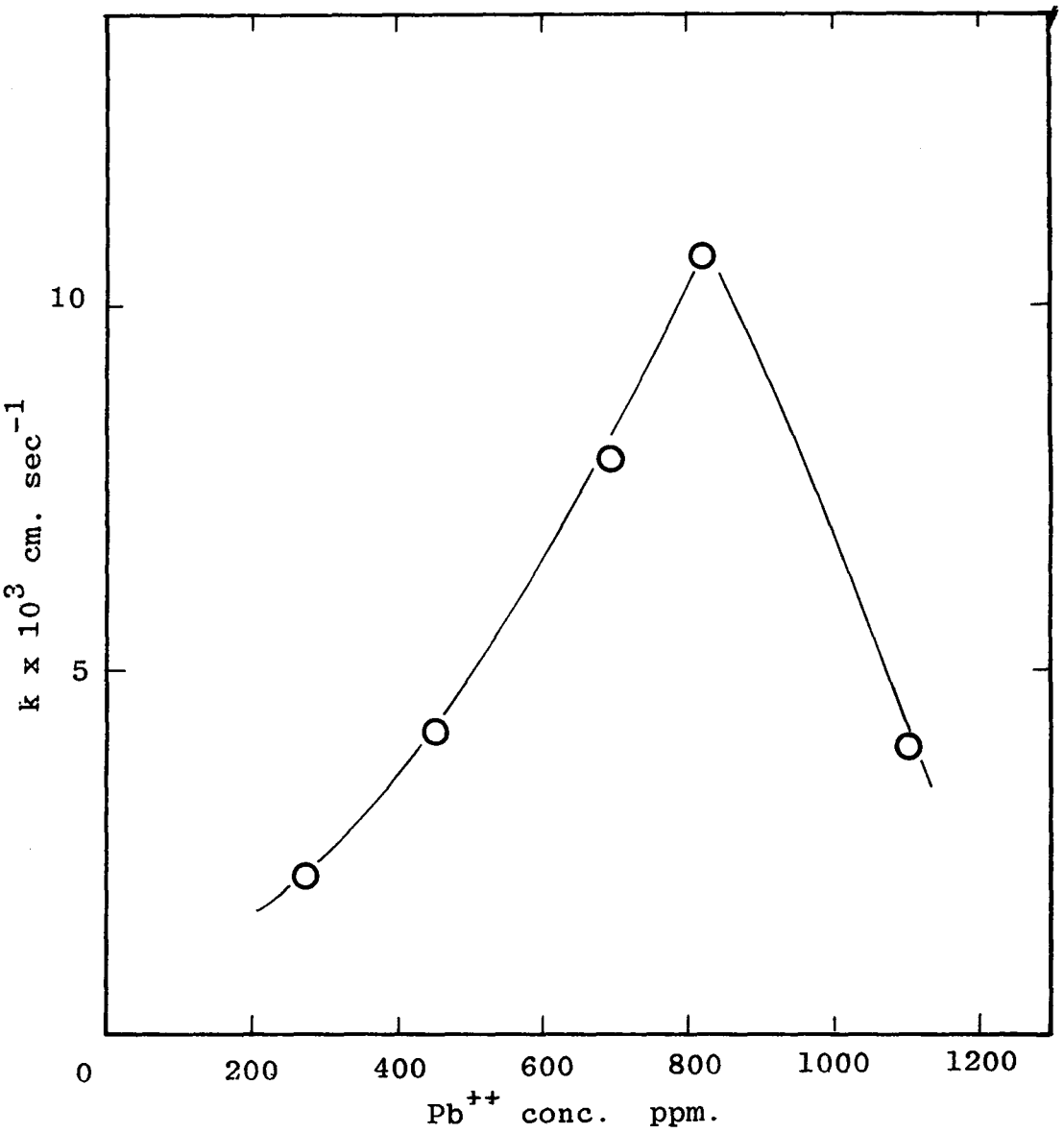


Figure 36. Effect of lead ion concentration on the specific rate constant for cementation in the recirculation column, flow rate = 60 ml/min. temperature = 45°C, bed height = 7.50 cm.

## 7.4 CONTINUOUS CEMENTATION

A column packed randomly with zinc cylinders was used to study the lead cementation of the leach liquor. The parameters influencing the cementation rate such as bed length flow rates, initial concentration were investigated at a constant temperature of 45°C. The apparent mass transfer coefficient was calculated from equation (42) developed for steady state conditions in the cementation process.

### 7.4.1 Determination of Effective Interfacial Area

Initially there were some doubts as to whether the inner surface of the cylindrical zinc packing material was available for the process of cementation. However, this point was clarified by conducting two similar experiments. One experiment was conducted with packing material whose inner surfaces were completely excluded from coming into contact with the liquid. This was achieved by coating the inside of the packings with an epoxy paint which was highly resistant to any form of alkaline attack. The results were compared with those of the experiment where the packings had both surfaces exposed for cementation. The results are shown in Table 9 , which indicates the apparent mass transfer coefficient obtained for the packings with both surfaces exposed to the diffusing lead ions gave a value of $2.10 \times 10^{-2}$ cm/sec. The corresponding value for packings whose insides were coated with paint gave a value of $0.76 \times 10^{-2}$cm/sec. The above results suggest that both surfaces of the packings were taking part in the lead cementation.

Table No. 9 Results with different interfacial areas

| Continuous Cementation Flow Rate = 260 ml/min | | |
|---|---|---|
| Time (mins) | Packings with coatings inside $a = 2.3703 \frac{cm^2}{cm^3}$ | Packings with both sides available $a = 4.7406 \frac{cm^2}{cm^3}$ |
| 0 | 525 | 550 |
| 10 | 425 | 550 |
| 20 | 375 | 375 |
| 30 | - | 350 |
| 40 | 345 | 287 |
| 50 | - | - |
| 60 | 355 | 200 |
| 80 | 322 | 50 |
| 100 | 337 | 25 |
| 120 | 282 | 25 |
| | $k_g = 0.0076$ cm/sec. | $k_l = 0.0210$ cm/sec. |

Based on the above confirmation the effective interfacial area for the packing material was calculated by including both surfaces as 4.7406 $cm^2/cm^3$. The detailed calculations are given in Appendix II. The interstitial velocity and bed voidage were determined by methods described in section 4.2.

7.4.2. Effect of Flow Rates

The effect of varying flow rate on the apparent mass transfer coefficient ($k_\ell$) was initially studied for a constant bed height of 15.0cm. Leach liquor with an initial lead ion concentration of 700 p.p.m. was used for flow rates ranging from 250 to 720 ml/min. The values of $k_\ell$ obtained for various flow rates used are shown in Figure 37. As Figure 37 indicates, the apparent mass transfer coefficient ($k_\ell$) increases with increasing flow rate. This was as expected for a diffusion controlled process. However, discrepancies in the $k_\ell$ values were seen in the flow rates from 400 to 820 ml/min. These results compare with those obtained with high flow rates in the recirculation column.

At high flow rates the transport of lead ions must be governed partly by convection and partly by diffusion. The role of diffusion becoming more important as the surface is approached. The transport of the lead ions from the bulk of the solution to the boundary layer will be by forced convection.

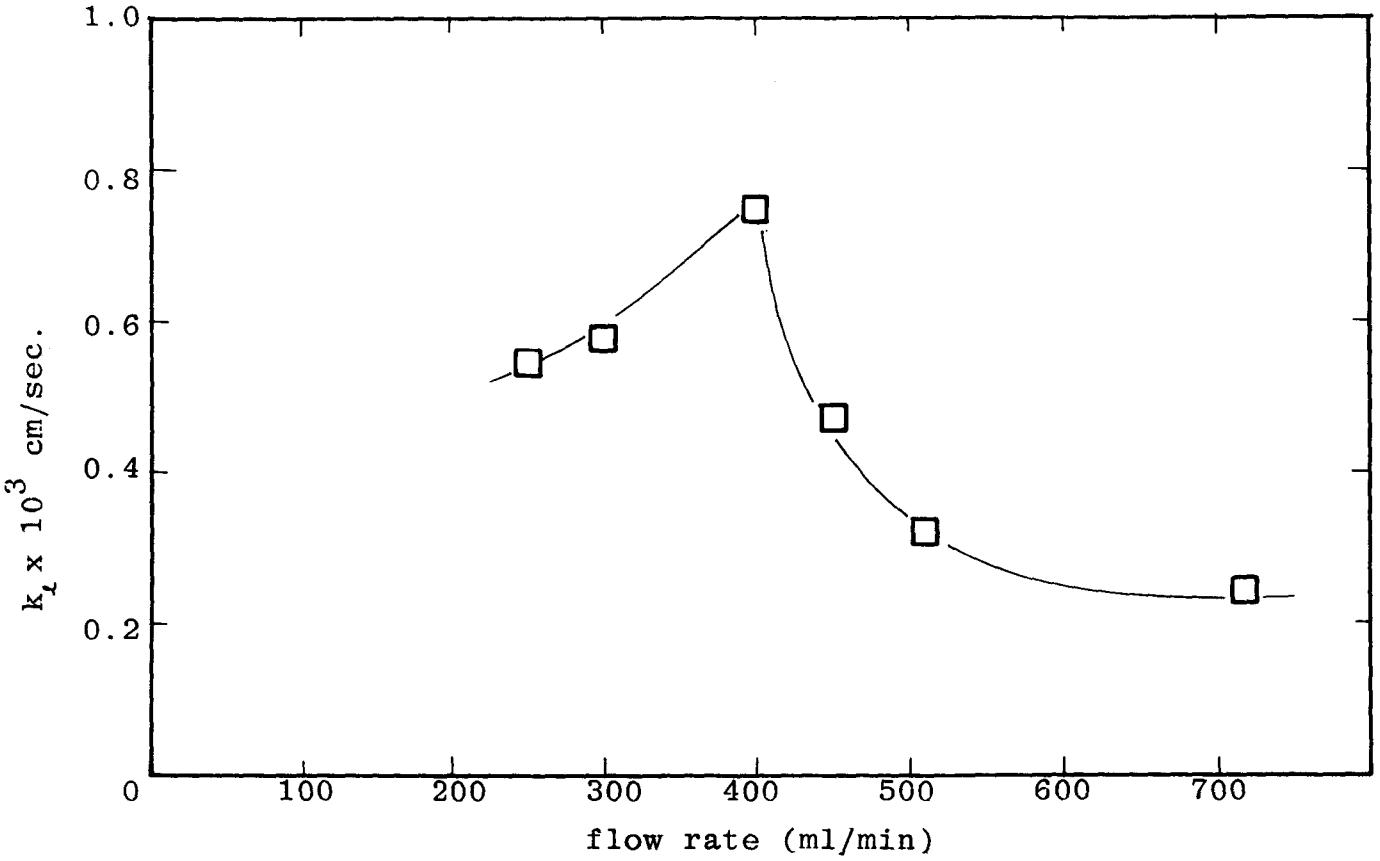


Figure 37. Relationship between flow rates and apparent mass transfer coefficient for continuous cementation, bed height = 15.0 cm. $Pb^{++}$ conc. = 700 ppm.

In the lead cementation process for runs < 400 ml/min. the transport to the solid surface was mainly by diffusion through the layer formed on the packing surface. The thickness of the diffusion layer decreased with increasing flow rate until it reached a limiting value and any further increase in flow rate should not increase the mass transfer rate. As the flow rate was increased above 400 ml/min. the velocity was likely to reach a point where the nature of the fluid flow near the surface altered abruptly and the flow mixed rapidly with the bulk fluid. This would result in an intensive mixing, which seemed to be an unsatisfactory condition for the diffusion process of the lead ions. Earlier experiments with the use of baffles have indicated that vigorous mixing conditions produced a diminishing effect on the rate of mass transfer.

### 7.4.3 Precipitation Efficiency

A quantitative study of the degree of lead removal from the leach liquor by a continuous cementation process may be expressed in terms of a precipitation efficiency (E) which could be defined as

$$E = \frac{C_o - C_t}{C_o}$$

where $C_o$ and $C_t$ are concentrations of lead ions in the inlet and outlet stream at time o and time t respectively. The

precipitation efficiency values were used to study the influence of initial lead ion concentration, flow rates on the rate of lead removal.

### 7.4.4. Effect of Lead ion Concentration

The effect of lead ion concentration on the precipitation efficiency was investigated by using a constant flow rate of 400 ml/min. and bed height of 15.0 cm. The lead ion concentration was varied from 200 to 900 p.p.m. and the calculated values of precipitation efficiency and the measured initial lead ion concentrations were plotted as shown in Figure 38. As Figure 38 illustrates, the diffusion of lead ion increased with increase in initial lead concentration. But the mechanism of lead diffusion changed at a concentration of 700 p.p.m. The deposits formed with lead ion concentrations above 700 p.p.m. were found to be non-porous. As reported in the previous cases, such deposits with low porosity often hinder the diffusion of the reactant cation. The experimental data showed that lead cementation with initial lead ion concentration of 900 p.p.m. gave a low efficiency of value. It also indicated that a maximum efficiency of 0.7 was achieved with concentration of 700 p.p.m. The overall effect on the precipitation efficiency was very similar to the results reported for industrial copper recovery by cementation.[44]

### 7.4.5 Influence of Bed Heights

The precipitation efficiency for bed heights ranging from 7.50 to 43.0 cm. was studied for varying flow rates. The

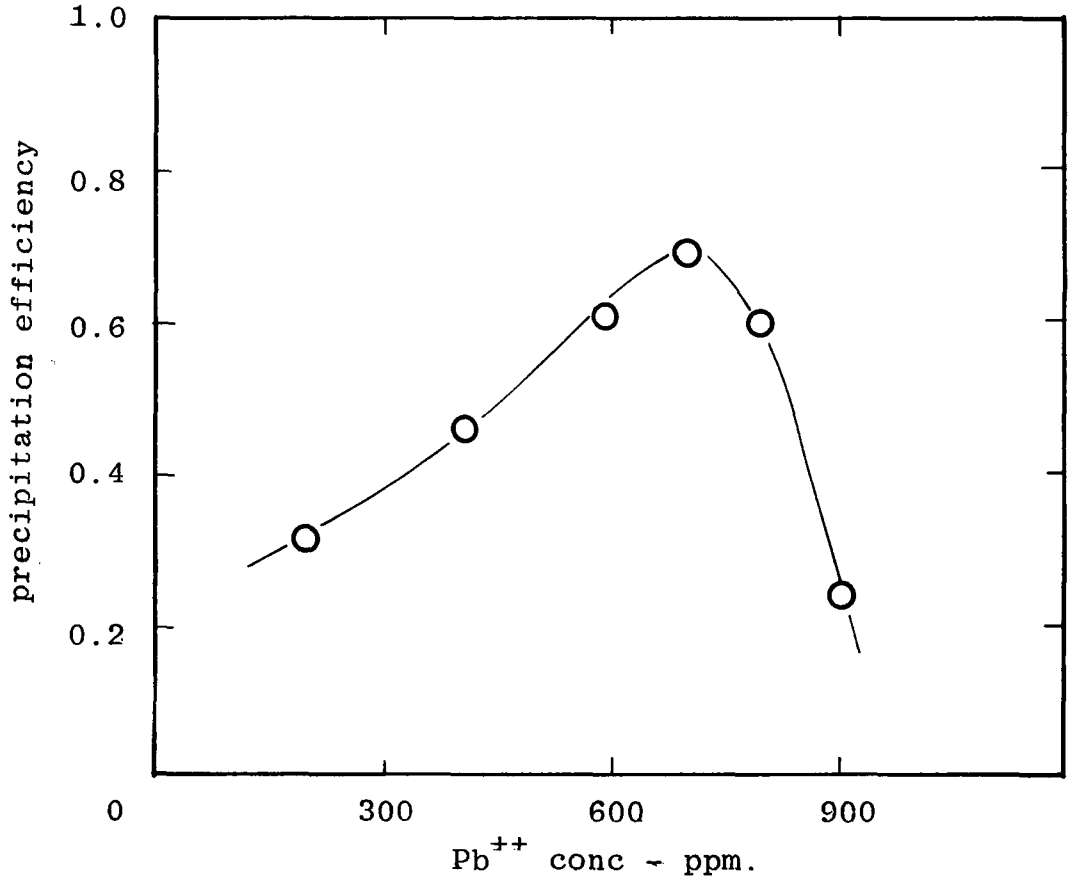


Figure 38 Effect of inlet lead ion concentration on the precipitation efficiency, temperature = 45°C. flow rate = 400 ml/min, bed height = 15.0 cm.

precipitation efficiency for one hour cementation from various bed heights were plotted against the flow rates in Figure 39. The flow rates ranging from 60 to 790 ml/min. were investigated. The results show that high efficiency values were obtained at low flow rates. It also indicates that generally the precipitation efficiency values increased with an increase in bed height as expected. The results indicate that an increase in flow rates for all bed heights resulted in a decrease in the precipitation efficiency value. It can be seen that an increase in flow rate above 400 ml/min. gave a constant precipitation efficiency which was characteristic for each bed height.

The results obtained for bed height of 15.0 cm. gave a maximum efficiency of 0.97 and 0.35 for flow rates of 125 and 500 ml/min. respectively. With larger bed height > 25 cm. the depositions on the packing surfaces were found to change with length of bed in the direction of the flow. Comparatively a higher rate of deposition appeared to prevail in the lower half of the packed bed.

### 7.4.6 Correlation of Mass Transfer Coefficient

In addition to an initial lead ion concentration of 700 p.p.m., further experiments with leach liquor with an initial lead ion concentration of 400 p.p.m. were carried out. The flow rates corresponding to Reynolds number in the range from 4.0 to 70.0 for varying bed heights were investigated.

C O N T E N T S

## ACKNOWLEDGEMENTS

I wish to express my sincere appreciation to Dr. M.S. Doulah for his guidance and supervision in all respects over the course of this work. I would also like to thank Dr. G.J. Rees, the co-supervisor, for his help.

The supplying of the steel making dusts used in this work by G.K.N. Tremorfa Steel Works, Cardiff, is gratefully acknowledged.

Thanks are also due to all the technical staff of the Department of Chemical Engineering for their hlep in the construction and maintenance of the experimental apparatus.

I acknowledge the help of the Chemistry and the Physics Sections of the Science Department for their help in the use of Atomic Absorption Spectrophotometer, Scanning Electron Microscope and X-ray diffraction equipment.

Finally, my thanks to Mrs. J. Suthers for typing this thesis.

## DECLARATION

This is to certify that neither this thesis nor any part of it has been presented or is being concurrently submitted in candidature for any other degrees

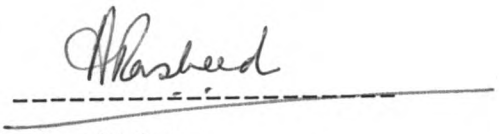

Candidate

Dated December 1981.

## Certificate of Research

This is to certify that, except where specific reference is made, the work in this thesis is the result of the investigation of the candidate.

H Rasheed

Candidate

M. S. Mourbek

Director of Studies

Dated December 1981.

## ABSTRACT

Previous studies on the utilization of electric arc furnace (e.a.f.) dusts and the recovery of valuable metals are based mostly on pyrometallurgical methods. Such methods are expensive to install and operate.

In the present study an attempt has been made to recover the main constituents such as iron, lead and zinc of e.a.f. dusts through a hydrometallurgical route by treating the dust with sodium-hydroxide solution. The iron compounds are obtained as a solid residue while lead and zinc remain in solution which is being used for the separation of lead by cementation. Along with this study the physico-chemical properties have been characterised.

Lead has been separated from the solution by a technique of cementation in batch and continuous systems using zinc as a precipitant metal. In the batch system the effect of temperature, stirring speed, caustic concentration, on the rate of cementation are investigated. The results confirm that the process is controlled by the counter diffusion of reactant and product cations through the mass transfer boundary layer. The results of tests with varying surface area necessitated the study of continuous cementation in a column packed with zinc cylinders.

The apparent mass transfer coefficients evaluated for continuous system with variables such as bed heights, flow rates and initial lead ion concentrations are expressed in terms of $j_D$ factor for mass transfer. The flow rates corresponding to a modified Reynolds number (Re') ranging from 4.0 to 70.0 are investigated and a correlation between $j_D$ and Re' for lead cementation is established.

# NOMENCLATURE

Dimensions of the symbols are given in terms of Mass(M), length (L) and time (T).

| | | Dimensions |
|---|---|---|
| A | frequency factor | $LT^{-1}$ |
| $A_p$ | cross-sectional area of column | $L^2$ |
| a | effective interfacial area | $L^{-1}$ |
| $C_B$ | bulk concentration of solute | $ML^{-3}$ |
| $C_i$ | concentration of solute at the interface | $ML^{-3}$ |
| $C_o$ | initial concentration (batch cementation)<br>inlet concentration (continuous runs) | $ML^{-3}$ |
| $C_t$ | concentration at time t(batch cementation)<br>outlet concentration (continuous runs) | $ML^{-3}$ |
| d | diameter of disc | L |
| $d_o$ | outside diameter of packings | L |
| $d_i$ | inside diameter of packings | L |
| dp | characteristic length | L |
| D | diffusivity | $L^2T^{-1}$ |
| E | activation energy | $ML^2T^{-2}$ |
| $E^o$ | standard electrode potential | volt |
| h | height of cylindrical packing | L |
| J,j | mass flux | $ML^{-2}T^{-1}$ |
| k | first order hetergeneous rate constant | $LT^{-1}$ |
| $k_c$ | rate constant for chemical reaction | $LT^{-1}$ |
| $K_l$ | apparent mass transfer coefficient<br>kinetics constant (continuous runs) | $LT_l^{-1}$<br>$T^{-1}$ |
| L | bed height | L |

| | | |
|---|---|---|
| m | weight of precipitate | M |
| $n_o$ | number of moles of solute initially present | dimensionless |
| $n_t$ | number of moles of solute at time t | do |
| Q | flow rate (continuous runs) | $L^3T^{-1}$ |
| R | gas constant | $L^2T^{2o}K^{-1}$ |
| R1 | inner cylinder radius | L |
| R2 | outer cylinder radius | L |
| S | surface area | $L^2$ |
| T | temperature | $^oK$ |
| t | time | T |
| u | peripheral velocity of cylinder | $LT^{-1}$ |
| $u_i$ | interstitial velocity (continuous runs) | $LT^{-1}$ |
| V | solution volume | $L^3$ |
| $V_s$ | slip velocity of particle | $LT^{-1}$ |
| X | distance | L |
| Greek symbols | | |
| $\omega$ | angular velocity | radians $T^{-1}$ |
| $\rho$ | density of solution | $ML^{-3}$ |
| $\upsilon$ | kinematic viscosity | $L^2T^{-1}$ |
| $\mu$ | solution viscosity | $ML^{-1}T^{-1}$ |
| $\theta$ | angle from pole of sphere | radians |
| $\theta_1$ | angular co-ordinate | radians |
| $\varepsilon$ | voidage of the packings | dimensionless |

Dimensionless Groups

| | | |
|---|---|---|
| Re' | modified Reynolds number | $\sqrt{A_p}G/\mu$ |
| Re | Reynolds number (rotating disc) | $\omega r^2/\upsilon$ |
| $Re_p$ | particle Reynolds number | $d_p V_s/\upsilon$ |
| Sc | Schmidt number | $\upsilon/D$ |
| Sh | Sherwood number (particle) | $kd_p/D$ |
| St | Stanton number | $k/u$ |

# CHAPTER ONE

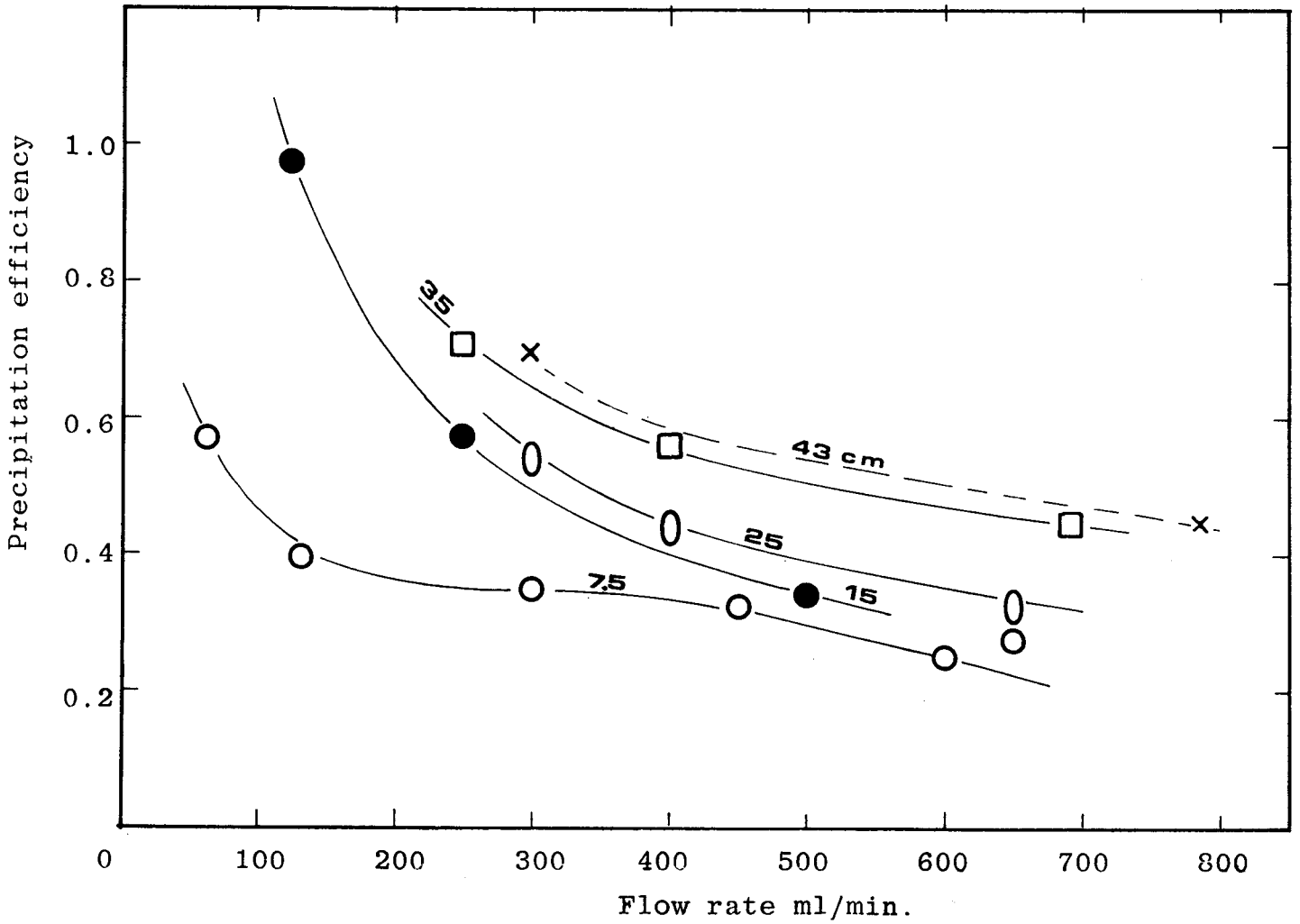


Figure 39. Precipitation efficiency versus flow rate curve for one hour (continuous), temperature $45 \pm 1^{\circ}C$, $Pb^{++}$ conc. = 700 ppm.

The apparent mass transfer coefficient calculated using equation (42) was treated by means of a dimensionless $j_D$ factor, $j_D = k_\ell Sc^{\frac{2}{3}}/u_i$. The evaluation of Schmidt number ($\upsilon/D$) and the interstitial velocity ($u_i$) are given in Appendix II. In the present study the calculated $j_D$ factor for the diffusion of leach ions was correlated to the modified Reynolds number and the results are presented on a log-log plot as shown in Figure 40.

The apparent mass transfer coefficients were determined for steady state cementation. In the present experimental set up, the experimental runs with a Reynolds number of less than 4.0 were impossible to achieve due to difficulties in maintaining very low flow rates. The relationship between $j_D$ factor and Reynolds number for mass transfer in a packed column can be expressed by the equation (24).

$$j_D = 1.15\ Re^{-\frac{1}{2}}$$

The results are shown in Figure 40. The experimental data show deviations from Carberry's model[84]. Such an increase in $j_D$ factors can be attributed to an increase in effective interfacial area, caused by the dissolution of zinc. Packings used for cementation process showed the presence of a large number of eroded areas mainly in the form of pits and grooves. The presence of such a rough surface resulted in an increase of $j_D$ factor.

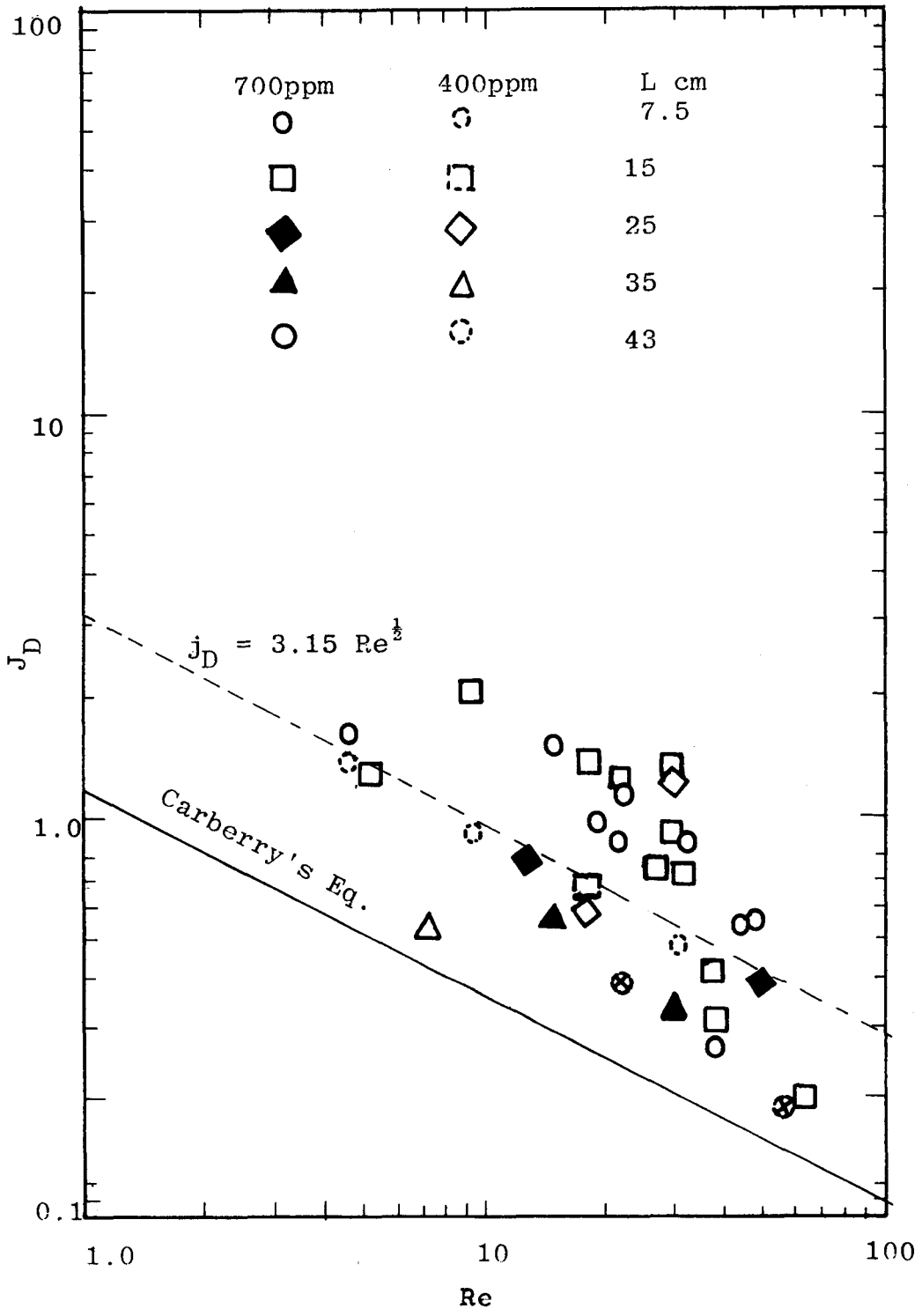


Figure 40. Plot of $j_D$ versus Re

During the cementation process it is possible for deposit formed on the surface to act as cathodic sites for more lead deposition. The overall effect on the lead cementation process would be an increase in mass transfer rates which would be greater than for those unetched surfaces of new packings. The cementation process is still limited by mass transfer of counterdiffusion of cations.

## 7.5 TOTAL ZINC CONSUMPTION

One of the critical factors for industrial use of any cementation process is the total consumption of the precipitant metal sacrificed for the recovery of noble metal. A typical industrial example is the cementation of copper by the use of iron. Machinon and Ingraham reported[62] an excess consumption of iron in the range of 36 - 182 per cent for the process.

In the proposed process for the treatment of e.a.f. leach liquor the excess consumption of zinc can be tolerated to a great extent as the dissolved zinc will be recovered during the next stage of the process. The amount of zinc consumed during the lead cementation was estimated from the stoichiometry of the reaction and the increase of zinc level in the samples taken during cementation.

The zinc consumption here is expressed in terms of "zinc factor"which can be defined as the ratio of amount of zinc used up to the lead precipitated. According to equation

$$Pb^{++} + Zn \rightarrow Zn^{--} + Pb^{o}$$

the theorectical value of the zinc factor is 0.3155. The calculated values for a series of experiments are shown in Table 10 . The results of cementation with varying temperaturesgave a mean value of 0.7104 and for varying stirring rates, the mean value was found to be 0.5658.

The excess consumption of zinc can be defined as

$$\text{Excess consumption} = \frac{(\text{actual} - \text{theoretical}) \times 100}{\text{theoretical}}$$

The values for the entire series of experiments both batch and continuous cementation ranged from 44 to 300%. The higher values were found in the recirculated runs. These values closely resemble the percentage quoted for copper cementation with iron. According to a recent publication[91] normally 60 to 260% can be expected for Cu - Fe systems.

Table 10. Total Zinc Consumption

| Temperature $^{o}C$ | Total Pb deposited (p.p.m) | Total Zn dissolved (p.p.m.) | Zinc Factor |
|---|---|---|---|
| 79 | 3405 | 3650 | 0.9380 |
| 70 | 3300 | 2825 | 0.7621 |
| 60 | 3300 | 2425 | 0.7348 |
| 40 | 3290 | 1825 | 0.5530 |
| 30 | 3180 | 1795 | 0.5644 |
| Rate of stirring (r.p.m.) | | mean = 0.7104<br>excess consumption = 125.16% | |
| 30 | 2250 | 1190 | 0.5288 |
| 650 | 315 | 1700 | 0.5396 |
| 800 | 3225 | 1725 | 0.5348 |
| 1260 | 3575 | 2250 | 0.6293 |
| 1600 | 3645 | 2175 | 0.5967 |
| | | mean = 0.5658<br>excess consumption = 79.34% | |

# C H A P T E R  E I G H T

## CONCLUSION

The lead and zinc contents of e.a.f. steel making dusts can be effectively extracted by treating with solution of sodium-hydroxide. The optimum leaching condition was found when caustic concentration of 400 gm/l at the boiling point of the slurry with solid-liquid ratio of about 20% (w/v) was used. The removal of lead from the leach liquor was studied both in batch and continuous systems.

The study of batch cementation consists of two separate investigations (i) simulated system containing lead ions only, and (ii) leach liquor containing lead and zinc ions. Based on the results obtained in this work the following conclusions can be drawn.

The lead cementation on a zinc surface was found to be a mass transfer process with diffusion as the controlling step. The activation energy obtained for the process also confirmed that the reaction is diffusion controlled with an activation energy ($E_a$) of 6.50 k cals/mole.

As in most diffusion controlled processes the rate of cementation increased with increasing stirring speed until a speed of approximately 1300 r.p.m. was reached. The results were in good agreement with the theory of Levich for mass transfer due to diffusion to a rotating disc.

The effect of deposit on the rate was minimal at low initial lead ion concentrations (< 700 p.p.m. $Pb^{++}$). However, high $Pb^{++}$ ion concentration can retard the rate of diffusion, due to the formation of a relatively smooth and non-porous type of deposit. The caustic concentration of the leach liquor was found to influence the rate of cementation. A decrease in rate constant (k) was observed with increasing caustic concentration.

Further observations were made on the physical nature of the deposit. The deposits were first formed as tiny dendrites on several active sites and developed to a bulbous, spongy structure which covered the entire surface. With stirring the loose deposits were detached from the surface in rapid succession. The deposits were mainly metallic lead with some oxides of lead and zinc. The results with varying initial lead ion concentrations have indicated that the nature of the deposit can significantly alter the rate of cementation.

The results obtained from the study of continuous cementation indicated that with initial low flow rates, the rate of mass transfer increased with increasing flow rates. At high flow rates > 400 ml/min. there were some discrepancies and these were due to a combined effect of intensive mixing condition and decrease in thickness of the diffusion layer to its limiting value.

The study of the effect of varying flow rates with different bed heights were expressed in terms of $j_D$ as a function of a modified Reynolds number ($Re'$). The results indicated an overall increase in effective interfacial area of the packings by a factor of 2.76. A correlation between $j_D$ factor and Re' was established.

Future Investigations

The present study indicates a number of possible areas of interest which demands further investigations.

Since the deposit formed at initial concentrations > 800 p.p.m $Pb^{++}$ has considerable influence on the cementation rates, it will be interesting to extend the study in terms of the deposit protrusions, the exact structure and composition.

From an industrial point of view, the future investigations involving techniques to improve the overall mass transfer rates with high flow rates are essential. Such improvements may be achieved by operating several columns of moderate height arranged in series.

## REFERENCES


1. WHALLEY, L. and BROADIE, V.E., UK - metal reclamation. Prospects for improvement, Resources Policy, 3, p.243-260, 1977

2. HIGLEY, L.W. and FUKUBAYASHI, H.H., Method for Recovery of Zinc and Lead from Electric Furnace Steel Making Dusts, Proc. 4th Mineral Waste Utilization Symp., Chicago, p.295-302, 1974

3. FUKUBAYASHI, H. and HIGLEY, L.W., Recovery of Lead and Zinc from Brass Smelter Dust., Met. Bull(U.K.), 2, p. 6004, 1975

4. SHARP, J.D., Elements of Steel Making Practice, Pergamon Press, London 1966

5. SZEKELY, J. The Steel Industry and the Environment. Marcel Dekker Inc., New York, 1973.

6. BARNARD P.G. et al., Proc. 3rd Mineral Waste Reclamation Symp., Chicago, p.63-68, 1972.

7. A NATIONAL WESTMINSTER BANK STUDY, The United Kingdom Waste Reclamation Industry. Nat. West. Bank Quart. Rev. (U.K.) p. 60-68, 1977

8. MOORE, J.J., Recycling of Non-ferrous Metals. Int. Metals Reviews 5, p.241=264, 1978

9. BASHFORTH, G.R., The Manufacture of Iron and Steel, Chapman and Hall, London p.1-5, 1964.

10. NADKARNI R.M. and WADSWORTH, M.E., Advances in Extractive Metallurgy, Proc. Inst. Min. and Met. p.918-941, 1968

11. HABASHI, F., Principles of Extractive Metallurgy, Vol.2. Hydrometallurgy, Gordon and Breach, New York, 1970

12. MANTELL, C.L., Solid Wastes, origin, collection, processing and disposal., John Wiley and Sons, London, 1975

13. KASHIWALA, M. and KUMAGI, T., Waelz Process for Leach Residues at Nisso Smelting Company, Ltd., Symp. A.I.M.E., World Symp. on Mining and Metallurgy of Lead and Zinc, p.409-422, 1970

14. BAN, T.E., U.S. Patent 3, 262, 771, 1966

15. THOM, G.G.W., U.S. Patent 3, 403, 018, 1968

16. U.S. BUREAU OF MINES, Reclaiming and Recycling Secondary Metals, Engng. Mining J. (U.S.A.) 176, 7, p.94-98, 1975

17. COCHRAN, A.A. and GEORGE, L.C., Recovery of Metals from a Variety of Industrial Wastes, Resource Recovery Conservation, (Holland), 2, 1 p.57-65, 1976.

18. HOLOWATY, M.O., A Process for Recycling of Zinc Bearing Steel Making Dusts, Chicago Regional Technical Meeting, A.I.S.I., 1971

19. POWELL, H.E. et.al., Converting Stainless Steel Furnace Flue Dusts and Wastes to a Recyclable Alloy, U.S. Bureau of Mines, Report Rl 8039

20. STIRLING, H.T., and KINSEY, F.W., Improved Techniques for Processing Steel Plant Fines, J. of Metals, 19, p.83-87, 1967

21. ANON. Recycling Steel/Zinc Dust, Met. Bull.(U.K.), 22, 6044, 1975.

22. LARPENTEUR, B.J., U.S. Patent 3.547.623, 1970.

23. THE OPEN UNIVERSITY, Metal Production, The Open University Press, Milton Keynes, 1979

24. BURKIN, A.R., The Hydrometallurgical Process, E. & F.N. Spon Ltd., London 1966

25. DAVIES, G.A., Unit Operations in Hydrometallurgy, Chemistry and Industry 13, 420-427, 1981

26. BAROCH, C.T., et.al. The caustic Electrolytic Zinc Process, J. Am. Electrochem, 100, 4, p.165-172, 1953

27. WINTER, U.S. Patent 3.326.783, 1967

28. WINTER et.al. U.S. Patent 3.515.510, 1970

29. HAAS, C.C., U.S. Patent 1.825.949, 1931

30. U.S. BUREAU OF MINES, Recycling of Steel Making Dusts, Research Report No.52, 1972

31. CUSANELLI, D.C., et.al. U.S. Patent 3.743,501, 1973

32. ABBRUZZESE, C., Caustic Leaching of Oxidized Lead-Zinc Ores, Proc. of Hydrometallurgy '81, U.M.I.S.T., U.K., Soc. of Chem. Ind. Symp., 1981

33. RINELLI, G., and ABBRUZZESE, C., U.S. Patent 4.191.729, 1980

34. MERRILL, C.C., and LANG, R.S., U.S. Bureau of Mines, Research Report No. 6576, 1965

35. KUPPER, R. and VOL ROLL, A.G., U.S. Patent 4.018.680, 1977

36. DUVAL, L.A., U.S. Patent 3.373.069, 1968.

37. GOENS, D.N. et.al. U.S. Patent 3.973.949. 1976.

38 BRAUN, R.L., LEWIS, A.E., WADSWORTH, M.E., In place Leaching of Primary Sulphide Ores, Proc. of the Solution Mining Symp. 103rd, A.I.M.E. Annual Meeting, Texas, p.295-323, 1974

39. WADSWORTH, M.E., Reduction of Metals in Solutions, Trans. Metall. Soc., A.I.M.E., 245, p.1381-1394, 1969

40. LAVENSPIEL, O., Chemical Reaction Engineering, John Wiley and Sons, Inc., New York, 1962

41. KUNII, D., and LAVENSPIEL, O., Fluidization Engineering, John Wiley and Sons, Inc., New York, 1969

42. POWER, G.P. and RITCHIE, I.M., A Contribution of the Theory of Cementation (metal displacement) Reactions, Aust. J. of Chemistry, 29, p.699-709, 1976

43. STRICKLAND, P.H. and LAWSON, F. The Measurement and Interpretation of Cementation Rate Data, Int. Symp. on Hydrometallurgy, Chicago, 1973

44. SPEDDEN, H.R., MALOUF, E.E., and PRATER, J.D., Cone-type Precipitations for Improved Copper Recovery, Min. Engng., 18, p.57-62, 1966

45. BAOK, A.E, Precipitation of Copper from Dilute Solutions Using Particulate Iron, J. of Metals, 19, p.27-29, 1967

46. CENTNERSZWER, M., and HELLER, W., Kinetik der Unwaldung der metallionen in neutralatome unter der cinwitkung des metallischen Zinks, S. fur Physik, Chemie, A161, p.113-128, 1932

47. KING, C.V. and BURGER, M.M. The Rate of Displacement of Copper from Solutions of Sulphate by Cadmium and Zinc. Trans. Electrochem. Soc., 65, p.403-411, 1934

48. KING, C.V. and MAYER, M. The Rate of Dissolution of Zinc and Cadmium in Chromic Chloride Solutions. J.Elec. Soc., 100, p.473-479, 1953

49. GLICKSMAN, R., et.al. Rate of Displacement of Silver from Aqueous Silver Nitrate by Zinc and Copper. J.Elect. Soc., 100, 12, p.580-585, 1953

50. LEE, E.C., et.al. Precipitation of Cadmium with Zinc from Dilute Aqueous Solutions: Under an Inert Atmosphere. Inst., Min. Met., p. c.87-91, 1975

51. LEE, E.C., et.al. Co-deposition of Copper and Cadmium onto Zinc. Inst. Min. Met. J. p.c.170-179, 1978

52. INGRAHAM, T.R. and KERBY, R., Kinetics of Cadmium Cementation on Zinc in Buffered Sulphate Solutions, Trans. Met. Soc. of A.I.M.E., 245, p.17-21, 1969

53. EPISKOPOSYAN, M.L., and KOKOVSKII, I.A., An Examination of Copper and Silver Cementation Kinetics with Metallic Iron from Chloride Solutions, Soviet J. Non-ferrous Metals, 6, 10, p.16-21, 1965

54. BISWAS, A.K., REID, J.G. Investigation of the Cementation of Copper on Iron. Proc. Aust. Inst. Min. Met. 242, p.37-45, 1972.

55. DROZDOV, B.V., Activation Energy of Contact Reduction of Copper on Solution by Nickel Powder. J. Applied Chem. U.S.S.R., 33, p.638-640, 1960

56. PAULIN, A. and ZLATKOVIC, Kinetics of Copper Precipitation with Iron in Sulphate and Chloride Solutions. Inst. Min. and Met. p.c.106-112, 1978

57. SAREYED-DIM, N.A., LAWSON, F., Cementation onto Particulates, Trans. Inst. Min. Metall. Section C, 85, p.c1-c6, 1976

58. LAWSON, F., and NHAN, L.T., Kinetics of Removal of Cobalt from Zinc Sulphate Electrolytes by Cementation. Proc. of Hydrometallurgy'81, Soc. of Chem. Ind. Symp. Manchester, U.K., 1981

59. GALECKI, A., and TOMASZEWSKI, J., Studja nad skladem chemicznymosadow stracajacych sie na cynku z roztworow siarczanu miedziowego, czesc 1, Rooznikii Chemii, 10, p.437-471, 1930

60. STRICKLAND, P.H., and LAWSON, F., Cementation of Copper with Zinc from Dilute Aqueous Solutions. Proc. Aust. Inst.. Min. Met. 236, p.25-34, 1974

61. LEVICH, V.G. Physicochemical Hydrodynamics, Prentice-Hall Inc., New Jersey, 1962

62. MACKINON, D.J. and INGRAHAM, T.R., Copper Cementation on Aluminium Canning Sheet, Can.Met. Quartz 10,3,p.197-201, 1971

63. VON HAHN, E.A. and INGRAHAM, T.R., Kinetics of Silver Cementation on Copper in Perchloric Acid and Alkaline Cyanide Solutions, Trans. Metall, Soc., A.I.M.E., 239, p.1895-1905, 1967

64. RICKARD R.S. and FUERSTENAU M.C., An Electrochemical Investigation of Copper Cementation by Iron, Trans. Metall. Soc., A.I.M.E., 242, p.1487-1493, 1968

65. MILLER, J.D., An Analysis of Concentration and Temperature Effects in Cementation Reactions, Miner. Sci. Eng., 5, p.242-254, 1973

66. FISHER, W.W. and GROVES, R.G., Physical Aspects of Copper Cementation on Iron, U.S. Bureau of Mines, Research Report. R1, 7761, 1973

67. KABONOVA, L.M., and KHAN, O.A., Cementation of Cadmium from Concentrated Sulphate Solutions, Trans. Altaisk Eorno-Met. Nauchn-Issled., Inst. Akad, Nauk Kazakhsk, S.S.R., 11, p.34-47, 1961 (Chem. Abst. 56:13909).

68. HAMDORF, C.J., Precipitation of Lead and Silver from Brine Solutions by Metallic Iron, Proc. Aust. Inst. Min. Met., 199, p.19-50, 1961

69. MILLER, J.D. and BECKSTEAD L.W., Surface Deposit Effects in the Kinetics of Copper Cementation by Iron, Trans. Met. Soc., A.I.M.E., 4, p.1967-1973, 1973

70. RICKARD, R.S. and FUERSTENAU, M.C., An Electrochemical Investigation of Copper Cementation by Iron, Trans. Metall. Soc., A.I.M.E., 242, p.1487-1493, 1968

71. KAMECKI, J., SEDZIMIR and GMYTRYK, M., Kinetyka Wytracania olowin zelazem i Gynkiem z roztworow chlorkowych., Polska Akad., Nauk., Arch. Hutnic, 1, p.195-216, 1956

72. HEIN, K., Cadmiumzementation aus technischen zinklaugen, Freiberger Forshungshefte, B29, p.155-214, 1958

73. NADKARNI R.M. and WADSWORTH, M.E., A Kinetic Study of Copper Precipitation on Iron: Part II Trans. Met. Soc. of A.I.M.E., 239, p.1066-1074, 1967

74. GABE, D.R. and ROBINSON, D.J., Mass Transfer in a Rotating Cylinder Cell I, Laminar flow, Electrochimica Acta, 17, p.1191-1127, 1972

75. GABE, D.R. and ROBINSON, D.J., Mass Transfer in a Rotating Culinder Cell II. Turbulent flow, Electrochimica Acta,17, p.1129-1137, 1972

76. NEWMAN, J., Mass Transfer to a Rotating Sphere at High Schmidt Numbers, J. Electrochem. Soc., 119, p.69-71, 1972

77. RIDDIFORD, A.C., The Rotating Disc System., Advances in Electrochemistry and Electrochem. Engng, Vol.4. Interscience, New York, 1966

78. BIRCUMSHAW, L.L., and RIDDIFORD, A.C., Transport Control in Heterogeneous Reactions., Quart. Review of Chem. Soc., 6, p.157-185, 1952

79. GREGORY, D.P. and RIDDIFORD, A.C., Transport to the Surface of a Rotating Disc., J. of Chem. Soc., p.3756-3764, 1956

80. BALBERYSZKI, T. and IBAGOS, L., Optimization of Process Parameters for a Continuous Copper Cementation System. Int. Symp. on Hydrometallurgy, A.I.M.E., 1973.

81. PLASKIN, I.N., and BUDNIKOVA, O.H., Oxidation Reduction Process During Precipitation of Metals from Cyanide Solutions, Izv. Akad. Nank, Otdel. Tekh, Nank, U.S.S.R., 2, p.267-272, 1951

82. SCHRADER, R., and CLAUSS, D. Uber die zementation von kupfer mit metallischen nickel im Ammoniakalischen beit., J. Prakt. Chem., 9, p.194-200, 1959

83. GUPTA, A.S. and THODES, G., Mass and Heat Transfer through fixed and Fluidized Beds., Chem. Engng. Prog. 58, p.58-62, 1962

84. CARBERRY, J.J. A Boundary-layer model of Fluid-Particle Mass Transfer in Fixed Beds., A.I.Ch.E. Jour., 6. p.460-462, 1960

85. INSTRUCTION MANUAL FOR COULTER COUNTER MODEL TA

86. INSTRUCTION MANUAL OF HAAKE VISCOMETER

87. PERRY, J.H. Chemical Engineers' Handbook, 4th Ed. McGraw-Hill, p.16-23

88. REYNOLDS, R.J. and ALDOUS, K., Atomic Absorption Spectroscopy, Griffin, London, 1970

89. VARIAN TECHTRON- Manual. Analytical Methods for Flame Spectroscopy.

90. POURBAIX, M. Atlas of Electrochemical Equilibria in Aqueous Solutions, Pergamon Press, London 1966

91. ANNAMALAI, V., and HISKEY, J.B. A kinetic study of Copper Cementation on Pure Aluminium, Soc.Min.Engrs., Min. Engng., p.650 - 659., 1978

# A P P E N D I X  I

Table No. 11. Pressure - Density Relationship of e.a.f. dusts

| Gauge Pressure in p.s.i. | Loading Pressure ($NM^{-2} \times 10^2$) | Compact Density in $gm/cm^3$ |
|---|---|---|
| 10 | 17 | 3.2890 |
| 30 | 110 | 3.8220 |
| 50 | 208 | 4.0411 |
| 65 | 268 | 4.1224 |

Table No. 12 Percentage Recovery of Lead and Zinc during the leaching for e.a.f. dusts at different temperatures

| Temperature - | 60°C | | | | 25°C | | | |
|---|---|---|---|---|---|---|---|---|
| Conc. of NaOH | 200 gm/l | | 400 gm/l | | 200 gm/l | | 400 gm/l | |
| Metals / Time (mins) | Pb | Zn | Pb | Zn | Pb | Zn | Pb | Zn |
| 10 | 84.00 | 23.00 | 71.00 | 31.00 | - | 13.00 | 44.20 | 8.39 |
| 20 | 86.00 | 26.50 | 74.00 | 46.50 | 66.00 | 15.00 | 59.30 | 16.42 |
| 30 | 79.50 | 27.00 | 74.00 | - | - | - | 62.00 | 20.15 |
| 40 | 79.10 | - | 74.20 | 44.00 | 80.00 | 21.00 | 72.00 | 25.00 |
| 60 | 81.00 | 33.00 | - | 48.00 | - | - | - | - |
| 80 | 84.50 | 28.90 | 74.30 | 48.60 | 80.30 | 20.72 | 76.60 | 31.00 |
| 120 | 91.00 | 35.80 | 84.00 | 55.00 | 81.50 | 20.48 | 73.00 | 35.10 |
| 180 | 98.00 | 37.00 | 86.00 | 57.50 | - | 24.00 | 74.00 | 36.18 |

Table 13 Order of reaction for lead cementation from leach liquor at temperature = 50°C rpm = 800

Experimental Data for Figure 23.

| Time (mins.) | $Pb^{++}$ conc. (ppm) |
|---|---|
| 0 | 3600 |
| 20 | 2000 |
| 40 | 850 |
| 60 | 400 |
| 80 | 190 |
| 100 | 100 |
| 120 | 50 |
| 140 | 25 |
| 160 | 25 |
| 180 | 50 |

Table No. 14 Results of Kinetic Data for Figure 16

| Temperature : 45°C | |
|---|---|
| Surface area $cm^2$ :19.6345 | |
| Stirring speed rpm : 800 | |
| Specific rate constant : $2.0536 \times 10^{-2}$ $cm.sec^{-1}$ | |
| Time (mins) | $(Pb^{++})$ in p.p.m. |
| 0 | 3675 |
| 5 | 3250 |
| 10 | 3100 |
| 15 | 2675 |
| 20 | 2575 |
| 40 | 1700 |
| 60 | 1250 |
| 80 | 975 |
| 100 | 650 |
| 120 | 450 |
| 140 | 350 |
| 160 | 225 |

Table No. 15 Effects of Temperature on the rate of cementation.
$Pb^{++}$ conc. in p.p.m. Data for Figure 17

| Temperature $^{o}C$ | 22.50 | 30.66 | 40.63 | 60.33 | 70.48 | 79.0 |
|---|---|---|---|---|---|---|
| Surface area $cm^2$ | 19.6345 | 19.6345 | 19.6345 | 19.6345 | 19.6345 | 19.6345 |
| Specific rate $cm.sec^{-1} \times 10^{-2}$ | 0.822 | 1.06 | 1.56 | 2.56 | 3.89 | 4.98 |
| Time (mins) | $(Pb^{++})$ | $(Pb^{++})$ | $(Pb^{++})$ | $(Pb^{++})$ | $(Pb^{++})$ | $(Pb^{++})$ |
| 0 | 3650 | 3550 | 3600 | 3600 | 3450 | 3750 |
| 20 | 3200 | 2950 | 2750 | 2250 | 1900 | 1700 |
| 40 | 2800 | 2500 | 2250 | 1500 | 900 | 750 |
| 60 | 2500 | 2150 | 1650 | 1000 | 500 | 450 |
| 80 | 2100 | 1770 | 1200 | 650 | 350 | 250 |
| 100 | 1850 | 1460 | 1000 | 450 | 220 | 160 |
| 120 | 1600 | 1200 | 750 | 300 | 150 | 120 |
| 140 | 1400 | 1000 | - | 280 | 150 | 120 |
| 160 | 1120 | 840 | 450 | 200 | 100 | - |
| 180 | 1050 | 720 | 360 | 200 | 100 | - |
| 200 | 900 | 600 | - | - | - | - |

Table No. 16 Results for Arrhenius Plot - simulated system

| Temperature $^{o}C$ | Specific Rate Constant cm/sec x $10^{-2}$ | $\frac{1}{T} \times 10^{-3}$ |
|---|---|---|
| 22.50 | 0.822 | 3.3818 |
| 30.66 | 1.06 | 3.2909 |
| 40.63 | 1.56 | 3.1864 |
| 70.48 | 3.89 | 2.9096 |
| 79.00 | 4.98 | 2.8392 |

Table No. 17 Data for Figures 20 and 21

| rpm | Specific Rate Constant cm/sec x $10^{-2}$ | Squareroot of rpm ($\omega$rad/sec) |
|---|---|---|
| 30 | 0.59 | 1.7724 |
| 60 | 0.86 | 2.5066 |
| 100 | 1.06 | 3.2360 |
| 280 | 1.55 | 5.4149 |
| 680 | 2.80 | 8.4385 |
| 900 | 3.03 | 9.7081 |
| 1260 | 3.10 | 11.4868 |
| 1600 | 3.37 | 12.9441 |

Table No.18 Effects of Stirring Speeds - Simulated System (Figure 19) on the rate of cementation

| Temperature $^{o}C$ | 45 | 45 | 50 | 45 | 45 | 45 | 45 |
|---|---|---|---|---|---|---|---|
| Stirring speed rpm | 30 | 100 | 250 | 680 | 800 | 1200 | 1600 |
| Specific Rate Constant $cm.sec^{-1} \times 10^{-2}$ | 0.59 | 1.06 | 1.55 | 2.80 | 2.05 | 3.10 | 3.37 |
| Time (mins) | ($Pb^{++}$) | ($Pb^{++}$) | ($Pb^{++}$) | ($Pb^{++}$) | ($Pb^{++}$) | ($Pb^{++}$) | ($Pb^{++}$) |
| 0 | 3650 | 3750 | 3650 | 3750 | 3675 | 3775 | 3750 |
| 20 | 3550 | 3050 | 2350 | 2160 | 2575 | 2450 | 2125 |
| 40 | 3000 | 2150 | 1600 | 1350 | 1700 | 1475 | 1250 |
| 60 | 2750 | 1750 | 1250 | 800 | 1250 | 975 | 700 |
| 80 | 2450 | 1540 | 800 | 500 | 975 | 575 | 410 |
| 100 | 1900 | 1250 | 480 | 340 | 650 | 300 | 220 |
| 120 | 1400 | 1100 | 300 | 210 | 450 | 200 | 105 |
| 140 | 1330 | 900 | 210 | 160 | 350 | 125 | 75 |
| 160 | 1250 | 830 | 150 | 100 | 225 | 50 | 50 |
| 180 | 1150 | 750 | 150 | 90 | - | - | 25 |
| 200 | 1050 | 700 | - | 50 | - | - | - |

$Pb^{++}$ conc. in p.p.m.

Table 19 Effect of stirring on the rate of cementation of leach liquor, $Pb^{++}$ conc. = 3600 ppm.

| Temperature = $45^{o}C$ | | | | |
|---|---|---|---|---|
| Stirring speed (rpm) | 250 | 550 | 900 | 1100 |
| Surface area ($cm^2$) | 19.6345 | 19.6345 | 19.6345 | 19.6345 |
| Specific rate constant $cm.sec^{-1}$ x $10^{-2}$ | 1.298 | 1.535 | 1.909 | 2.385 |
| Time (mins) | $Pb^{++}$ | $Pb^{++}$ | $Pb^{++}$ | $PB^{++}$ |
| 20 | 2875 | 2700 | 2750 | 2000 |
| 40 | 2350 | 2050 | 1946 | 1425 |
| 60 | 1800 | 1750 | 1370 | 1125 |
| 80 | 1550 | 1475 | 1143 | 825 |
| 100 | 1225 | 1025 | 905 | 600 |
| 120 | 1025 | 850 | 780 | 450 |
| 140 | 850 | 735 | 473 | 400 |
| 160 | 650 | 515 | - | 390 |
| 180 | 550 | 440 | - | 175 |

Table 20 Effect of baffles on the rate of cementation

| Concentration of NaOH = 400 gm/l | | |
|---|---|---|
| Stirring speed (rpm) = 550 | | |
| Surface area. $cm^2$ = 19.6345 | | |
| Specific rate constant $cm.sec^{-1} \times 10^{-2}$ | 1.57 | 2.12 |
| Time (mins) | Baffles ($Pb^{++}$) | Without baffles ($Pb^{++}$) |
| 0 | 3675 | 3690 |
| 20 | 2650 | 2400 |
| 40 | 1950 | 1820 |
| 60 | 1500 | 1270 |
| 80 | 1350 | 950 |
| 100 | 1000 | 650 |
| 120 | 750 | 500 |
| 140 | 500 | 450 |
| 160 | 300 | 375 |
| 180 | 200 | - |

Table No.21 Effects of Surface Area on the rate of cementation of Leach liquor - ($Pb^{++}$) conc. in p.p.m.

| Temperature $^{o}C$ | 45 | 45 | 45 | 45 |
|---|---|---|---|---|
| Surface area $cm^2$ | 4.9087 | 7.0685 | 9.6211 | 12.566 |
| Specific Rate Constant $cm/sec^{-1} \times 10^{-2}$ | 3.94 | 8.42 | 7.57 | 8.64 |
| Time (mins) | ($Pb^{++}$) | ($Pb^{++}$) | ($Pb^{++}$) | ($Pb^{++}$) |
| 0 | 2975 | 2875 | 2875 | 3000 |
| 20 | 2625 | 2250 | 2325 | 2450 |
| 40 | 2200 | 1100 | 1200 | 1825 |
| 60 | 1875 | 775 | 650 | - |
| 80 | 1500 | 450 | 250 | 175 |
| 100 | 1200 | 240 | 75 | 45 |
| 120 | 875 | 150 | 25 | 25 |
| 140 | 400 | 90 | 0 | 45 |
| 160 | 360 | 75 | 0 | 45 |
| 180 | 325 | 50 | 0 | - |

Table 22 Experimental Data for Cementation with Different Initial lead ion concentration of leach liquor, rpm = 550, temperature = 45°C

| Time (mins) \ Initial lead ion conc. (ppm) | 1250 | 2500 | 3500 | 5500 |
|---|---|---|---|---|
| 20 | 950 | 1625 | 2700 | 3750 |
| 40 | 800 | 1300 | 2050 | 2800 |
| 60 | 612 | 875 | 1750 | 2100 |
| 80 | 462 | 600 | 1475 | 1550 |
| 100 | 375 | 390 | 1025 | 1125 |
| 120 | 275 | 275 | 850 | 900 |
| 140 | 212 | 200 | 735 | 650 |
| 160 | 125 | 100 | 515 | 550 |
| 180 | 100 | 75 | 440 | 400 |

Table No. 23 Effect of Stirring - Simulated System

Data for Figure 26

| r.p.m. | ω(rad/sec) | k cm/sec | Sh | Re | $Re^{\frac{1}{2}}$ | $Re^{\frac{1}{2}}SC^{\frac{1}{3}} \times 10^{-3}$ |
|---|---|---|---|---|---|---|
| 30 | 3.1414 | 0.0059 | 90.1864 | 404.0697 | 20.1014 | 0.134 |
| 60 | 6.2830 | 0.0086 | 131.4582 | 808.1652 | 28.4282 | 0.189 |
| 100 | 10.4716 | 0.0106 | 162.0299 | 1346.9335 | 36.7005 | 0.244 |
| 280 | 29.3211 | 0.0155 | 236.9306 | 3771.4936 | 61.4124 | 0.409 |
| 680 | 71.2082 | 0.0280 | 428.003 | 9159.3177 | 95.7043 | 0.638 |
| 900 | 94.2472 | 0.0303 | 463.1611 | 12122.7600 | 110.1034 | 0.734 |
| 1260 | 131.9465 | 0.0310 | 473.8612 | 16971.9200 | 130.2763 | 0.869 |
| 1600 | 167.5497 | 0.0337 | 515.1329 | 21551.4630 | 146.8041 | 0.979 |

Table 23(contd) Effects of stirring-Leach Liquor

| r.p.m. | (rad/sec) | k cm/sec | Sh | Re | $Re^{\frac{1}{2}}$ | $Re^{\frac{1}{2}}SC^{\frac{1}{3}} \times 10^{-3}$ |
|---|---|---|---|---|---|---|
| 250 | 26.1799 | 0.0128 | 195.6588 | 3367.452 | 58.0297 | 0.387 |
| 550 | 57.5958 | 0.0233 | 356.1608 | 7408.3948 | 86.0720 | 0.574 |
| 650 | 68.06 | 0.0181 | 276.6737 | 8755.0 | 93.5701 | 0.624 |
| 900 | 94.2477 | 0.0202 | 308.7740 | 12122.817 | 110.1036 | 0.734 |
| 1100 | 115.1917 | 0.0255 | 389.7890 | 14816.78 | 121.724 | 0.812 |

Table 24 Effect of Initial Lead ion Concentration on Cementation in the Recirculation column. Experimental Data for Figure 35.

| Bed height = 7.5cm | | Flow rate = 300 ml/min | | |
|---|---|---|---|---|
| Time (mins) | $Pb_o^{++}$ = 1100 ppm | $Pb_o^{++}$ = 825 ppm | $Pb_o^{++}$ = 450 ppm | $Pb_o^{++}$ = 275 ppm |
| 10 | 900 | 700 | 425 | 250 |
| 20 | 750 | 512 | 375 | 225 |
| 30 | 562 | 312 | 300 | 225 |
| 40 | 487 | 150 | 250 | 225 |
| 50 | 450 | 57 | 175 | - |
| 60 | 312 | 62 | 125 | 175 |
| 70 | 262 | 37 | 112 | - |
| 80 | 262 | 37 | 87 | 138 |
| 90 | 175 | 25 | 75 | - |
| 110 | 175 | 25 | 75 | 105 |
| 130 | 170 | - | 78 | 88 |
| 140 | - | 25 | - | - |

Table 25 Effect of Flow rates on lead cementation
$Pb^{++}$ = 1800 ppm.
Experimental Data for Figure 33.

Recirculation Column

Packing height = 7.5cm Temperature = $45 \pm 0.5^{o}C$

| Flow rate ml/min / Time (mins) | 1,000 | 800 | 600 | 415 | 230 |
|---|---|---|---|---|---|
| 10 | 1,250 | 1,038 | 1,012 | 1,025 | 1,100 |
| 20 | 788 | 563 | 725 | 500 | 712 |
| 30 | 600 | 313 | 450 | 337 | 525 |
| 40 | 438 | 175 | 313 | 200 | 412 |
| 50 | 250 | 100 | 173 | 125 | 300 |
| 60 | 162 | 75 | 125 | 50 | 125 |
| 70 | 137 | 55 | 88 | 37 | 45 |
| 80 | 88 | 45 | 70 | 30 | 45 |
| 90 | 88 | 38 | 50 | 25 | - |
| 110 | 85 | 25 | 38 | 25 | - |
| 130 | - | - | 38 | - | - |

Table 26 Experimental Data of Continuous Cementation.

| Run | Flow rate (ml/min.) | Interstitial Velocity, u (cm/sec) | Bed Height L (cm) | Initial lead ion conc.(ppm) | Modified Reynolds No. Re' | Apparent mass transfer coefficient $k_\ell \times 10^{-3}$ (cm/sec) | $j_D$ |
|---|---|---|---|---|---|---|---|
| 70 | 60 | 0.0553 | 7.5 | 380 | 4.5172 | 1.1936 | 1.3746 |
| 71 | 60 | 0.0553 | 7.5 | 700 | 4.5172 | 1.5279 | 1.6217 |
| 72 | 125 | 0.1154 | 7.5 | 700 | 9.4109 | 1.6467 | 0.9087 |
| 73 | 200 | 0.1846 | 7.5 | 682 | 15.0574 | 4.3043 | 1.4849 |
| 74 | 300 | 0.2769 | 7.5 | 682 | 22.5862 | 3.8690 | 0.8898 |
| 75 | 450 | 0.4154 | 7.5 | 725 | 33.8793 | 5.2420 | 0.8036 |
| 76 | 600 | 0.5539 | 7.5 | 735 | 45.1724 | 4.8713 | 0.5599 |
| 77 | 650 | 0.6001 | 7.5 | 720 | 48.9367 | 5.2944 | 0.5618 |
| 78 | 125 | 0.1154 | 15.0 | 700 | 9.4109 | 3.7920 | 2.0926 |
| 79 | 250 | 0.2308 | 15.0 | 380 | 18.8218 | 2.4908 | 0.6873 |
| 80 | 300 | 0.2769 | 15.0 | 685 | 22.5862 | 5.2400 | 1.2051 |
| 81 | 400 | 0.3693 | 15.0 | 725 | 30.1149 | 7.5457 | 1.3012 |
| 82 | 450 | 0.4154 | 15.0 | 715 | 33.8793 | 4.6657 | 0.7153 |
| 83 | 510 | 0.4708 | 15.0 | 737 | 38.3965 | 2.9782 | 0.4028 |

Table 26 (continued)

| RUN | Flow rate (ml/min.) | Interstitial Velocity, u (cm/sec) | Bed Height L (cm) | Initial lead ion conc.(ppm) | Modified Reynolds No. re' | Apparent mass transfer coefficient $k \times 10^{-3}$ (cm/sec) | $j_D$ |
|---|---|---|---|---|---|---|---|
| 84 | 835 | 0.7707 | 15.0 | 685 | 62.8645 | 2.4068 | 0.1988 |
| 85 | 250 | 0.2308 | 25.0 | 425 | 18.8218 | 2.1671 | 0.5979 |
| 86 | 400 | 0.3693 | 25.0 | 412 | 30.1149 | 7.5457 | 1.3012 |
| 87 | 690 | 0.6370 | 25.0 | 737 | 51.7482 | 3.9641 | 0.3963 |
| 88 | 165 | 0.1523 | 25.0 | 700 | 12.5000 | 1.7673 | 0.7390 |
| 89 | 200 | 0.1846 | 35.0 | 725 | 15.0574 | 1.5492 | 0.5344 |
| 90 | 87 | 0.0877 | 35.0 | 385 | 7.2000 | 7.1248 | 0.5173 |
| 91 | 400 | 0.3693 | 35.00 | 682 | 30.1149 | 1.9365 | 0.3339 |
| 92 | 300 | 0.2769 | 43.0 | 375 | 22.5862 | 1.7224 | 0.3961 |
| 93 | 790 | 0.7293 | 43.0 | 375 | 59.4770 | 2.1530 | 0.1891 |

# A P P E N D I X  II

Calculation of Effective Interfacial Area

The effective interfacial area 'a' is evaluated from the dimension of a single packing, using the definition

$$a = \frac{\text{area of packing}}{\text{volume of packing}}$$

The preliminary, effective interfacial area is calculated by considering only the outer surface of the packing is used in the transfer operation. The dimensions of a single packing are as follows

$d_o$ = 1.2732 cm $\qquad$ $d_i$ = 1.1332 cm

h = 1.7000 cm $\qquad$ thickness = 0.0700 cm

The total area of a single cylinder (inner surface not considered)

$$A = \pi d_o h + 2\pi(d_o^2 - d_i^2)/4$$

Assuming that the packings are touching one another, and considering the area of a single cylinder in a stacked position

$$A = \pi d_o h$$

The mean area available to transfer

$$= \tfrac{1}{2} \left| \pi d_o h + 2\pi(d_o^2 - d_i^2)/4 + \pi d_o h \right|$$

$$= \pi d_o h + \pi(d_o^2 - d_i^2)/4$$

$$\therefore A_{av} = \pi \times 1.2732 \times 1.7 + \pi(1.2732^2 - 1.1322^2)/4$$

$$= 7.0643 \text{ cm}^2$$

Area of five holes = $5 \times \frac{\Pi}{4} \times 0.32^2$

$= 0.4021 \text{ cm}^2$

$A_{av} = 7.0643 - 0.4021$

$= 6.6622 \text{ cm}^2$

Volume of packing $V = \Pi(d_o^2 - d_i^2)1.7/4$

$= \frac{\Pi}{4}(0.3369)1.7$

$= 0.4498 \text{ cm}^2$

Total volume of 5 holes $= \frac{\Pi}{4} \times 0.32^2 \times 0.07 \times 5$

$= 0.0281 \text{ cm}^3$

$\therefore V = 0.4498 - 0.0281$

$= 0.4216 \text{ cm}^3$

$\therefore$ The effective interfacial area 'a'

$= \frac{\text{Net area of a packing}}{\text{Net volume of a packing}}$

considering the bed voidage e = 0.85

$$a = (1 - e)\frac{6.6622}{0.4216}$$

$= \underline{2.3703} \text{ cm}^2/\text{cm}^3$

If both sides of the packings are considered

$$A_{av} = \pi d_o h + \pi d_i h + \pi(d_o^2 - d_i^2)/4 = 13.3244$$

$$\therefore \quad a = \frac{13.3244 \times 0.15}{0.4216}$$

$$= \underline{4.7406} \text{ cm}^2/\text{cm}^3$$

Calculation of Schmidt Number

The kinematic viscosity ($\upsilon$) and the Schmidt number (Sc) are calculated for the operating temperature of 45°C.

kinematic viscosity, with caustic concentration of leach liquor = 100 gm/l.

$$\upsilon = \frac{\mu}{\rho} = \frac{0.042}{1.13} = 37.10 \times 10^{-3} \text{cm}^2/\text{sec}$$

Schmidt number:

$$Sc = \frac{\upsilon}{D}$$

$$= \frac{37.10 \times 10^{-3}}{7.3 \times 10^{-5}} = 508.21$$

This value was used in determining the $j_D$ factor for mass transfer.

A Sample Calculation of interstitial velocity ($u_i$) - Continuous cementation.

Example: Flow rate (Q) = 400 ml/min

e = 0.85. Cross-sectional area of Column A = 21.2371cm$^2$

$$u_i = \frac{Q}{A.e} = \frac{400}{21.2371 \times 0.85 \times 60} = 0.3693 \text{ cm/sec}$$

# A P P E N D I X  III

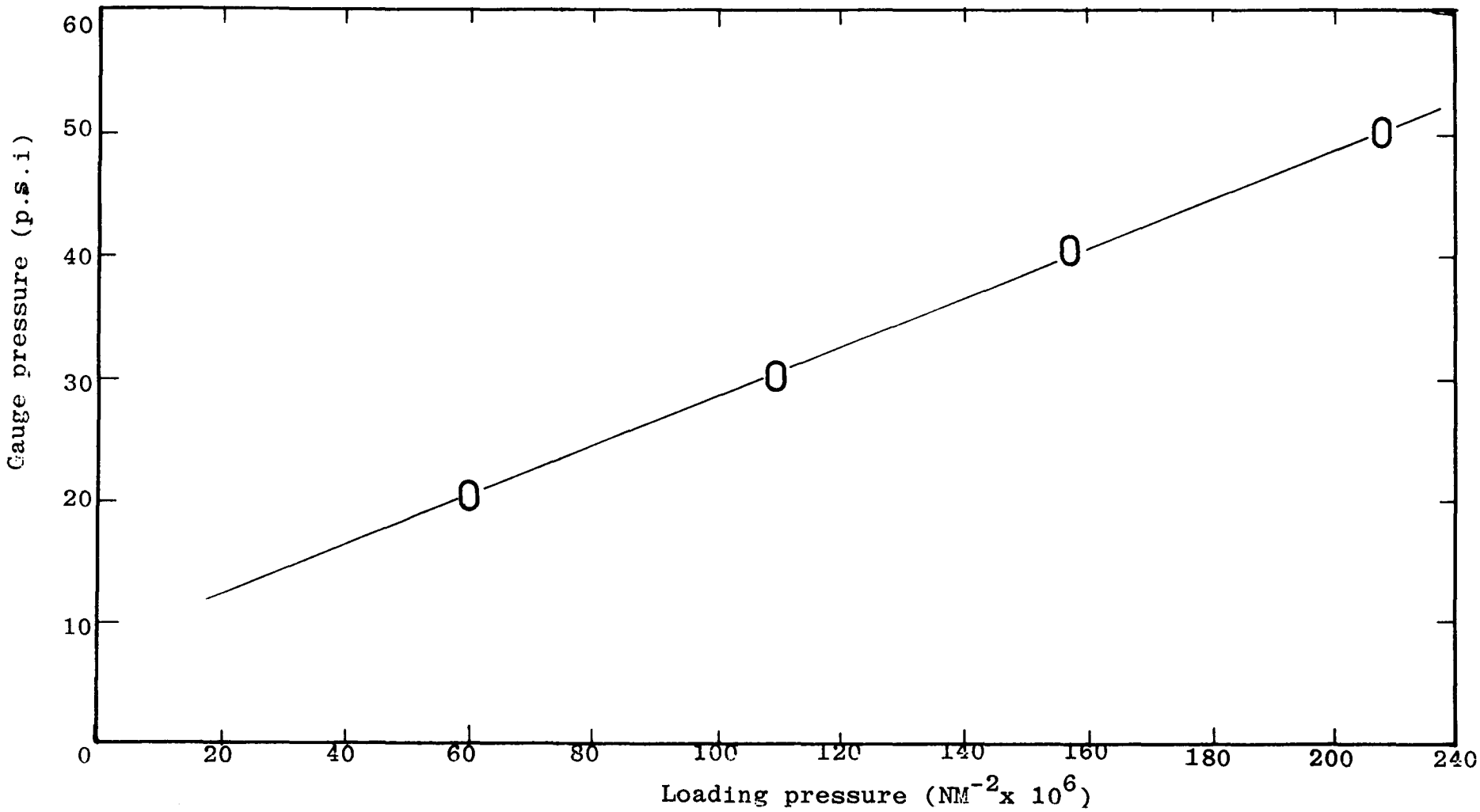


Figure 3.1 Calibration diagram for compact density measurement of e.a.f. dusts.

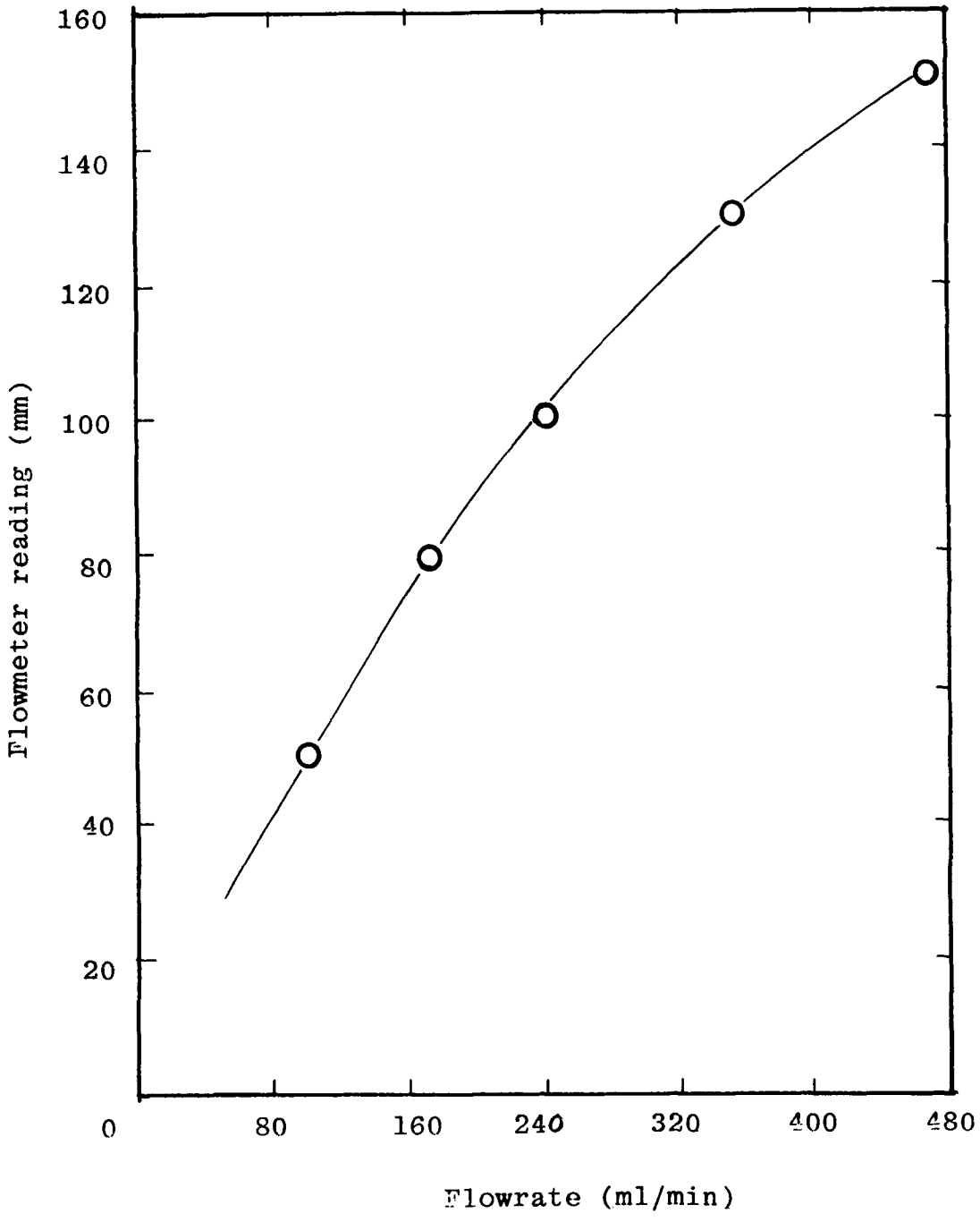


Figure 6.1 Calibration curve for flowmeter

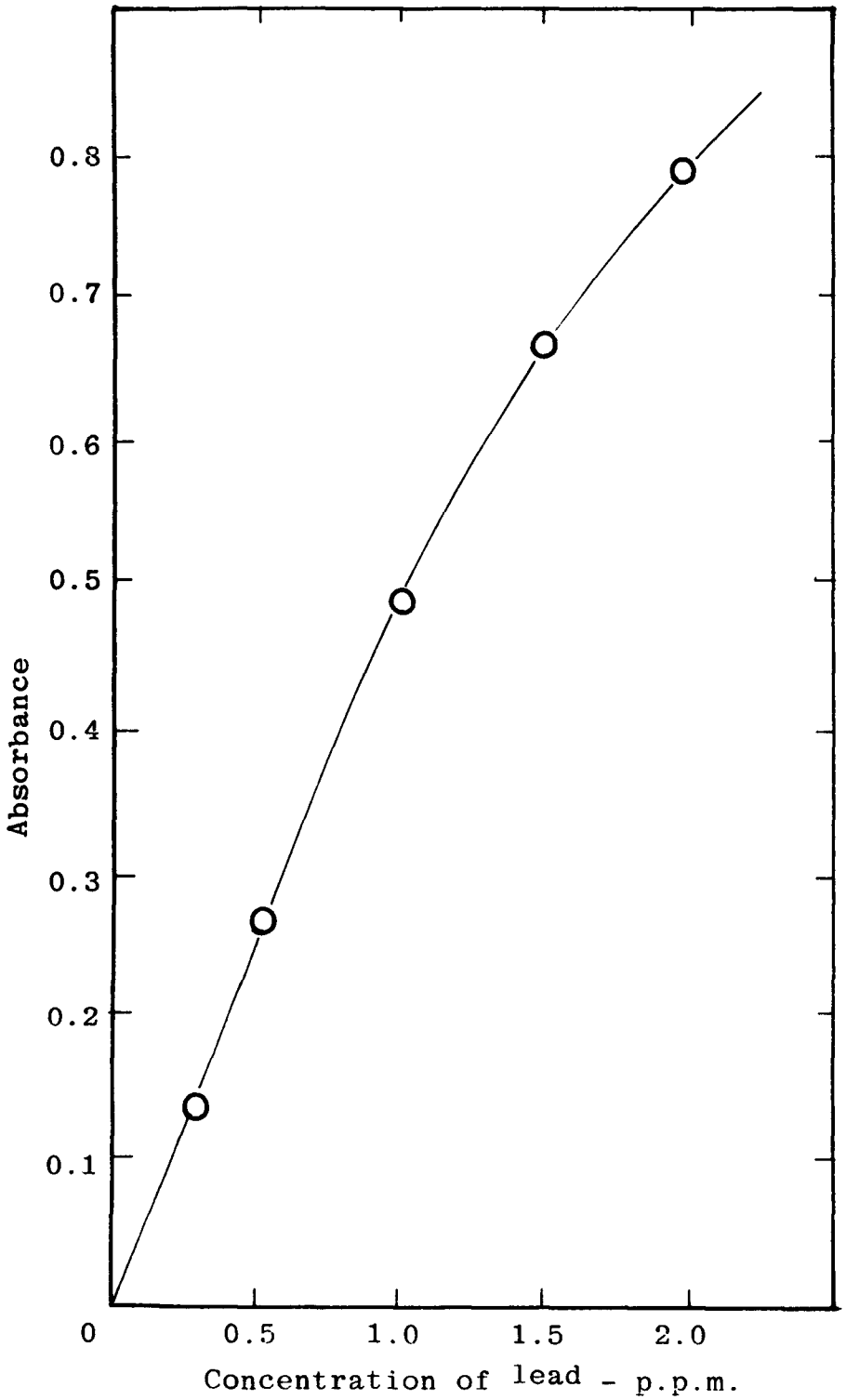


Figure 8.1 Calibration curve for lead analysis by atomic absorption spectophotometry

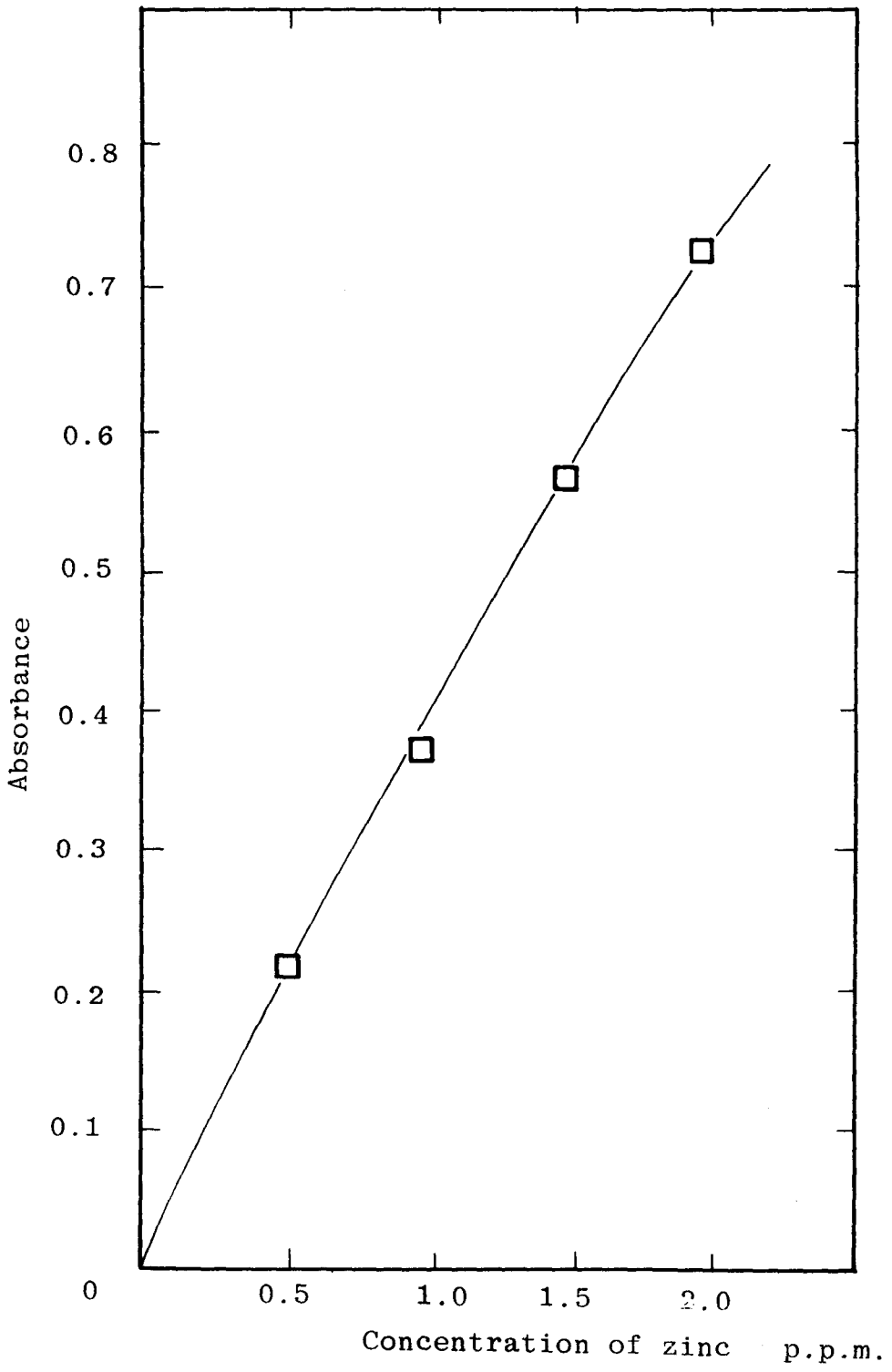


Figure 8.2 Calibration curve for zinc analysis by atomic absorption spectrophotometry

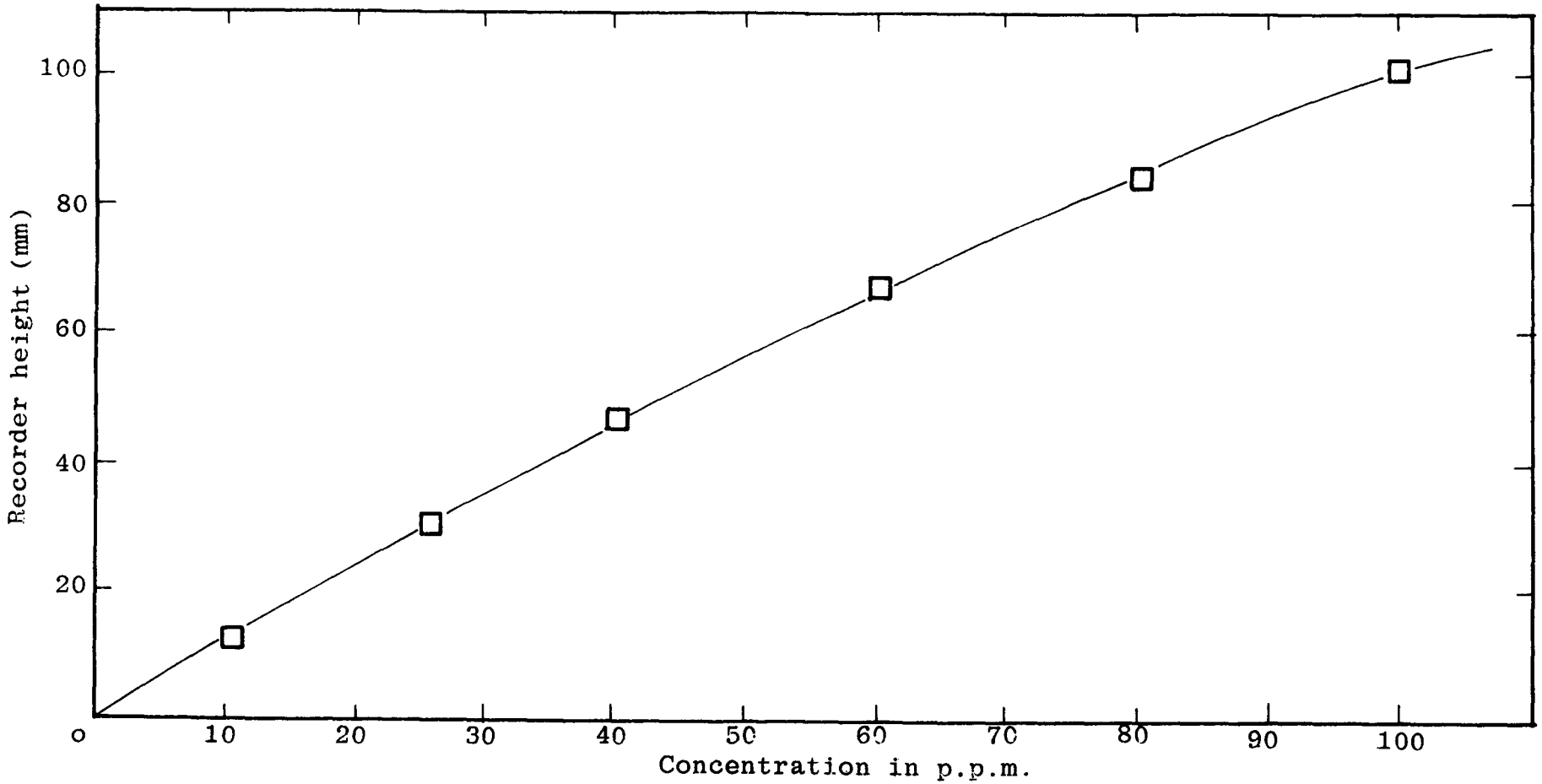


Figure 8.3 Calibration curve for total inorganic carbon analysis

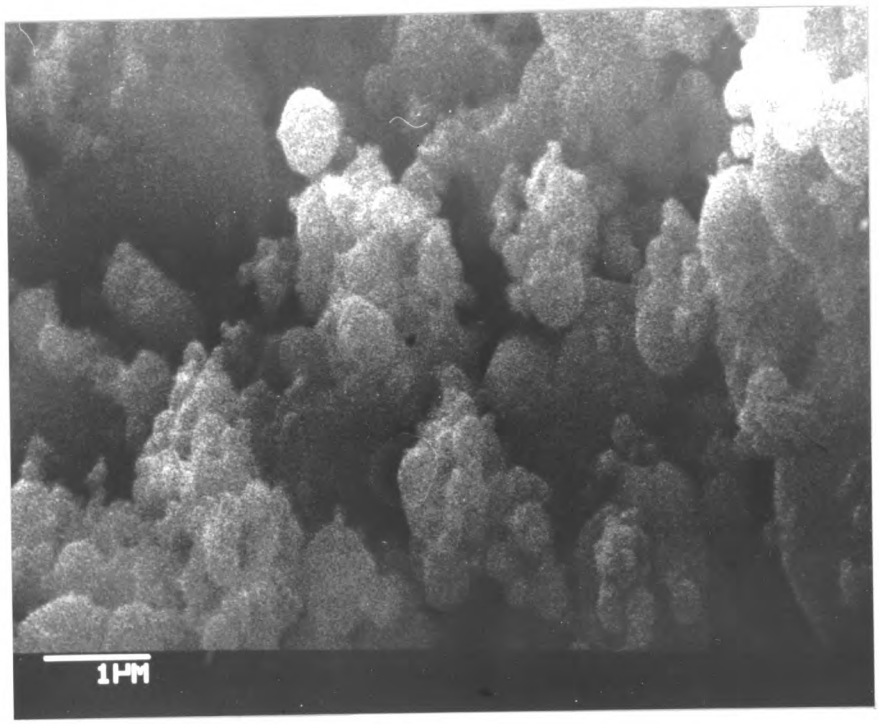


a

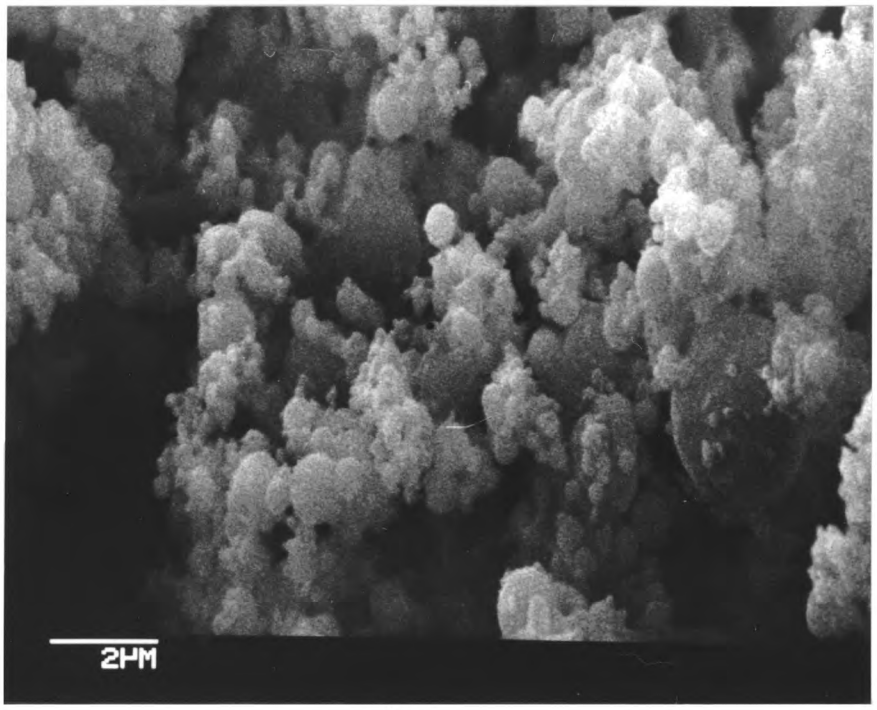


b

Scanning Electron Micrographs of E.A.F. Dusts.
Magnification : a = 20 x $10^3$, b = 10 x $10^3$,
c = 5 x $10^3$, d = 2 x $10^3$

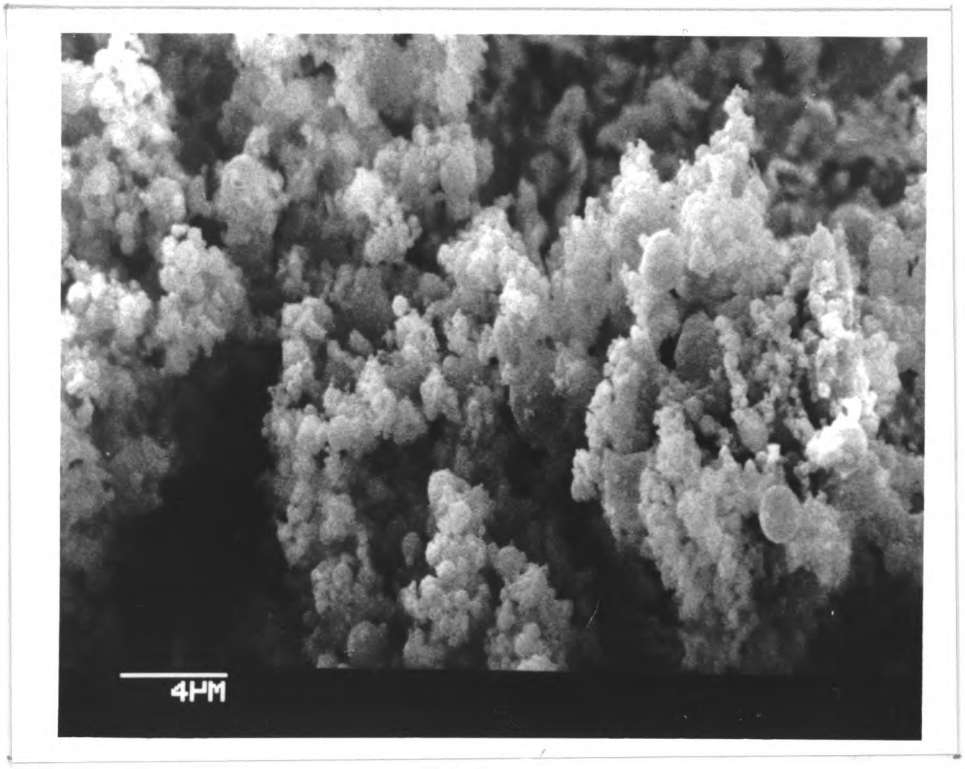


c

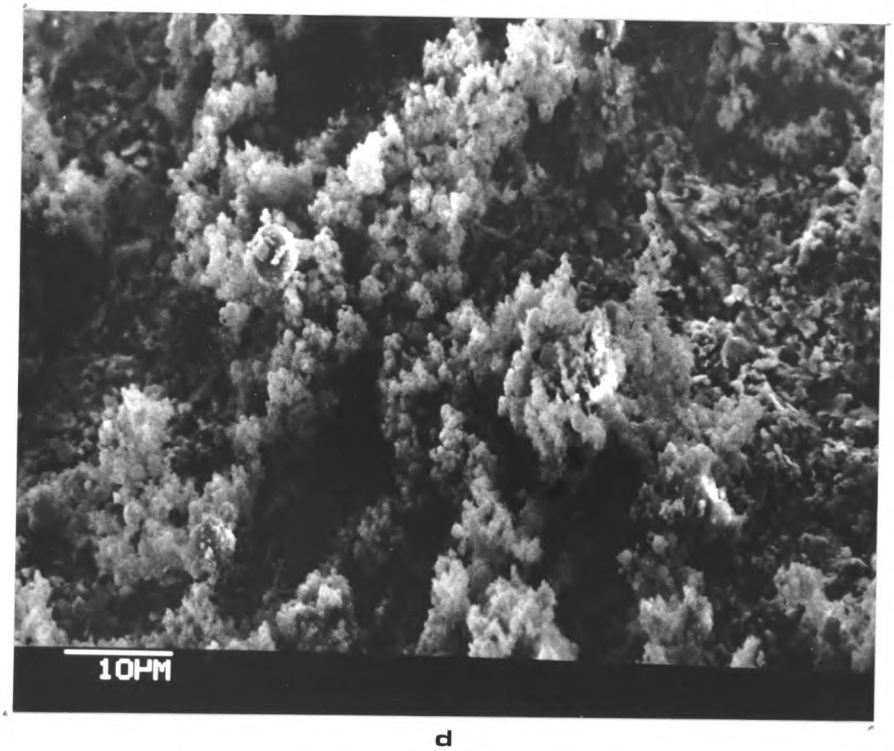


d

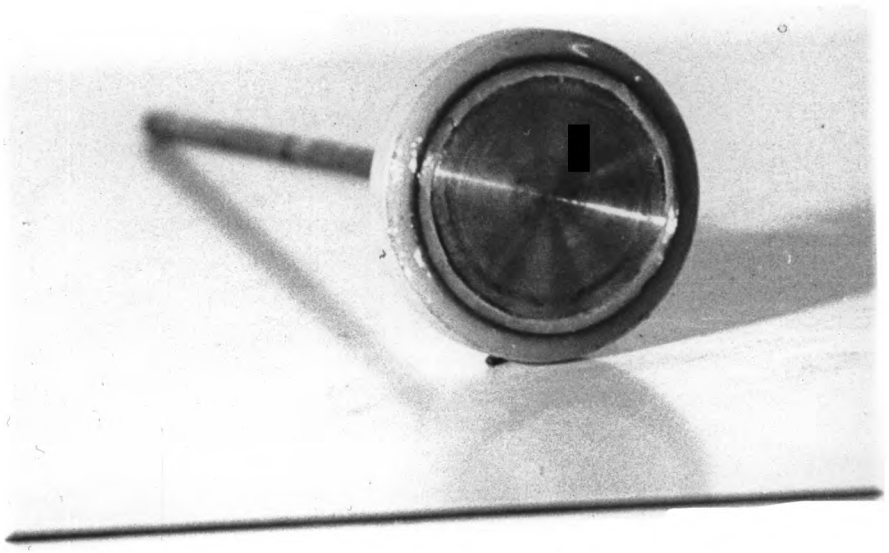

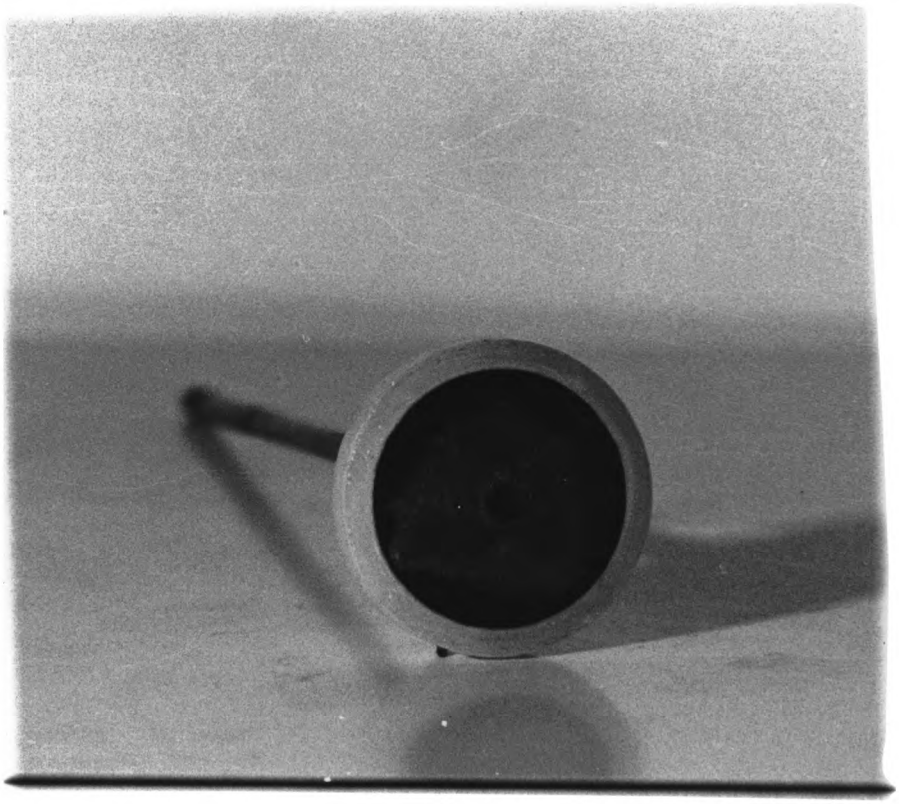

Lead cementation on zinc disc.

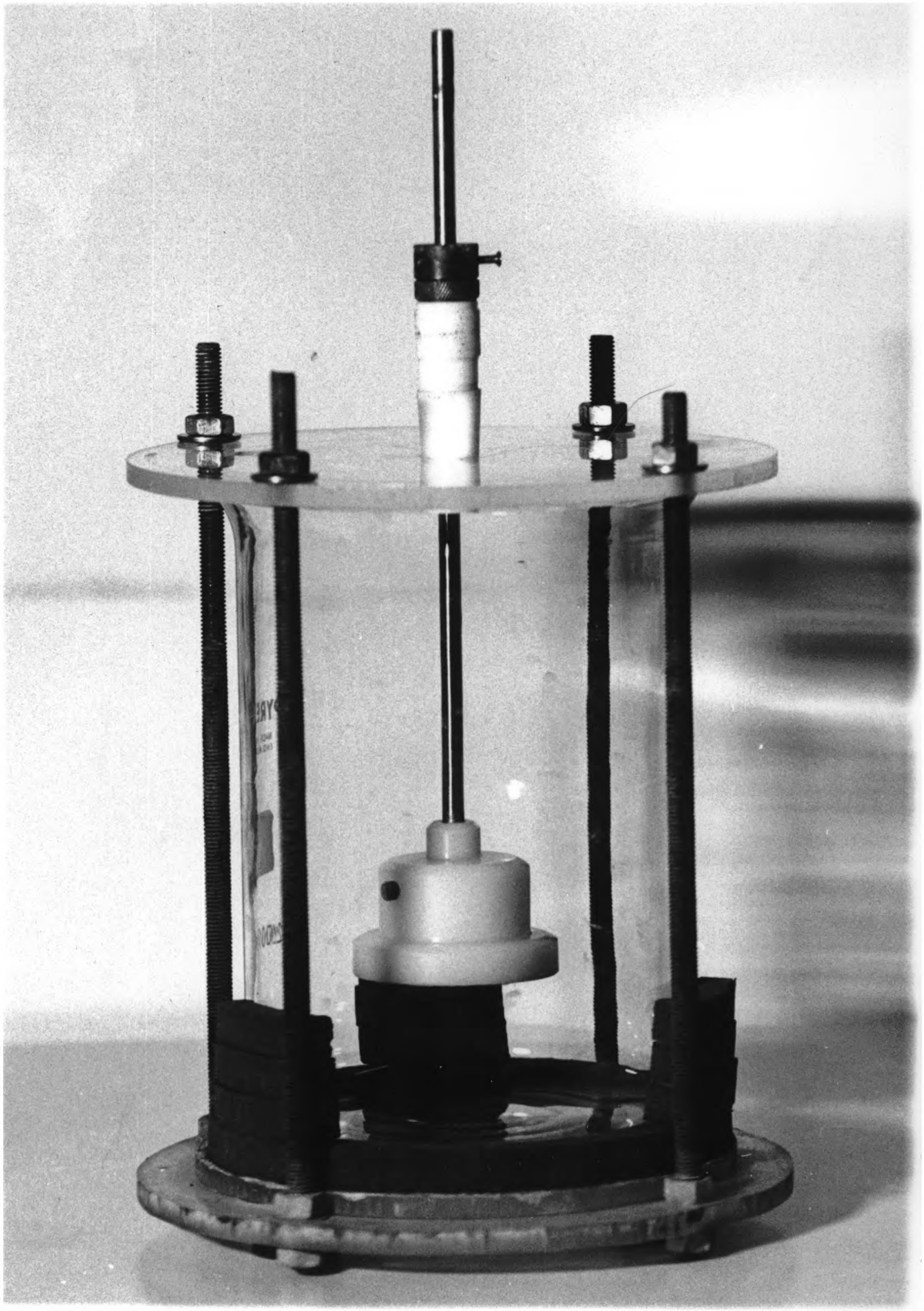

Apparatus for Batch cementation

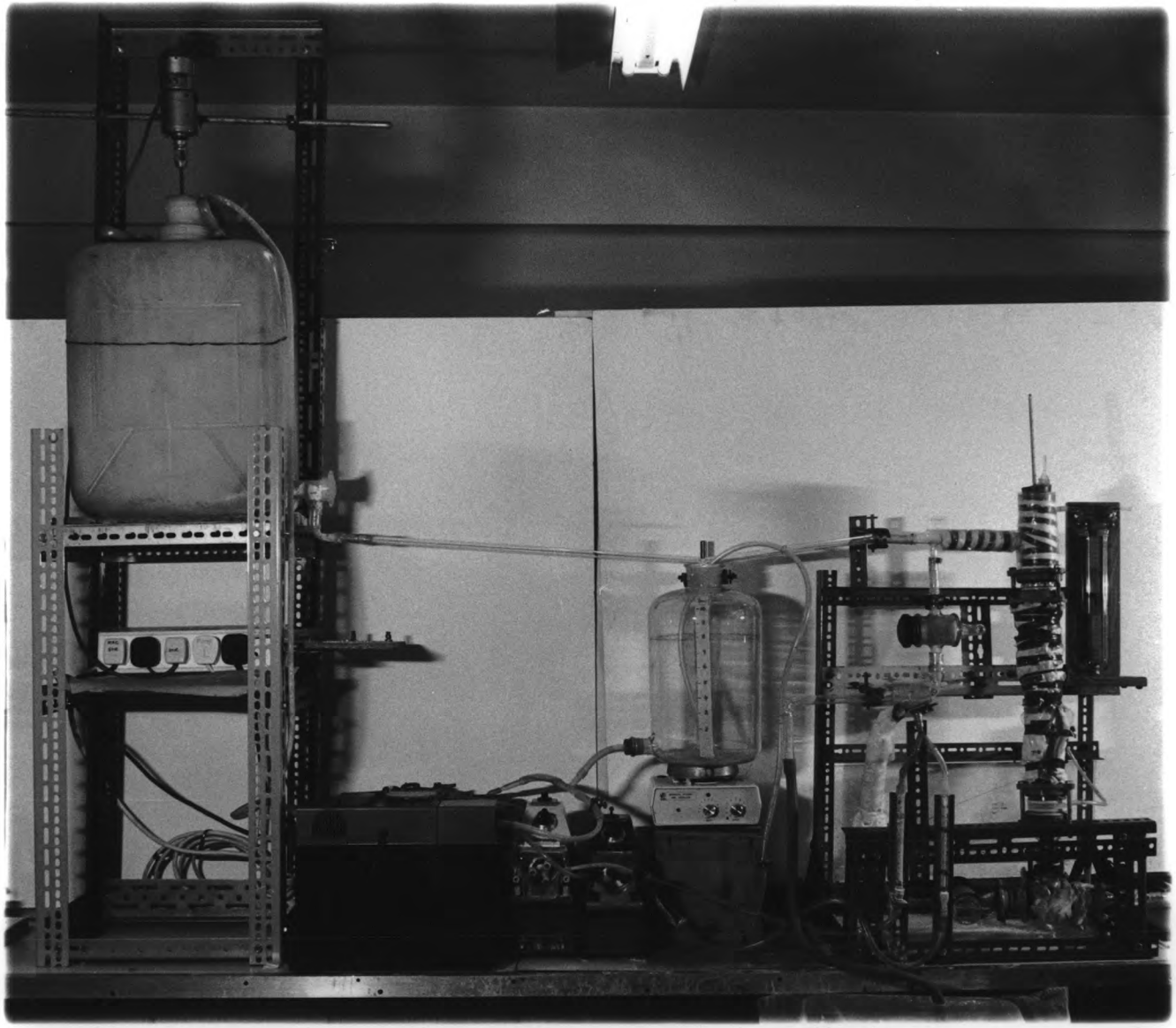

Apparatus for Continuous Cementation